PUB-5420

Report on
Ernest Orlando Lawrence
Berkeley National Laboratory

Laboratory Directed Research and Development Program

FY 1995

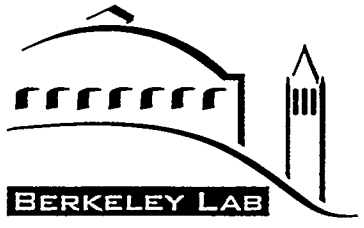

ERNEST ORLANDO LAWRENCE
BERKELEY NATIONAL LABORATORY
UNIVERSITY OF CALIFORNIA
BERKELEY, CALIFORNIA 94720

Prepared for the U.S. Department of Energy under Contract No. DE-AC03-76SF00098

PUB-5420

Report on
Ernest Orlando Lawrence
Berkeley National Laboratory

Laboratory Directed Research and Development Program

FY 1995

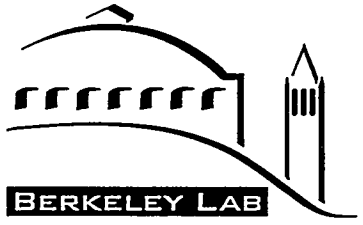

ERNEST ORLANDO LAWRENCE
BERKELEY NATIONAL LABORATORY
UNIVERSITY OF CALIFORNIA
BERKELEY, CALIFORNIA 94720

Prepared for the U.S. Department of Energy under Contract No. DE-AC03-76SF00098

Table of Contents

Introduction

The *Ernest Orlando Lawrence Berkeley National Laboratory (Berkeley Lab) Laboratory Directed Research and Development Program FY 1995* report is compiled from annual reports submitted by principal investigators following the close of the fiscal year. This report describes the projects supported and summarizes their accomplishments. It constitutes a part of the Laboratory Directed Research and Development (LDRD) program planning and documentation process that includes an annual planning cycle, projection selection, implementation, and review.

The Berkeley Lab LDRD program is a critical tool for directing the Laboratory's forefront scientific research capabilities toward vital, excellent, and emerging scientific challenges. The program provides the resources for Berkeley Lab scientists to make rapid and significant contributions to critical national science and technology problems. The LDRD also advances the Laboratory's core competencies, foundations, and scientific capability, and permits exploration of exciting new opportunities. Areas eligible for support include:

- Work in forefront areas of science and technology that enrich Laboratory research and development capability;
- Advanced study of new hypotheses, new experiments, and innovative approaches to develop new concepts or knowledge;
- Experiments directed toward proof of principle for initial hypothesis testing or verification; and
- Conception and preliminary technical analysis to explore possible instrumentation, experimental facilities, or new devices.

The LDRD program supports Berkeley Lab's mission in many ways. First, because LDRD funds can be allocated within a relatively short time frame, Berkeley Lab researchers can support the mission of DOE and serve the needs of the nation by quickly responding to forefront scientific problems. Second, LDRD enables the Laboratory to attract and retain highly qualified scientists, and supports their efforts to carry out world-leading research. Finally, the LDRD program also supports new projects that involve graduate students and postdoctoral fellows, thus contributing to the education mission of the Laboratory.

Berkeley Lab has a formal process for allocation of funds for LDRD. The process relies on individual scientific investigators and the scientific leadership of the Laboratory to identify opportunities that will contribute to scientific and institutional goals. The process is also designed to maintain compliance with DOE Orders, in particular DOE Order 5000.4A. From year to year, the distribution of funds among the scientific program areas will change. This flexibility optimizes the Laboratory's ability to respond to opportunities.

Berkeley Lab LDRD policy and program decisions are the responsibility of the Laboratory Director. The Director has assigned general programmatic oversight responsibility to the Deputy Director for Research. Administration and reporting on the LDRD program is supported by the Directorate's Office for Planning and Communications. LDRD accounting procedures and financial management are consistent with the Laboratory's accounting principles and stipulations under the contract between the University of California and the Department of Energy, with accounting maintained through the Laboratory's Chief Financial Officer.

In FY 1995, Berkeley Lab was authorized by the Department of Energy to establish a funding ceiling for LDRD based on 3% of the Laboratory's FY 1995 operating and capital equipment budgets. This funding level was provided to develop new scientific ideas and opportunities and allow the Laboratory Director an opportunity to initiate new directions. However, budget constraints limited available resources, so only $6.0 M was allocated for operating and $0.4 M for capital equipment.

In FY 1995, scientists submitted 128 proposals requesting over $17 M. A total of 49 projects were funded, with awards ranging from $33 K to $467 K. These projects are summarized in Table 1.

To bring its overhead structure under new Cost Accounting Standards, Berkeley Lab started in FY 1995 to charge a scientific burden for LDRD projects. To an initial operating budget of $5.51 M for the program, an additional $641 K was allocated for this purpose. One effect is that the budget for an average project, as well as for the program as a whole, is about 12% higher than for prior years. The figures given in the previous paragraphs for actual allocations include this scientific burden.

Table 1: FY 1995 Laboratory Directed Research and Development Program.

Investigator	Project Title	($)
Accelerator and Fusion Research Division		
Richard Gough	Femtosecond X-ray Pulse Generation	520,300
Alan Jackson Clyde Taylor	"Superbend" — A 5 T Bending Magnet for the ALS	292,500
William C. Turner	Technology for Proton Colliders at High Energy and Luminosity	206,000
Chemical Sciences Division		
Charles B. Harris	Magnetic Properties and Electron Localization at Interfaces	116,200
David K. Shuh	Structure and Chemistry of Adsorbates at Semiconductor Interfaces Investigated by Synchrotron Radiation Techniques	49,900
Earth Sciences Division		
Gudmundur S. Bodvarsson	Studies in the Geologic Disposal of Nuclear Waste	21,000
Donald De Paolo Mark Conrad Terrence Leighton Bob Buchanan	Characterization and Monitoring of Subsurface Biologic Activity Using Stable Isotope Soil Gas Analysis	82,400
Harvey E. Doner Mavrik Zavarin Tetsu K. Tokunaga	Soil Carbonate Sorptive Properties for Trace Elements: Advanced Methods in Determination of Microscopic and Molecular Level Associations	36,400
Hoi-Ying Holman Yvonne W. Tsang	Laboratory Studies of Microbial Transformation of Diesel Fuel in a Transient Subsurface Environment	115,300
Jiamin Wan	Microbial Transport and Microbial and Nutrient Delivery in Subsurface Environments	75,100
Energy and Environment Division		
Susan L. Anderson	Toxicity at Mare Island Naval Shipyard	78,000

Table 1. Continued.

Investigator	Project Title	($)
Stephen P. Cramer Jeffrey Beeman Eugene Haller Norman Madden Mark Le Gros Eric Silver	Broad-Band High-Resolution Microcalorimetry for Biological and Materials Science Applications on the ALS	102,900
M.D. Levine N. Brown D. Grether R. Harley D. Hopkins K. Jackson D. Littlejohn D. Lucas M. Madou F. McLarnon R. Sawyer I. Shepherd H. Stadler H. Taha T. Wenzel	Research to Improve the Development of Energy-Efficient, Low-Polluting Automobiles	138,000
Stephen E. Selkowitz	Building Performance Assurance	369,800
Engineering Division		
Joseph M. Jaklevic Jocelyn C. Schultz	Development of Microchemical Methods for Biological Assays	69,400
Jacques Millaud Thomas Earnest Howard Padmore David Nygren	Advance Towards the Next Generation of Pixellated Detectors for Protein Crystallography	293,700
Life Sciences Division		
Damir Sudar Joe W. Gray	Integrated Molecular Cytogenetics Workstation	57,200
Bing Jap	Electron Crystallography of Selected Membrane Proteins	147,600
Maria Pallavicini Malak Shoukry George Brecher	Propagation of Genetically Damaged Hemopoietic Stem Cell Progeny	49,000

Table 1. Continued.

Investigator	Project Title	($)
Edward M. Rubin	Creation of Transgenic Mice Containing a Library of P1 Clones Encompassing the Down's Syndrome Region from Chromosome 21	265,900
G. Shyamala	A Transgenic Model for Clinical Testing of Progestins and Analysis of Progesterone Receptor Function	69,500
Diane L. Tribble Elaine L. Gong Edward M. Rubin Mary Helen Barcellos-Hoff	Variations in Susceptibility to Environmental Oxidants as Studied Using Transgenic Mice	110,000
Paul Yaswen	Isolation of Genetic Supressor Elements in Human Mammary Epithelial Cells	67,000
Materials Sciences Division		
Jeffrey Bokor	Electronic Thermalization in Metals and Semiconductors	122,400
Shimon Weiss D. Frank Ogletree Daniel S. Chemla	Near-Field Scanning Optical Microscopy/ Spectroscopy of Low-Dimensional Systems at 50-nm Resolution	112,100
John Clarke	Electron-Beam Lithographic Fabrication of Submicron Junctions for Coulomb Blockade Arrays	89,000
Ulrich Dahmen	New Directions for *In Situ* Electron Microscopy at High Spatial Resolution	158,400
Dung-Hai Lee	Quantum Hall Plateau Transitions and the Hubbard Model	86,400
Roya Maboudian	Interaction of Hydrogen and Hydrocarbon Molecules with Indium Antimonide Surface: Chemistry of Etching	77,700
Paul L. McEuen	A Low Temperature AFM for Imaging Current Flow in Nanostructures	54,900
W. Meyer-Ilse J.T. Brown D. Attwood	Biological X-ray Microscopy	40,500
Joseph Orenstein Stuart Parkin	Optical Spectroscopy and Microscopy of Magnetic Multilayers	51,400

Table 1. Continued.

Investigator	Project Title	($)
Norman Phillips	Establishment of the Thermodynamic Temperature Scale in the mK Region	53,100
Zi Q. Qiu	Investigation of Nanometer Magnetism by Using Surface Magneto-Optic Kerr Effect (SMOKE)	59,800
Peter G. Schultz Paul McEuen	Nanosynthesis	91,500
Peter G. Schultz	A Combinational Approach to Materials Science	83,600
Neville Smith	Spin-Polarized Photoemission Studies of Magnetic Surfaces, Interfaces, and Films	409,900
Gabor A. Somorjai Mark D. Alper Alexis T. Bell Peter G. Schultz Jay Keasling Fabio H. Ribeiro	Catalytic Routes to a Cleaner Environment	173,300
Harry W.K. Tom	Time-Resolved Studies of VUV, XUV, and Soft-X-Ray Photo-Induced Chemistry at Surfaces	78,000
Wladyslaw Walukiewicz Kin Man Yu Lei Wang Christian Kisielowski Edith Bourret	Application of Synchrotron Radiation to Processing of Semiconductor Materials	56,400
Shimon Weiss D. Frank Ogletree Daniel S. Chemla	Ultrafast Surface Dynamics with Atomic Resolution	101,400
Alex K. Zettl Marvin L. Cohen Steven G. Louie	Conducting and Semiconducting Boron–Nitrogen–Carbon Nanowires	43,800
Nuclear Science Division		
Claude Lyneis	New Techniques for Low-Energy Nuclear Beams	182,500

Table 1. Continued.

Investigator	Project Title	($)
Robert G. Stokstad Henry J. Crawford Douglas M. Lowder Martin E. Moorhead David R. Nygren Austin Richards	New Research Directions in Nuclear and Particle Astrophysics (INPA)	57,700
Physics Division		
Randy Baadhio	Global Gravitational Anomalies in Three Dimensions	30,100
Michael E. Levi Frederic Kral	Integrated Instrumentation System for Drift Chambers, TOF, Cerenkov, and Silicon Detectors	195,900
S. Perlmutter G. Goldhaber C. Pennypacker H. Spieler S. Holland R. Stover P. Suni	Development of High-Resistivity Charge-Coupled Devices for Imaging	87,800
Structural Biology Division		
Rosalind Kim	Hyperthermophilic Microorganisms	99,900
Multidivisional		
Thomas McKone Sally Benson Nancy Brown Joan Daisey Lois Gold Jane Macfarlane	SELECT, An Integrated, Science-based Environmental Software Framework	434,400
TOTAL		6,365,000

Accelerator and Fusion Research Division

Femtosecond X-ray Pulse Generation

Principal Investigator: Richard Gough

Project No.: 93002

Funding: $520,300 (FY 95)
$487,700 (FY 94)
$477,700 (FY 93)

Project Description

The purpose of this project was to develop a novel tunable source of femtosecond x rays based on right-angle Thomson scattering of terawatt laser pulses with a tightly focused beam of relativistic electrons. In addition, we proposed development of ultra-sensitive time-integrated diagnostics, as well as time-resolved diagnostics for source characterization. The x rays are strongly forward directed (along the electron beam) and are of femtosecond duration because the interaction time between the laser and the electron beam is limited by the transverse dimension of the focused electron beam. Femtosecond x-ray pulses are potentially important for the study of fast chemical reactions in a time-resolved manner, coherent intramolecular dynamics in chemistry, and phonon dynamics in the solid state.

Accomplishments

Installation of the Laser System at the ALS Linac

We have completed installation and integration of the laser system at the Beam Test Facility.

Scattering Chamber and Accessories

We have installed all components required to carry out the interaction experiment, including delay stages to adjust the temporal overlap between the e-beam and laser pulses, and mirror controls to adjust the spatial overlap. We have implemented ultrafast photodiodes for timing purposes, feedback systems for timing jitter control, and a quadrant detector for position monitoring of the laser beam. We have also developed electron beam diagnostics based on Optical Transition Radiation. These diagnostics have allowed us to measure the jitter performance of the system, measure for the first time the ALS Linac bunch length, and measure and monitor the spot size at the interaction point.

X-ray Detection

We have succeeded in producing the Thomson scattered x-rays. The x-ray beam (Fig. 1) was detected by means of a high-sensitivity GadoliniumOxide:Tb phosphor screen imaged onto a slow-scan 16-bit CCD camera.

The laser and electron beams were scanned across each other both in space and time. The electron-beam bunch length was measured to have a full width half maximum of about 25–30 ps with a typical charge of about 1.2–1.3 nC. The electron beam was focused down to a spot size (rms) of about 65 μm. By tuning the electron-beam transport line for zero dispersion, the electron-beam pointing was found to be better than 25 μm. The laser pulse had a pulse length of about 70 fs with an energy of around 40 mJ. The phosphor screen sensitivity and linearity were calibrated with a NIST traceable radioactive I^{129} source (a 30 keV x-ray line emitter), using direct comparison with the yield on a high purity Ge-detector. The overall system efficiency was found to be 1.2

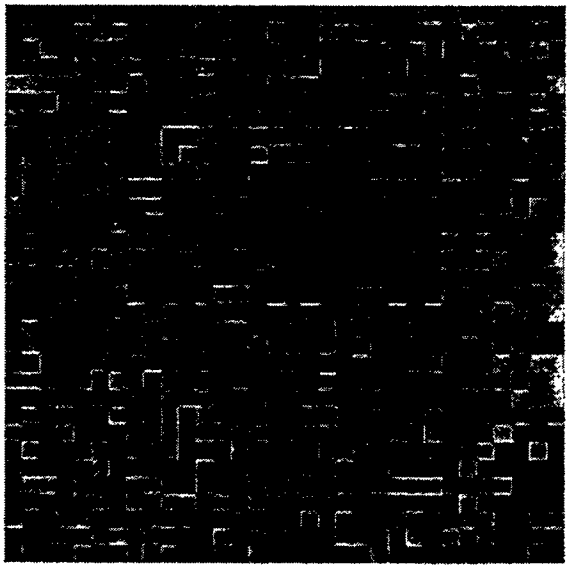

Figure 1. Image of a femtosecond x-ray pulse incident on the phosphor screen. The 1.62 cm × 1.62 cm screen was imaged onto a CCD camera. The beam size was about 6–7 mm corresponding to a beam divergence on the order of 12–15 mrad. The total x-ray yield was about 5–6 × 10^4.

x rays/count, where the CCD camera saturates at 32,000 counts. By integrating the total amount of counts from an x-ray image, we found that about 50,000 to 60,000 x rays were generated, compared to a calculated value on the order of 65,000.

Using the Ge-detector, we have also been able to measure the energy of the x-ray photons. At the present, a spectrum has been obtained for the on-axis photons. Experiments are under way to angularly resolve the spectrum. Development of temporally resolving x-ray diagnostic systems is still under way. The x-ray pulse duration will be measured with picosecond time resolution using conventional x-ray streak cameras. A cross-correlation technique with femtosecond time resolution, has been developed and tested on a soft-x-ray (400 Å) radiation source.

In conclusion, for the first time we have generated femtosecond x rays through 90° Thomson scattering of a high-power laser beam off of a relativistic electron beam. The x-ray beam was observed on a phosphor screen after scanning both beams across each other in time and space. Full spatial, spectral, and temporal characterization of the beams is still in progress.

Publications

K.-J. Kim, S. Chattopadhyay, and C.V. Shank, "Generation of Femtosecond X-Rays by 90° Thomson Scattering," *Nucl. Instrum. Meth. in Physics Research A* 341, 351–354 (1994).

J. Bengtsson, W. Leemans, and T. Byrne, "Emittance Measurement and Modeling of the 50 MeV Linac to Booster Transport Line at ALS," *Proceedings of the 1993 Particle Acceleration Conference*, 567–569.

W. Leemans, G. Behrsing, K.-J. Kim, J. Krupnick, C. Matuk, F. Selph, and S. Chattopadhyay, "The 50 MeV Beam Test Facility at LBL," *Proceedings of the 1993 Particle Acceleration Conference*, 83–85.

B. van der Geer, M. de Loos and W. P. Leemans, "Characterization of the 50 MeV ALS Linac Beam with Optical Transition Radiation," *Proceedings of the 1994 European Particle Acceleration Conference*, London, U.K.

W. Leemans, S. Chattopadhyay, M. Conde, E. Glover, K.- J. Kim, R. Schoenlein, and C. V. Shank, "Status of the LBL Experiment on Femtosecond X-Ray Generation through 90° Thomson Scattering," *Proceedings of the 1994 European Particle Acceleration Conference*, London, U.K.

W. Leemans, R. Schoenlein, A. Chin, E. Glover, M. Conde, S. Chattopadhyay, K.-J. Kim, and C.V. Shank, "Femtosecond X-Ray Generation Through 90° Thomson Scattering: Status of the LBL Experiment," *AIP Conference Proceedings 335 of the 1994 Advanced Accelerator Concepts Workshop*, 209–223 (1995).

T. E. Glover, R. W. Schoenlein, A. H. Chin, and C.V. Shank, "Observation of Laser Assisted Photoelectric Effect and Femtosecond High Order Harmonic Radiation," submitted to *Phys. Rev. Lett.*

W. Leemans, R. Schoenlein, A. Chin, E. Glover, R. Govil, P. Volfbeyn, S. Chattopadhyay, K.- J. Kim, and C. V. Shank, "Femtosecond X-rays from 90° Thomson Scattering," *Proceedings of the 1995 Particle Accelerator Conference*, Dallas, TX.

A. Chin *et al.*, "Progress Report of the Femtosecond X-Ray Experiment," CBP Tech Note.

P. Volfbeyn, W. Leemans, and L. Archambault, "Time Integrated Measurement Techniques for the Femtosecond X-ray Experiment," CBP Tech Note.

"Superbend"—A 5 T Bending Magnet Design for the ALS

Principal Investigators: Alan Jackson and Clyde Taylor

Project No.: 95002

Funding: $292,500 (FY 95)

Project Description

The ALS can be upgraded by replacing some of the gradient bend magnets with superconducting (SC) dipoles, and extra quadrupoles to match the lattice functions. The short ~ 4 T dipoles (at 1.5 GeV) can be ramped to ~ 5.1 T for operation at 1.9 GeV. These magnets would provide bend-magnet synchrotron radiation with a critical energy of 6 keV, which is much better suited to protein crystallography and other small sample x-ray diffraction and adsorption studies than is currently available at the ALS. We will design, build, and test a prototype magnet to verify

the concept. If successful, it is anticipated that the changeover (ALS-II) could occur in FY 97 supported by ARIM funding. The proposed design is unique, yet it would seem that similar magnets could be developed for other light sources and accelerators.

A prototype magnet complete with cryostat will be constructed by the SC Magnet Program. The prototype will be tested for magnetic field quality, quench safety, electrical stability, mechanical positioning, stability, and alignment after cool down. These results would be the basis for building three magnets for installation in ALS-II.

The C-shaped "cold iron" design has "internal" pole-piece iron driven to about 5.5 T, and it has a magnetic length of only ~ 24 cm along the beam direction. The magnet (in its cryostat) is to be installed around the existing ALS beamline, bringing the pole faces as close together as possible. Since the magnet is very short, it is important to understand the end effects determined by the gap.

Accomplishments

The magnet design, shown in Fig. 2, has been optimized during the past year and is much simpler

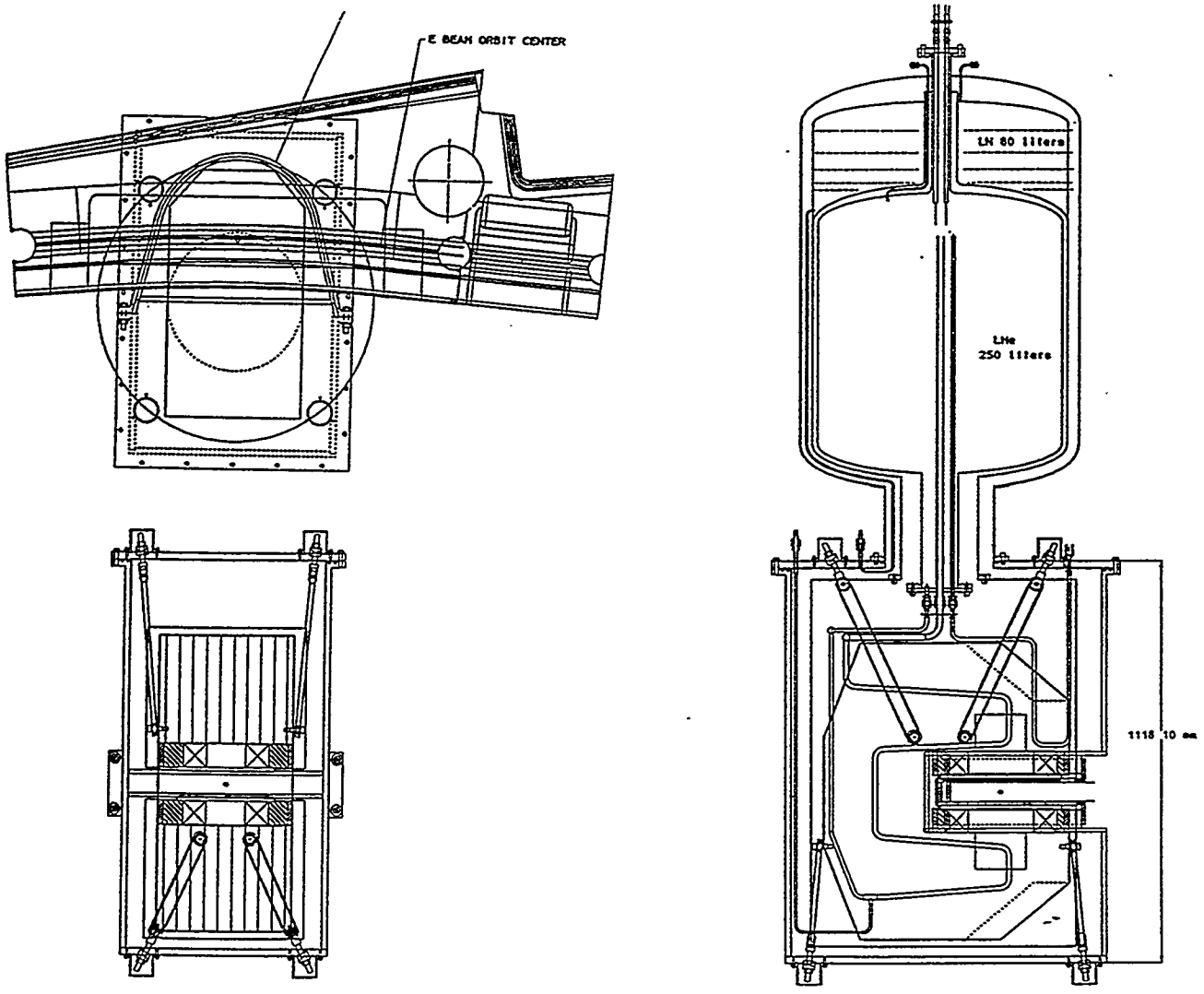

Figure 2. Top Left: plan view of the superbend assembly around the existing ALS vacuum chamber. Bottom Left: elevation cross section of the magnet. Right: bird's eyeview of the magnet and cryostat.

than the original conceptual design. A single magnet now provides the required 10-degree bend instead of two 5-degree bend magnets spaced 0.5 m apart. The coil and coil support design have been simplified: each pole has a single pole-face coil with a circular support hoop instead of the original multicoil "Vobly" design. Beam simulation studies were performed using the three-dimensional field of this magnet design and show that the ALS will operate satisfactorily with three such Superbend magnets placed symmetrically in the ring. Some material will be removed from the aluminum beamline walls at the bend locations to allow the magnet pole gap to be as small as possible.

Saturated liquid helium at atmospheric pressure can circulate through a coolant manifold via natural convection. Coil and yoke are attached to the manifold and cooled by conduction.

A detailed design has been completed. A superconductor was purchased, and prototype coils were fabricated by Wang NMR, Inc. These prototype coils will be tested in early FY 96 in an existing helium dewar using a dummy iron yoke.

Technology for Proton Colliders at High Energy and Luminosity

Principal Investigator: William C. Turner

Project No.: 95001

Funding: $206,000 (FY 95)

Project Description

The DOE response to the recent recommendation of the Drell subpanel of the High Energy Physics Advisory Panel makes it likely that the U.S. will participate in the construction of the Large Hadron Collider (LHC) at CERN. The proposed Berkeley Lab program consists of (1) superconductor R&D for interaction region quadrupoles; (2) design and construction of the collider room temperature insertion region vacuum systems; and (3) accelerator physics studies. The work builds on longstanding Berkeley Lab expertise in superconducting magnet and vacuum technology. We are developing design approaches and fabrication techniques in collaboration with the CERN teams. Our work concentrates on time-critical studies of ternary superconductors for the quadrupole and conceptual design of the warm beam tube vacuum systems.

Accomplishments

One of the more critical elements in the performance of a collider is the quadrupole lens at the beam collision points. These quadrupoles normally form a set of triplets around the interaction region. Their focal power directly affects the luminosity available at the crossing point. An improved Fermilab two-layer design can serve as the basis for an alternative to a more intricately graded, four-layer design now envisioned for the LHC, provided it can obtain the proposed gradient. Detailed studies through this project demonstrate that these two-layer designs should achieve the required operational gradient of 250 T/m with at least a 5% margin on the short-sample load-line intersection. These high current densities also require turn-off times < 0.2 s after transition to the normal state. Such a short time requires the development and testing of an advanced protection heater design. New design concept quadrupole calculations were also done. The concept of using an active flux return is proposed as a possible candidate design for a future higher gradient requirement.

Especially relevant to the LHC beam tube vacuum requirements is determining how to deal with the magnitude of gas desorption and power deposition by synchrotron radiation while satisfying resistivity, impedance, and space constraints in the cryogenic environment of superconducting magnets. A beam tube vacuum model was developed that treats photodesorption of tightly bound H, C, and O; photodesorption of physisorbed molecules; and the isotherm vapor pressure of H_2. Experimental data on cold tube vacuum performance were applied to model calculations of beam tube vacuum performance for simple cold beam tube and liner configurations. This analysis was then extended to include ion desorption, in addition to thermal desorption and synchrotron-radiation-induced photodesorption. The new ion desorption terms introduced the possibility of vacuum instability. Experimental data were used to evaluate the H_2 sojourn time for the conditions of the LHC, and this situation was found to be stable. Also evaluated were stability margins and inclusion of gases heavier than H_2.

Additional efforts included studies in electrical performance of a string of superconducting magnets, modeling of an 80 K liner vacuum system, studies of

loss in pressurized Rutherford cables, and determining the effect of Nickel and Stabrite coatings and resistive cores on such AC loss.

Seven publications were completed that were wholly or partially supported by LDRD funds. The results of this work were also reported at technical meetings and workshops: the 1995 Cryogenic Engineering and International Cryogenic Materials Conference; the 1995 Particle Accelerator Conference; and the 1995 IUVSTA International Workshop on Wall Conditioning in Large UHV Devices. An AFRD scientist spent three months at CERN participating in experiments with the first string of three LHC superconducting dipole magnets. In addition, at CERN's request, small samples of superconducting cable with a thin stainless steel strip inserted to suppress eddy current losses were prepared and delivered to CERN for testing.

Publications

F. Rodriguez, L. Coull, K. Dahlerup-Peterson, D. Hagedorn, G. Krainz, A Rijllart, and A. McInturff, "Electrical Performance of a String of Magnets Representing a Half-Cell of the LHC Machine," LBL-37413, presented at the MT14 Conference.

E.W. Collins, M.D. Sumption, R. M. Scanlan, S.W. Kim, M. Wake, and T. Shintomi, "Magnetic Studies of AC Losses in Pressurized Rutherford Cables with Coated Strands and Resistive Cores," presented at the 1995 Cryogenic Engineering and International Cryogenic Materials Conference, July 17–21, 1995.

M.D. Sumption, R.M. Scanlan, A. Nijhuis, H.H.J. ten Kate, and E.W. Collings, "Calorimetric Measurements of the Effect of Nickel and Stabrite Coatings and Resistive Cores on AC Loss in Accelerator Cables Under Fixed Pressure," presented at the 1995 Cryogenic Engineering and International Cryogenic Materials Conference, July 17–21, 1995.

A.D. McInturff, J.M. van Oort, and R.M. Scanlan, "Two Alternate High Gradient Quadrupoles; an Upgraded Tevatron IR and a 'Pipe' Design," LBL-36531; presented at the 1995 IEEE PAC, May 1–5, 1995.

W.C. Turner, "Beam Tube Vacuum in Future Superconducting Proton Colliders," *AIP Conf. Proc.* 326 (1995).

W.C. Turner, "Model of an 80 K Liner Vacuum System for the 4.2 K Cold Bore of the SSC 20 TeV Proton Collider," *JVST A*, 13, 2241 (1995).

W.C. Turner, "Ion Desorption Stability in Superconducting High Energy Physics Proton Colliders," LBL-37408 (1995); submitted for publication to *JVST A*.

Chemical Sciences Division

Magnetic Properties and Electron Localization at Interfaces

Principal Investigator: Charles B. Harris

Project No.: 95003

Funding: $116,200 (FY 95)

Project Description

We endeavor to study magnetic properties and the spatial extent of electrons at scientifically and technologically interesting interfaces. We are applying recent advances in Ti:sapphire laser technology and nonlinear optics to enable us to study magnetic interfaces. High-resolution, time- and angle-resolved two-photon photoemission (TPPE) is being used to determine the spatial extent, band structure, tunneling and carrier dynamics, and magnetic splittings of electrons localized at atomically thin interfaces. The important nanometer scale structures under investigation include magnetic thin layers, metal–semiconductor junctions and metal–polymer interfaces. The unifying theme of this work is the study of the unoccupied electronic states at interfaces where these excited states control the electronic and magnetic dynamics and/or serve as sensitive probes of important interface physics.

First, *metal–polymer interfaces* have become technologically relevant junctions due to successful initial work on polymer LEDs and batteries. The metal–polymer contact is an integral feature of the class of devices, so the conduction bands of the interface form a crucial part of the electrical pathway through the device. An understanding of the band structure at the metal–polymer interface and the coupling between the interface states and the metal states is crucial to modeling the current-voltage characteristics. We will attack these problems by studying model metal–polymer junctions where the overlayers are various single- and double-bonded hydrocarbons. By studying the conduction band structure of the interface as a function of overlayer chain length, branching, and electronic structure, we will derive general principles for understanding the electronic states at metal–polymer interfaces.

Important aspects of the metal–polymer interface to be addressed include electron localization and tunneling lifetimes.

Second, Schottky barriers, or *metal–semiconductor junctions*, comprise an important class of interface in microelectronics. Almost all work in the literature on Schottky barriers concerns metal layers on semiconductor substrates. Very little research has been done for semiconductor layers on metal substrates. The TPPE techniques developed in our laboratory are uniquely suited for the study of the excited electronic states and dynamics of atomically thin semiconductor layers on metal substrates. Localization effects may also be observed at these interfaces.

Third, *thin-film magnetism and layered magnetic materials* are an important area of research for magnetic storage devices, nanotechnology, and the 2-D physics of highly correlated systems. Interface and low-dimensionality effects may dominate the physics in these systems and yield new phenomena. Magnetic coupling across ultrathin layers can induce magnetism in the substrate and adsorbate or induce magnetically dead layers in the overlayer. Potentially useful giant magnetoresistance effects have been observed in multilayer metal-on-metal systems.

Accomplishments

In FY 95, we achieved femtosecond time-resolution in the TPPE spectroscopy of metal substrates and at interfaces. The output of a femtosecond Ti:Sapphire oscillator-regenerative amplifier combination is being used to pump an optical parametric amplifier, producing a 200 KHz train of sub-100 femtosecond light pulses tunable from 240–2400 nm. The apparatus has been used to measure $n = 1$ and 2 image potential state lifetimes of 32 fs and < 20 fs, respectively. The increased wavelength range and ultrafast time resolution, in conjunction with good angle and energy resolution, provide the capabilities necessary to carry out the proposed research.

The test case for these capabilities was done by taking the first time-resolved data of a model metal–polymer system. The dynamics of the $n = 1$ image potential state population for zero, one, and two layers of n-heptane on Ag(111) are shown in Fig. 1. The approximately exponential increase in lifetime is consistent

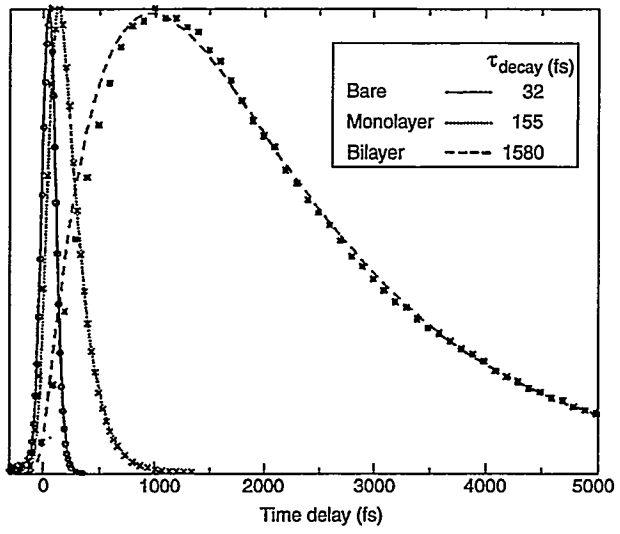

Figure 1. The femtosecond population dynamics in the $n = 1$ state for bare Ag(111), monolayer n-heptane/Ag(111), and bilayer n-heptane/Ag(111).

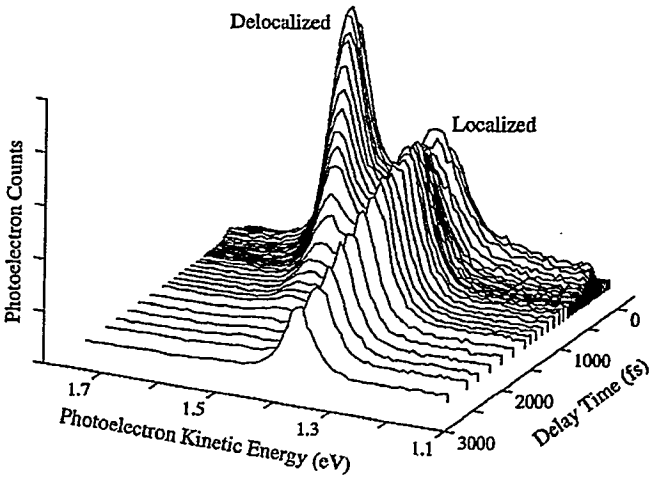

Figure 2. The dynamics of delocalized and localized states for bilayer n-heptane/Ag(111) studied by time- and angle-resolved TPPE at 18.4 degrees. To clearly show the time dependence, the localized feature has been magnified by a factor of three.

with a tunneling picture in which the adlayer forms a barrier that slows the decay of an image potential electron back into the metal. The existence of the tunneling barrier is consistent with the repulsive electron affinity of the longer chain n-alkanes in the condensed phase. The lifetimes of the higher quantum states indicate that the presence of even a monolayer significantly reduces coupling of the image states to the bulk band structure of the metal, so that further changes in lifetime are determined by the adlayer barrier and an attempt rate related to the classical oscillation time in the modified image potential well.

The work on metal–polymer interfaces is also proceeding by measurements of the time and momentum dependence of electron localization. The dynamics of delocalized and localized electron states are shown in Fig. 2. The difference in temporal dynamics is obvious for the respective spectral features. The delocalized feature decays relatively quickly, while the localized feature persists for several picoseconds. We believe that the decay of the delocalized feature is mainly due to fast intraband transitions from high-momentum states to low-momentum states, whereas direct transition from the high-momentum state into the localized state is a relatively slow process. We are currently investigating the nature of the transition from low-momentum states into the localized state.

Work on the metal–semiconductor junctions requires similiar dynamical measurements, particularly in studying the localization effects, as with those for metal–polymer interfaces, but with different samples requiring different growth techniques. We have begun our studies on these junctions by measuring the femtosecond dynamics of conduction electrons at the rare gas solid/Ag(111) interface. These model interfaces are useful because they allow us to study quantum well electronic structure and dynamics in a simple system before moving to the more complicated interfaces of interest. First, time resolved data on the Xe/Ag(111) interface indicate that the lifetimes of the $n > 1$ image potential higher quantum states become shorter than the $n = 1$ state for more than two layers of Xe/Ag(111). This confirms that the higher quantum states of the bare metal surface evolve into quantum well states of the overlayer for greater than four or five layers. We have adapted for our use a model for analyzing the layer-by-layer development of quantum well structures and are using it to make the most accurate measurements to date of the 3-D conduction band structures of rare gas solids. The use of this model will allow us to evaluate the momentum and energy-dependence of future lifetime measurements on magnetic and metal–semiconductor interfaces.

We have tested the laser system now in place and established the production of wavelengths necessary for the intended studies in thin-film magnetism and layered magnetic materials. The next target in this area is to make the necessary modifications to the existing vacuum chamber, timing this to minimize disruption to our entire research program.

Publications

R.L. Lingle, Jr., R.E. Jordan, D.F. Padowitz, and C.B. Harris, "Image and Quantum Well States of Xe, Kr adsorbed on Ag(111)," submitted to *J. Chem. Phys.*

R.L. Lingle, N.-H. Ge, J.D. McNeill, C.M. Wong, and C.B. Harris, "A Time-Resolved Study of the Two-Dimensional Localization of Electrons at Interfaces," in preparation.

Structure and Chemistry of Adsorbates at Semiconductor Interfaces Investigated by Synchrotron Radiation Techniques

Principal Investigator: David K. Shuh

Project No.: 93004

Funding: $49,900 (FY 95)
$74,300 (FY 94)
$76,100 (FY 93)

Project Description

This research project utilizes Synchrotron Radiation (SR) surface characterization techniques to study the relationship between structure and chemistry of compound semiconductor interfaces with and without simple adsorbates. The SR investigations provide fundamental information on binary semiconductor interfaces to improve existing materials processing technologies and to implement new electronic materials. The SR techniques employed will become available at the Advanced Light Source (ALS), and the scientific program is designed to take full advantage of ALS facilities in the near future. A modest laboratory surface science chamber, that will be used as a simple SR endstation at the ALS, continues to be developed.

The investigations employ several SR techniques to characterize semiconductor interfaces: Soft X-ray Photoelectron Spectroscopy (SXPS); Near Edge X-ray Absorption Fine Structure (NEXAFS); and X-ray Standing Waves (XSW). SXPS characterizes the chemical behavior, NEXAFS the electronic structure, and XSW the interfacial structure. These electron spectroscopy experiments use existing endstations at the Stanford Synchrotron Radiation Laboratory (SSRL) and the National Synchrotron Light Source (NSLS), and there have been initial activities at the ALS. A simple surface science system that has basic analytical capabilities continues to be developed in the laboratory to support the SR projects. This surface science capability permits preliminary research on experimental systems of interest, testing of experimental apparatus, and use as a SR endstation. The research program will shift entirely to the ALS once the beamline facilities to perform these experiments are completed.

Accomplishments

Halogen Adsorbates on Compound Semiconductors

The adsorption of iodine on GaAs(110) chemisorbs without the formation of higher iodides, as shown by the fitted GaAs core levels in Fig. 3. Iodine is found to saturate the surface largely at the expense of the surface core level shifts. Iodine exposures have also been performed on the (001) surfaces of GaAs and other III-V materials. Iodine bonds with both surface atoms and the predominant bonding occur to the element that is the majority species independent of surface reconstruction. Studies of the chlorine etching interactions have also been continued. The XSW experimental activities have been severely limited as a result of lack of available beamtime at NSLS and

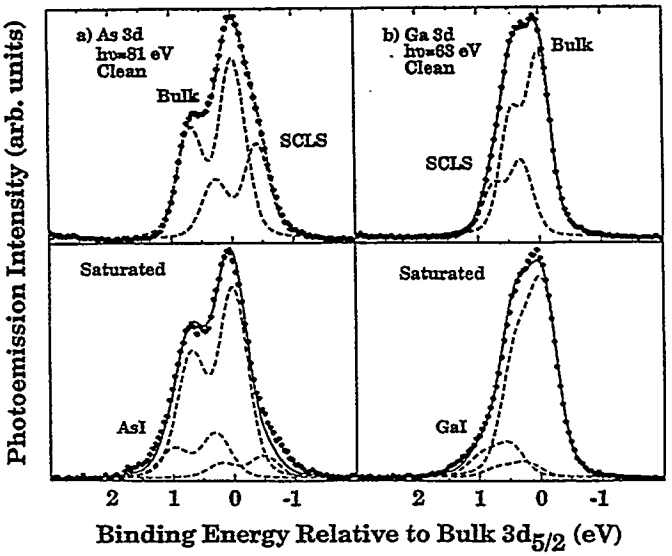

Figure 3. Surface sensitive SXPS from the 3d core levels of the clean surface and the surface saturated with iodine: (a) arsenic collected with hν=81 eV, and (b) gallium collected with hν = 60 eV. The experimental points less the background are the filled circles, the components of the fit are the dashed lines, and the solid line is the sum of the fit components.

SSRL. XSW investigations can now be performed at the ALS as a beamline to perform these measurements has been recently commissioned, especially since several iodine systems have been characterized by SXPS.

Novel Nitride Materials

Many of the basic electronic and physical properties of GaN that will lead to implementation of the material have yet to be characterized. Epitaxial single crystal thin films produced by pulsed laser deposition have been investigated by SXPS at the ALS and by NEXAFS at the SSRL to form the foundation for material contacting and processing technologies. The NEXAFS spectra from the series of GaN thin films is presented in Fig. 4, which illustrates the sp^3 bonding

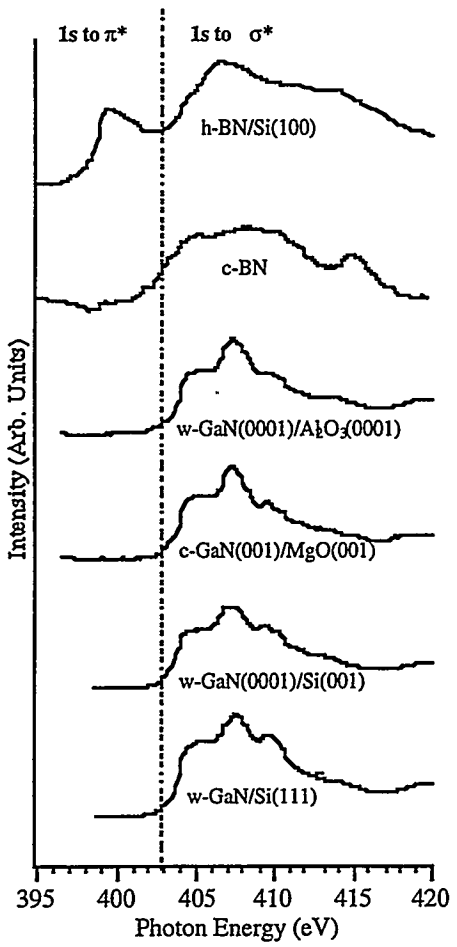

Figure 4. Nitrogen K edge NEXAFS spectra from the GaN thin films along with hexagonal (h) and cubic (c) BN reference materials.

by lack of π^* features. Although the nitrogen K edge is understood for simple gas-phase species, the electronic structure of nitrogen is not well characterized in the solid state. This study of GaN–nitrogen bonding in an ideal zincblende/wurtzite environment is one from which more complex nitride systems can be understood.

Beamline 8.0 Participating Research Team at the ALS

The commissioning of the display spectrometer endstation has been completed and the rotating experimental platform installed to permit rapid interchanging of the PRT endstations, in collaboration with the other PRT members. The insertion device beamline optical elements were characterized and optimized, and the overall operation of the beamline facility became routine. The collection of SXPS data was performed for several of the nitride-based semiconductor systems.

Surface Science System and SR Endstation

The laboratory surface science system, which can also function as a simple SR endstation, continues to perform simple measurements and tests of experimental apparatus prior to their use at SR beamlines. The analytical capabilities and instrumentation of the system were improved and updated to meet increased experimental characterization requirements. The laboratory efforts are an essential component of the SR program, enhancing the productivity of the outside user-based SR efforts, and provide a laboratory system that can perform rudimentary experiments to complement the SR experiments.

Publications

F.J. Himpsel, D.A. Lapiano-Smith, H. Akatsu, J.A. Carlisle, E.A. Hudson, L.J. Terminello, T.A. Callcott, J.J. Jia, M.G. Samant, J. Stohr, D.L. Ederer, R.C.C. Perera, and D.K. Shuh, "Synchrotron Radiation Techniques in Industrial Research," monograph submitted to *Am. Chem. Soc.* (1995).

P.R. Varekamp, C.M. Håkansson, D.K. Shuh, J. Kanski, U.O. Karlson, and J.A. Yarmoff, "A Synchrotron Photoemission Study of the Reaction of Iodine With GaAs(001)," *Vacuum* 46, 1231 (1995).

W.C. Simpson, W.M. Tong, C.B. Weare, D.K. Shuh, and J.A. Yarmoff, "The Temperature Dependence of the Cl_2/GaAs(110) Surface Product Distribution," accepted by *J. Chem. Phys.* (1995).

W.C. Simpson, D.K. Shuh, and J.A. Yarmoff, "Room-Temperature Chlorination of As-rich GaAs(110)," submitted to *J. Chem. Phys.* (1995).

P.R. Varekamp, M.C. Hankansson, J. Kanski, D.K. Shuh, M. Bjorkqvist, M. Gothelid, W.C. Simpson, U.O. Karlsson, and J.A. Yarmoff, "Reaction of I_2 with the (001) Surfaces of GaAs, InAs, and InSb: Chemical Interactions With the Substrate," submitted to *Phys. Rev. B,* (1995)

W.M. Tong, I. Jimènez, D.K. Shuh, J.A. Carlisle, D. G.J. Sutherland, L.J. Terminello, F.J. Himpsel, D. Feiler, R.S. Williams, "Near Edge X-ray Absorption Fine Structure Investigation of GaN Films Grown by Pulsed Laser Deposition," to be submitted to *J. Appl. Phys.*

Studies in the Geologic Disposal of Nuclear Waste

Principal Investigator: Gudmundur S. Bodvarsson

Project No.: 95004

Funding: $21,000 (FY 95)

Project Description

The purpose of this project was to identify and begin addressing critical scientific areas pertaining to geologic disposal of nuclear waste of interest to both the U.S. and France. These areas include multiphase flow of water and radionuclides in fractured rocks, thermal loading strategies/constraints, and repository stability.

This analysis involved the following:

- Exchanging information on strategies for geologic disposal of nuclear waste,
- Examination of ongoing R&D programs to support these efforts,
- Identification of critical gaps in knowledge regarding the scientific and engineering foundations for geologic repositories, and
- Scoping additional research on critical joint problems.

This preliminary effort will be the basis for ongoing, indepth collaborative efforts between the French and U.S. scientific and engineering communities involved in nuclear waste disposal programs.

Accomplishments

Problems of relevance to both governments' nuclear waste disposal programs were reviewed by U.S. and French scientists. This review ranged in content and complexity from simple technical exchanges to actual joint research projects on some various common problems. We have grouped individual projects either conducted or identified into four major areas of collaborative research as follows.

Flow and Transport Process

Colloidal and Multiphase Transport. Colloidal transport of radionuclides under multiphase conditions plays an important role in performance assessment of Yucca Mountain and other nuclear waste repositories. The colloid transport processes may be controlled by liquid saturation, electrical fields, gas formation and migration, and some other factors. However, our understanding of colloidal multiphase transport is very limited due to few studies conducted in this area.

Solubility/Sorption. Aqueous-phase solubility and sorption on rock surfaces are fundamental mechanisms that govern radionuclide and chemical transport in porous/fractured media. The origins of recent circulations of aqueous solutions in porous/fractured rocks are subject to multiple interpretations and should be understood for the future evaluation of Yucca Mountain and other potential repositories.

Heterogeneous Media. Large heterogeneous systems are commonly encountered when studying flow and transport related to nuclear waste repository sites. Such systems are difficult to model and the related uncertainties are difficult to quantify. To better understand these systems, we need to explore ways to improve our modeling capabilities and use *in situ* tracers to characterize the potential transport of radionuclides in these media. The information from these projects will help in the design of field tests for site characterization, repository design, performance assessment, and demonstration of regulatory compliance.

Coupled Process Studies

Thermo-Mechanical-Hydrological Behavior of Single Fractures. The subsurface environment for waste repositories is subject to thermo-mechanical-hydrological combining effects. Through model development and laboratory tests, we are studying the thermomechanical and hydrological coupled behavior of rocks of interest to both groups.

Thermo-Mechanical-Hydrological Block Tests. Through model development and field tests, we are studying thermally induced coupled processes.

Field Studies of Excavation Effects. These studies evaluate the extent of disturbance induced by the excavation process/thermal load in low-matrix permeability rock.

Characterization of Fractured/Faulted Rocks

Investigation of Geometry, 3-D Models, Tectonic Effects of Fracture Networks and Major Faults. Model development, testing, and evaluation are among important procedures used in characterizing fracture system morphology and geometry and the effects of tectonic activity and fault proximity for rock blocks near a repository.

Field Testing Methodology Studies at a Prototype Site for Fractured Rocks (Raymond, CA). The rock mass at the Raymond Field Site is fractured granite. The site will be used to develop techniques and instrumentation for planned tests at both the Yucca Mountain and the French fractured sites.

Testing in Underground Laboratories. With direct application to both the French and U.S. fractured rock programs, studies of the hydromechanical behavior of fractures will be conducted utilizing laboratory measurements and theoretical models.

Natural Analog Studies

Investigation of Natural Analogs for Flow and Transport. Natural analog sites allow investigation of features and processes likely to be encountered at a repository site.

Cooperative Studies on the Oklo-A Natural Nuclear Waste Repository. The Oklo site is the only natural analog of nuclear waste disposal with long-term data. We can use our study of this site to develop confidence in the feasibility studies of safe geologic disposal and ensure that all relevant processes are included.

Clearly, much of this work requires further support in both countries. We hope that some of the more important projects can be identified and jointly funded and supported by the appropriate U.S. and French agencies. Proposals and summaries are being prepared and will be disseminated among scientists and government agencies within the nuclear waste disposal community.

Characterization and Monitoring of Subsurface Biologic Activity Using Stable Isotope Soil Gas Analysis

Principal Investigators: Donald De Paolo, Mark Conrad, Terrence Leighton, and Bob Buchanan

Project No.: 94003

Funding: $82,400 (FY 95)
$78,400 (FY 94)

Project Description

In situ bioremediation of petroleum hydrocarbon contaminants is one of the most promising new technologies for environmental restoration. It provides an attractive alternative to costly "pump and treat" or "burn and bury" techniques that are currently employed to remove hydrocarbons from contaminated groundwater and soils. However, there are significant difficulties associated with monitoring and optimizing *in situ* bioremediation efforts. The only techniques currently available for this purpose involve analyzing the effects of subsurface biologic activity in samples collected from bore holes. The disadvantages of drilling as a means to monitor bioremediation include high cost and site perturbation. In addition, subsurface heterogeneity can significantly compromise the accuracy of bore-hole data.

Measurements of changes in the levels of microbial byproducts in soil gas and groundwater samples present a potential method for monitoring *in situ* bacterial activity. Bacterial degradation of petroleum hydrocarbons results in the production of compounds such as CO_2 in soil gases and dissolved inorganic carbon compounds (DIC) in groundwater. There are, however, other sources for these compounds besides subsurface bacterial activity (e.g., root respiration, dissolution of soil carbonates, atmospheric contamination). In addition, bacteria have other substrates to choose from besides contaminants (e.g., soil organic matter). In order to identify the sources

of these metabolic byproducts, we use measurements of the isotopic compositions of the byproducts. For many of the microbial byproducts, there are large differences in the isotopic compositions of compounds produced from bacterial degradation of hydrocarbons and those produced from other substrates, such as soil organic matter. In several studies, changes in the stable isotope ratios of soil gas CO_2 and groundwater DIC have been cited as evidence of intrinsic biodegradation of hydrocarbons. When complemented with measurements of the ^{14}C concentrations in carbon compounds, this method presents a promising way of identifying and quantifying *in situ* levels of subsurface microbial activity.

The utility of stable isotope data is limited, however, by a lack of knowledge about the effects of bacterial metabolic activity on the stable isotopic compositions of substrates and byproducts. Most physical, chemical, or biologic processes cause shifts in the isotopic compositions of the materials. As noted above, there is a complex mix of processes occurring in subsurface systems (see Fig. 1). The $^{13}C/^{12}C$ ratios of CO_2 produced (or consumed) by these processes are related to the isotopic composition of the source by a fractionation factor. The magnitudes of these fractionation factors for processes such as carbonate dissolution or plant respiration have been carefully determined by researchers working in other fields (e.g., botany, oceanography). The importance of bacterial processes in natural systems has only recently been realized, and, as a result, very little work has been done in this area.

Accomplishments

Our research has concentrated on two topics; (1) demonstrating the applicability of isotope monitoring at sites contaminated with hydrocarbon compounds, and (2) quantifying the isotopic fractionation effects of bacterial metabolic activity. For the first part, we conducted a field study at a former gas station site at the Naval Air Station at Alameda, California (ANAS). A leaking underground storage tank at the site resulted in shallow gasoline contamination. Figure 1 is a schematic diagram outlining the potential sources and sinks of soil gas CO_2 and groundwater DIC at the site. Using a combination of stable carbon isotope and radiocarbon measurements, we were able to demonstrate that intrinsic bioremediation at the site was effectively preventing migration of volatile organic carbon compounds to the surface.
For the second part of our research, we have been conducting a series of culture experiments, growing bacteria on carbon substrates with known isotopic compositions.

We started by studying aerobic degradation of glucose by two well-characterized soil bacteria. The first, *Bacillus subtilis*, is a Gram positive bacterium that has a demonstrated ability to remove heavy metal contaminants, such as selenium, from solution. The second bacterium, *Psuedomonas putida*, is Gram negative and is capable of degrading a wide variety of hydrocarbon compounds. Both bacteria initially produced CO_2 depleted in ^{13}C relative to the original substrate. For *Bacillus*, the $\delta^{13}C$ value CO_2 was about 3‰ lower than the $\delta^{13}C$ value of the glucose substrate. As the number of cells increased during log phase, the $\delta^{13}C$ values of the CO_2 became progressively lower, representing a strongly fractionating process associated with vegetative growth. Once the cultures entered the stationary phase, the trend reversed and the $\delta^{13}C$ value of the CO_2 became higher as the glucose remaining in the culture became enriched in ^{13}C. The initial carbon isotope ratios of CO_2 produced by *Psuedomonas* were about 6‰ lower than that of the substrate. As biomass accumulated during log phase, the $^{13}C/^{13}C$ ratios of the CO_2 increased rapidly. Unlike *Bacillus*, however, there was no obvious change in the magnitude of carbon isotopic fractionation by *Psuedomonas* when it shifted metabolic mode from log to stationary phase. The results of these experiments suggest that it may be possible to use changes in the carbon isotopic compositions of soil gas CO_2 to recognize changes in the metabolic mode of different types of soil bacteria capable of degrading different kinds of pollutants.

As the next step in our experiments, we have begun growing cultures of *Psuedomonas* on butyrate, an analog for petroleum hydrocarbon compounds. The initial results of these experiments indicate that the degree of fractionation for butyrate is much less than for glucose (1–2 per mil). We are now expanding this work to measure fractionation effects resulting from biodegradation of other organic compounds found in petroleum products.

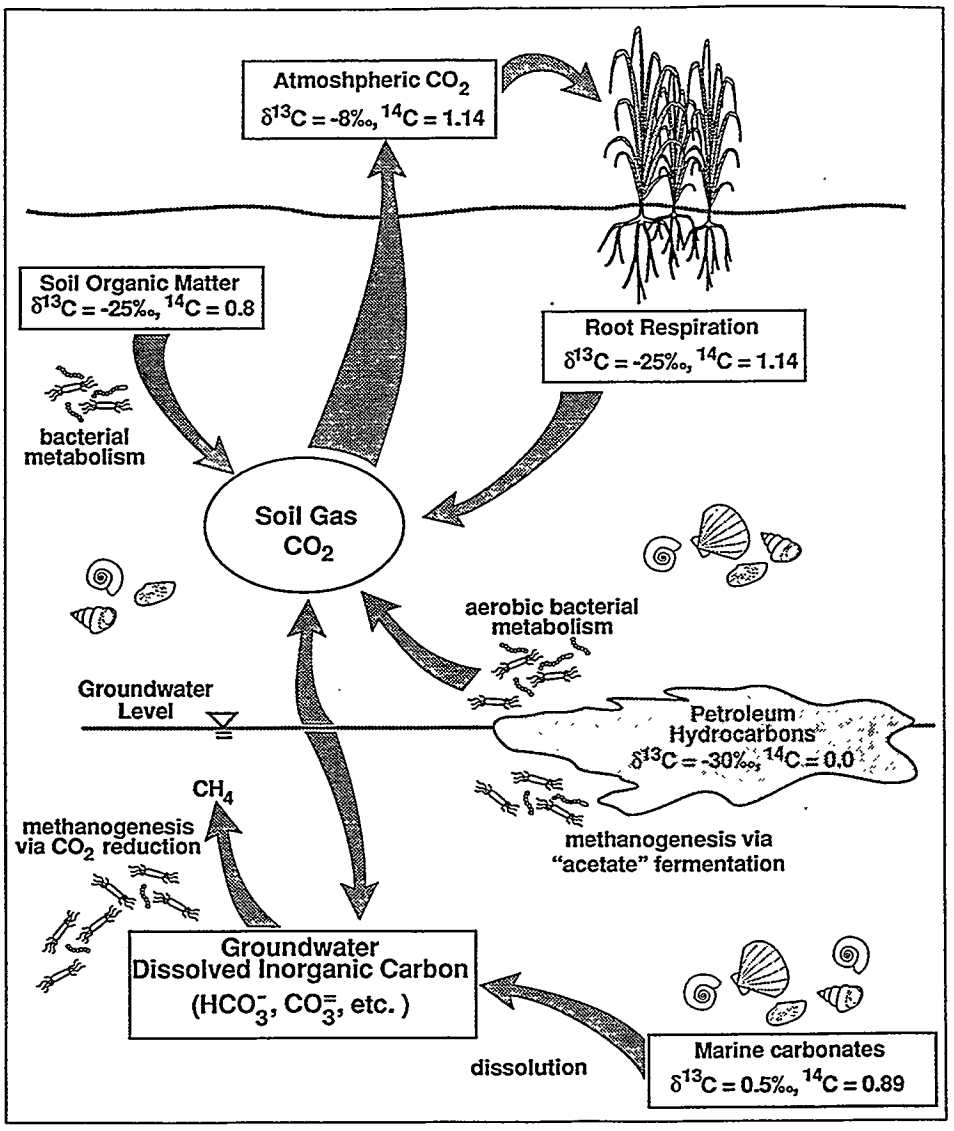

Figure 1. Schematic diagram showing potential sources and sinks of carbon at Site 7C at ANAS. Also shown are the approximate $\delta^{13}C$ and ^{14}C values of different carbon sources at the site.

Publications

M.E. Conrad, T. Leighton, and B.B. Buchanan, "Carbon Isotope Fractionation by *Bacillus subtilis*," *Geol. Soc. of Am. Abstracts with Programs* 26(7), A-510 (1994).

M.E. Conrad, P.F. Daley, M.F. Fischer, B.B. Buchanan, and T. Leighton, "Carbon Isotope Evidence for Subsurface Bacterial Activity at the Naval Air Station, Alameda, California," *EOS, Trans., Am. Geophys. Union* 76(17), S119 (1995).

M.E. Conrad, P.F. Daley, M.F. Fischer, B.B. Buchanan, T. Leighton, and M. Kashgarian, "Carbon Isotope Evidence for Intrinsic Bioremediation of Petroleum Hydrocarbons," submitted to *Nature* (1995).

M.E. Conrad, T. Leighton, B.B. Buchanan, and D. Carlson, "Fractionation of Carbon Isotopes by Bacteria During Aerobic Metabolism," in preparation.

Soil Carbonate Sorptive Properties for Trace Elements: Advanced Methods in Determination of Microscopic and Molecular Level Associations

Principal Investigators: Harvey E. Doner, Mavrik Zavarin, and Tetsu K. Tokunaga

Project No.: 94002

Funding: $36,400 (FY 95)
$17,800 (FY 94)

Project Description

The two main goals of this research are (1) developing a better understanding of the role of soil carbonates in controlling mobility of trace elements, and (2) to develop standardized methods for conducting and interpreting synchrotron x-ray fluorescence microprobe experiments involving soils. Current limitations in understanding transport of trace elements such as Ni, As, Se, and Sr in carbonate soils are in part due to lack of information of spatial distributions with sufficiently high spatial resolution. Previously observed elevated concentrations of some potentially toxic trace elements in certain carbonate formations indicate the need to understand the environmental conditions controlling their accumulation as well as their possible release. The synchrotron x-ray fluorescence microprobe is especially well suited for such research since it permits elemental mapping with exceptionally high spatial resolution on essentially undisturbed samples. The x-ray microprobe at the Advanced Light Source is ideal for studies of Ni, Cr, and other trace element accumulation in carbonates since it offers an exceptionally favorable combination of spatial resolution and detection limits. Application of this tool to research in soil systems requires further methods development as these media tend to exhibit extreme variations in mineralogical composition and mass density over very short distances.

The ALS microprobe as well as the National Synchrotron Light Source (NSLS) microprobe were used to determine trace element (Ni, Se, Sr, and As) distributions within calcite nodules from the Panoche Creek area (California). Extended X-ray Absorption Fine Structure (EXAFS) was performed on both natural and synthetic trace metal accumulated carbonates. Supplemental chemical analyses were performed to obtain information on distributions of organic matter, clay, and other minerals. Laboratory experiments were performed to study trace element partitioning into carbonates under controlled conditions. Additional research was conducted to systematically characterize the influence of soil particle-size distribution and localized variation in soil mineralogy on x-ray microprobe fluorescence spectra. These latter studies were conducted on natural soil and fine-grained natural calcite in which heterogeneities in these parameters are well defined.

Accomplishments

Wet-Chemical Studies of Equilibrium State of Soils from Panoche Creek

Soils are often thought to be supersaturated with respect to calcite; it has been argued that this is a function of Ca-silicate solubility control, carbonate surface poisoning, and organic matter coatings on carbonates. An experiment was set up to determine whether the Panoche Creek soils are generally supersaturated with respect to calcite. We found that much of the soil is highly supersaturated with respect to both calcite and barite. These results point to two hypotheses for explaining how the solubility effect may be indicative of varied sorptive behavior: (1) molecular level surface structure of natural carbonates tends to increase mineral solubility relative to synthetic calcite, and this structural ordering influences sorptive properties; and (2) known equilibrium constants do not fully describe speciation in soil solutions while sorptive properties of synthetic and soil carbonates are equivalent. Future sorption studies on natural carbonates will help elucidate the significance of the apparent supersaturation of soils with respect to calcite and determine its effect on trace metal sorption.

Laboratory Analysis of Factors Affecting Trace Element Coprecipitation

The rate of selenite incorporation as a function of calcite precipitation rate was examined with the use of constant pH/constant supersaturation state apparatus. Results indicate that calcite removes extensive amounts of selenite from solution. Additionally, the relative amount of selenite incorporation was found to increase as the precipitation rate increased. This indicates that two types of incorporation may exist: site-specific selenite coprecipitation and disordered incorporation. EXAFS analysis of the same samples was performed and results are described in section D below.

Modeling X-ray Behavior in Heterogeneous Systems

Experiments were performed to account for sample heterogeneity when determining the concentration of trace elements in heterogeneous systems. The initial experiments were set up to understand the effect of heterogeneity on trace-element fluorescence. Figure 2(a) shows the side view of constructed samples used to test the effect of depth on fluorescence yield from a constant concentration of trace element. Figure 2(b) presents results from the Cu-deposited calcite wedge; the sample was scanned from the thin end (~ 0 microns, left side) to the thick end (~ 200 microns, right side). The relative fluorescence of Ca, Fe, and Cu is shown; Fe is relatively homogeneously distributed in the calcite. The relative fluorescence of copper decreases by two orders of magnitude over the 200-μm-calcite-thickness range. Clearly, quantitative analysis would be strongly affected by heterogeneity in the sample. Note, on the other hand, that there is a very strong change in the relative fluorescence between the Cu-Kα and Cu-Kβ intensities as the thickness of overlaid calcite increases. This is more clearly shown by looking at the ratio of Cu-Kα and Cu-Kβ fluorescence (Fig. 2[c]). The thickness of calcite can decrease the relative intensity of the Cu-Kα peak more than the Cu-Kβ peak because the mass absorption of calcite at those two energies is different. This effect is potentially useful for determining heterogeneity effects in natural samples and may provide a method for quantitative analysis of heterogeneous system by Synchrotron X-ray Fluorescence Microprobe (SXRFM) methods.

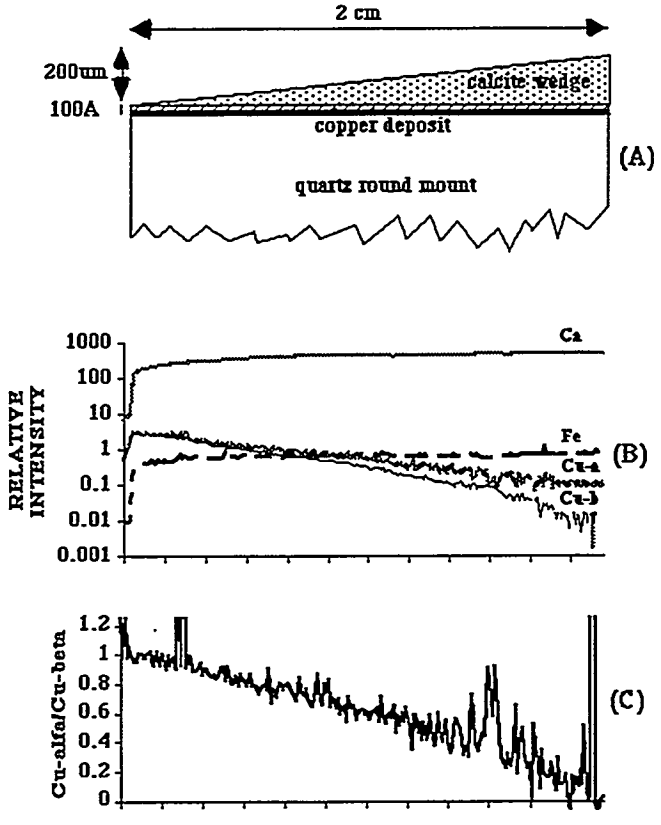

Figure 2. Modeling x-ray behavior in heterogeneous systems.

Extended X-ray Absorption Fine Structure (EXAFS) Studies of Synthetic Sorption Samples and Natural Carbonates

EXAFS of coprecipitated SeO_3^{2-} samples described in section B were analyzed to determine if precipitation rates altered the configuration of selenite in the calcite system. Figure 3 shows the Fourier transforms of these samples as well as those of sorbed SeO_3^{2-} and sorbed SeO_4^{2-}. (It is important to note that these transforms were not corrected for phase shift; the distances, therefore, cannot be related to real bond distances at this time.) Selenite coprecipitated at the lowest rate (Fig. 3, line A) has peaks at 1.4, 3.2, 3.8, and 5.1 Å. The peak at 1.4 is clearly due to the Se–O bond in selenite. The peaks at 3.2 and 3.8 are most likely second-shell bond distances, which may be Se–Se, Se–Ca, Se–C, or Se–O. The peak at 5.1 is most likely a scattering peak which cannot be deconvoluted to give bond distance information but can be used as a characteristic scattering peak. The Fourier transform of the high precipitation rate sample (Fig. 3, line B) indicates that at this rate, most of the structure beyond the first shell is lost. The Fourier transform of sorbed selenite

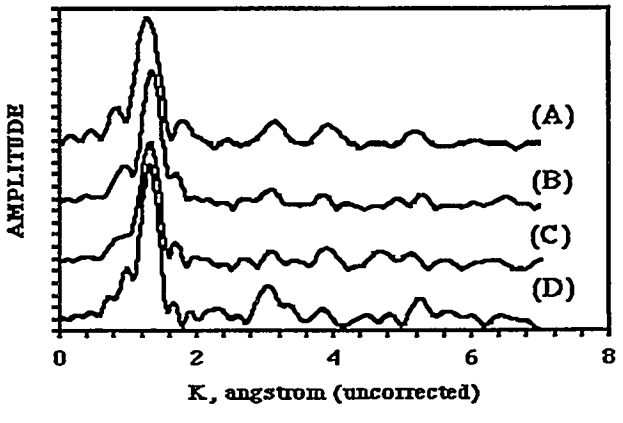

Figure 3. EXAFS studies of selenium sorbed to synthetic calcite.

(Fig. 3, line C) shows peaks at 3.2 and 3.8 Å. These distances are equivalent to those found in the slow precipitation rate sample, although they have a reduced amplitude. This suggests that the structure around sorbed and coprecipitated selenite is similar. Sorption of selenate on calcite (Fig. 3, line D) shows only a single distance for the second nearest neighbor at 3.1 Å. This would indicate that selenate sorption on calcite may be inner sphere, as is selenite, although the structural ordering of the two oxidation states is clearly different.

Ni EXAFS of natural carbonate and parent rock from the Panoche Creek soil were run. The technique shows promise in its use for identifying the coordination of trace elements in natural samples. From a preliminary analysis of the Ni EXAFS, we find that there is little difference between the apparent structure of Ni in the parent rock versus the carbonate. This would indicate that the high Ni concentration in the carbonates may be due to the preservation of parent nickel by occlusion rather than by dissolution and coprecipitation with calcite.

We wish to thank the many people involved in this research project. Tim Teague and John Donovan of the Geology and Geophysics Department, UC Berkeley, helped with running the electron microprobe, preparing thin sections, and preparing calcite wedges. Hau-Wai Wong conducted most of the solubility studies. Karen Chapman and Al Thompson of the ALS, Berkeley Lab, and Patt Nuessle of the NSLS, Brookhaven, helped set up SXRFM scans. We wish to especially thank Andrea Foster, as well as others in the Dr. Gordon E. Brown Jr. research group, for assistance in running our first samples at SSRL and assistance with the EXAFSPAK and FEFF software.

Publications

H.E. Doner and M. Zavarin, "The Role of Soil Carbonates in Trace and Minor Element Chemistry," submitted to *Adv. in Geoecol.*

M. Zavarin, and H.E. Doner, "Sorptive Properties of Soil Carbonates Relative to Synthetic Carbonates and the Factors which Influence Their Dissimilarities," presented at the SSSA Conference, St. Louis, Missouri, Oct. 29–Nov. 2, 1995.

M. Zavarin and H.E. Doner, "Sorptive Properties of Trace Elements for Ni, Se, and Mn: X-ray Absorption Studies," presented at the NCR-174 Meeting, Berkeley Laboratory, Berkeley, California, June 24–26, 1995.

M. Zavarin and H.E. Doner, "The Role of Soil Carbonates in the Retention of Ni and Se," presented at the Third International Conference on the Biogeochemistry of Trace Elements, Paris, May 15–19, 1995.

Laboratory Studies of Microbial Transformation of Diesel Fuel in a Transient Subsurface Environment

Principal Investigators: Hoi-Ying Holman and Yvonne W. Tsang

Project No.: 94004

Funding: $115,300 (FY 95)
$99,500 (FY 94)

Project Description

This experimental study is a continuation of the ongoing microcosm studies on the intrinsic biodegradation of petroleum hydrocarbons in the vadose zone under a transient environment. The study was motivated by the fact that the success of enhanced biodegradation processes observed in the laboratory was seldom transferred to field-scale operation. This discrepancy partly arises from the inherent gaps between fundamental/applied microbiological research and the engineering application. More importantly, however, the discrepancy may be attributed to the fact that laboratory studies are usually performed in an experimental environment that is highly idealistic, and not representative of the transient field conditions encountered by microorganisms in nature. One of the most important transient environmental parameters in the vadose zone is the fluctuation of aeration status and the soil moisture content, which are associated with the rainfall infiltration and the rise and fall of groundwater tables. The purpose of this work is to test the hypothesis that intrinsic biodegradation of petroleum hydrocarbons in the vadose zone can be significantly altered by the rise and fall of the water table.

Accomplishments

The project was designed to measure the change of biodegradation of diesel fuel in a soil that undergoes

the rise and fall of the water table. This study consisted of a series of microcosm experiments conducted inside partially saturated soil columns equipped with sampling ports. The water level inside each column was controlled by a custom-designed flow system.

Background groundwater from a diesel-fuel-contaminated site was collected and filtered through an activated charcoal cartridge and a 0.2-μ sterile filter. This treated water was further phosphate-buffered to pH 7.3 and stored at 4°C until use. Background soil from the same site was collected aseptically about four feet below the ground surface, air dried, and passed through a 1.7-mm sieve. To represent a highly polluted soil, 72 ml of sterile, nonlabeled diesel oil was first injected into 720 grams of air-dried soil inside an airtight bag, mixed well, and kept in the dark at 21°C for six months. At the end of the this time, microcosms were prepared by packing 40 grams of the acclimated soil into each glass cylinder. The cylinders were equipped with sampling ports.

To quantify the kinetics of mineralization of these model compounds, ^{14}C-labeled substrates were used. For simplicity, only five labeled compounds were used to represent different biodegradable hydrocarbon groups in the diesel fuel. They are: (1) *n*-[1-^{14}C]hexadecane, representing the long-chain aliphatic components; (2) [1-^{14}C]naphthalene, the volatile, slightly water-soluble diaromatic components; (3) [9-^{14}C]phenanthrene, the slightly water-soluble nonvolatile polyaromatic components; (4) [*side ring*-^{14}C]anthracene, the almost water-insoluble nonvolatile polyaromatic components; and (5) [4,5,9,10-^{14}C]pyrene, the water-insoluble nonvolatile polyaromatic components. These radioactive chemicals were mixed individually into diesel oil in nanomolar amounts. The $^{14}CO_2$ produced and released by soil microbes was sampled periodically through the sampling ports and counted by a liquid scintillation counter.

Three types of column microcosms were constructed for each model compound: one represented the abiotic degradation, and the other two represented the biotic degradation process. A total of fifteen column microcosms were monitored in this study.

We demonstrated that the $^{14}CO_2$ measurements show the biodegradation process can be accelerated by the rise and fall of the water table. This is established by the following observations. At a given water level, the time course of cumulative $^{14}CO_2$ production increased initially and plateaued after about six weeks. A change of the water level caused the $^{14}CO_2$ production to increase with time again. However, not all five groups of the hydrocarbons studied display this kind of behavior. For the volatile, slightly water-soluble diaromatic components (e.g., naphthalene), the slightly water-soluble nonvolatile polyaromatic components (e.g., phenanthrene), and the almost water-insoluble nonvolatile polyaromatic components (e.g., anthracene), production of $^{14}CO_2$ increased drastically with a change of the water table. For the water-insoluble nonvolatile polyaromatic components (e.g., pyrene) and the long-chain aliphatic components (e.g., *n*-hexadecane), there was no measurable benefit with the change of the water level. Because of the slow kinetics, the time interval between the adjustments of the water table is typically six to eight weeks. To obtain a more complete understanding of the effect of transient environmental factors on the biodegradation process, we are allowing the experiments to continue over several additional cycles of water level variations.

Microbial Transport and Microbial and Nutrient Delivery in Subsurface Environments

Principal Investigator: Jiamin Wan

Project No.: 95005

Funding: $75,100 (FY 95)

Project Description

Efforts towards improving *in situ* biodegradation (both enhanced and intrinsic) of contaminants in soils and groundwaters has received much recent attention. Although *in situ* processes are attractive because of potentially much lower costs, the many uncertainties associated with controlling transport and transformations in heterogeneous subsurface environments have hindered progress. Rate limitations to in-situ bioremediation are typically due to the inability to bring (and sustain) microorganisms, nutrients, and contaminants into sufficiently close proximity for permitting rapid contaminant degradation. Remediation strategies may involve nutrient delivery to stimulate native microbial populations, delivery of preselected microorganisms, and/or displacement of contaminant phases. In all cases, better understanding of basic transport

processes is needed in order to improve the efficiency of field-scale clean-up activities.

The research proposed here is directed towards improving our understanding of these controlling transport processes through various laboratory experiments. The objectives of this study are: (1) to identify the potential importance of sedimentation on bacterial transport in groundwaters, (2) to quantitatively study the dependence of bacterial transport on matric potential and water-film thickness in vadose environments, (3) to explore the possibility of injecting foam to deliver bacteria and nutrients to desired locations for enhancing *in situ* bioremediation, and (4) to develop techniques of visually and quantitatively studying *in situ* microbial behavior from bacteria to porous medium scales. The approaches taken in this research combine visualization with quantification in both glass micromodels and soil columns, which permits systematic evaluation of various mechanisms controlling microbial transport and microbial and nutrient delivery. Mechanisms responsible for microbial transport are studied visually in micromodels subjected to controlling boundary conditions. The observed and measured processes in micromodels are tested in columns at three dimensional and porous medium scales.

Accomplishments

Bacterial Sedimentation Through Porous Medium

Past studies of bacterial transport in groundwaters and to deep aquifers and sediments have either neglected, or regarded as insignificant, the contribution of bacterial sedimentation. In this study, we examined the potential significance of sedimentation as a mechanism for bacterial transport. We developed a model to predict the behavior of particles (bacterial or inorganic colloids) sedimenting through granular porous media under hydrostatic conditions. The conventional assumption of neutral buoyancy of bacteria was demonstrated to be invalid through buoyant density measurements on 25 subsurface bacterial strains. Stokes Law sedimentation velocities for two bacterial strains calculated from our measurements of buoyant densities and characteristic sizes was found to be in good agreement with direct measurements of free sedimentation through water columns. Sedimentation rates through saturated sand columns were consistent with the model developed in this research. Bacterial breakthrough in sand columns by sedimentation exhibited trends consistent with first-order attenuation with distance. The results suggest that if time scales are sufficiently long, spanning many generations, sedimentation can become a significant mechanism for bacterial transport. This research contributes to the field of bacterial transport in both theoretical and practical aspects, and has implications in deep subsurface microbiology, and deep subsurface bacterial origins. Our article "Bacterial Sedimentation Through Porous Medium" was published in *Water Resources Research.*

Unsaturated Straining

Conventional filtration theory is concerned with removal of particulates suspended in a single-fluid phase flowing through a porous medium. Most research in this field has addressed either fully liquid-saturated or essentially gas-saturated systems. In such single-fluid-phase systems, straining is one basic mechanism of filtration which results from trapping of suspended particles at locally restrictive pores within the porous medium. When the characteristic diameter of suspended particles is very small relative to the porous media grains, straining during single-phase flow has been shown to be insignificant. However, in partially water-saturated soils, the air–water interface presents an additional constraint on particle movement. The pore-scale geometry of the aqueous and gas phases needs to be considered in mechanistic analyses of particle (microorganisms and suspended colloids) transport through soils. The microscale visualization and measurement experiments were conducted by using a special micromodel device designed and constructed for this study. Latex microspheres with three different sizes, 1.0, 2.0, and 4.2 μm, were used as idea colloids. Particle straining phenomena were observed as matric potential decreased (more negative pressures) and were video recorded with micrometer spatial resolution. Matric potential (subatmospheric water pressure) was controlled and measured with high resolution (10 Pa) at the micromodel boundaries. Further research is in progress, including using different sized bacterial strains in the microscopic experiments and implementing column studies. We found that even in the limit of ideal hydrophilic particles, unsaturated straining retards transport when water-film thicknesses approach or become less than characteristic particle diameters, regardless of the porous media grain size. We believe this result will be a realistic and significant extension of classical filtration theory to colloid and bacterial transport in partially saturated soils and porous rock.

Innovations in Experimental Technique

Conventional micromodels are typically used for studies of phase displacement in subsurface porous media. In these conventional two-dimensional micromodels, only one fluid can be continuous at the pore scale. No significant three-dimensional pore structure is included that would allow local occupancy by two separate fluid phases. This limitation has prevented conventional micromodels from representing more realistic, complex three-dimensional flow and transport processes. We have developed a new type of micromodel, designed and manufactured to represent more realistic two-phase flows in porous media. The newly developed technique allows two-phase flow to occur down to the pore scale. These new micromodels will also contribute to a wide range of other research activities, such as those aimed at improving petroleum recovery, and those related to contaminant transport and cleanup in subsurface environments. A patent invention disclosure was filed (1162-IB).

Laboratory studies of flow and transport in subsurface fractured rock systems can provide mechanistic insights into larger-scale phenomena that are critical in many areas, such as repositories for high-level nuclear wastes, contaminant migration and cleanup, and improved petroleum recovery. Transparent rock fracture replicas have been used as analogs of natural rock fractures. Previous to the invention to be described next, rock fracture casts have been made with epoxy resin. However, the wettability of rock surfaces is often not well represented by epoxy surfaces. In this study, we developed a new method to fabricate the rock fracture cast with glass. The new glass fracture casts provide wettabilities more representative of many natural fractures. A clean glass fracture surface has zero contact angle, and wettability of the glass fractures can be easily altered with chemicals by using established methods. The new glass casts also provide accurate aperture structure of rock fracture and excellent optical clarity. Therefore, microbial transport, multiphase flow, and transport visualization experiments conducted in glass fracture casts will be more generally relevant to real rock systems. A patent invention disclosure has been filed (1171-IB).

Publications

J. Wan, T.K. Tokunaga, and C.F. Tsang, "Bacterial Sedimentation Through Porous Medium," *Water Resources Research* **31**, 1627–1636 (1995).

J. Wan, and T.K. Tokunaga, "Influences of Matric Potential on Unsaturated Colloid and Bacterial Transport," an abstract to be submitted to the 1996 AGU Spring meeting.

J. Wan, and T.K. Tokunaga, "A New Method for Constructing Glass Micromodels Resulting in a Wide Distribution of Pore Sizes," *Patent Disclosure*, 1162-IB (1995).

J. Wan, T.R. Orr, and J. O'Neill, "Glass Casting of Rock Fractures," *Patent Disclosure*, 1171-IB (1995).

Energy and Environment Division

Toxicity at Mare Island Naval Shipyard

Principal Investigator: Susan L. Anderson

Project No.: 95006

Funding: $78,000 (FY 95)

Project Description

The primary goal of this project is to assess the potential for remediation of contaminated wetland sites at Mare Island Naval Shipyard using toxicity-based methods. This work will advance the application of ecological hazard assessment techniques to the important problems of wetland restoration and military base closures. This effort has established us as lead ecotoxicologists in a UC Davis effort to develop a wetlands research consortium at Mare Island and has helped to establish our credibility for work on a second Navy project at the Alameda Naval Air Station.

Sediment pore-water toxicity tests have been used to rank several wetland sites according to levels of toxicity. Toxicity levels have been confirmed in follow-up surveys. Our research in FY 95 extends this approach to evaluation of the potential of *in situ* toxicity testing to predict hazards at selected sites. Our studies have been coupled with research conducted by ecologists and engineers on other UC campuses. Results of the group effort will be used to determine which sites have the greatest potential for cost-effective and ecologically beneficial remediation. In general, improved integration of ecological and engineering concerns is needed to restore wetlands at decommissioned military bases.

Accomplishments

Our research has helped the Navy team to discern that determining what constitutes a toxic hazard at a specific site is often not intuitive. For example, metals contamination at the highly contaminated "Green Sands" site appears to pose little hazard to sediment-dwelling organisms because the metals do not appear to be biologically available (e.g., no appreciable toxicity was observed). (Fig. 1, GS sites.) These findings have stimulated further intensive studies to determine whether costly restoration activities are appropriate at this site. In contrast, sites that were suggested to us as reference locations on the base (for which little or no toxicity was anticipated) have produced highly toxic responses in a range of test organisms (Fig. 1, PP sites). These results are being used to determine whether these previously unknown hazards should receive priority for restoration. Another important finding was our determination that toxicity in the mitigation pond is attributable to unionized ammonia. This suggests that naturally generated ammonia is a positive interference in these sediment toxicity test results.

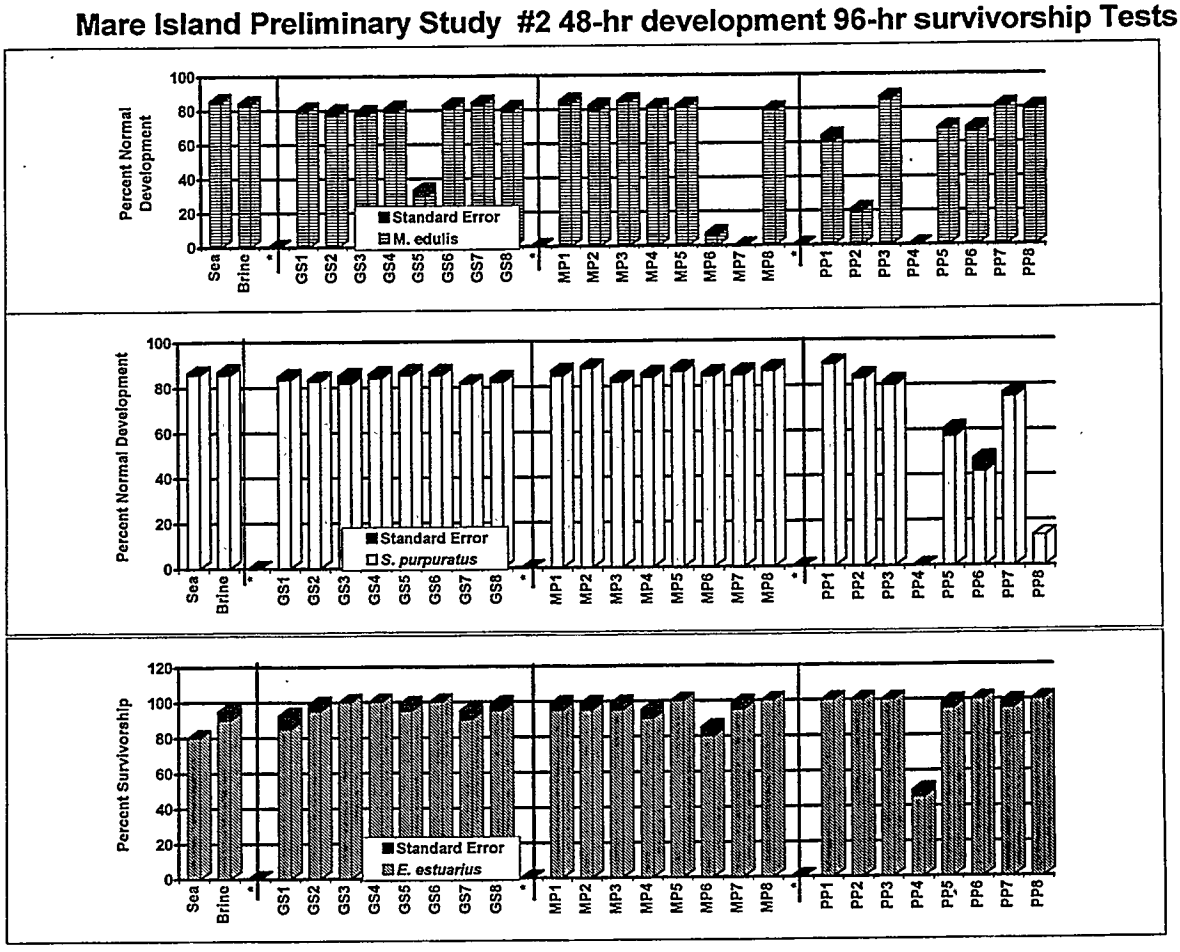

Figure 1. Toxicity in three test species exposed to pore-water samples collected at the Mare Island Naval Shipyard. The three species/lifestages are embryos of the bivalve Mytilus edulis, *embryos of the sea urchin* Strongylocentrotus purpuratus, *and adults of the amphipod* Eohaustorius estuarius. *Eight field replicates are taken at each location, and standard errors are computed for four laboratory replicates for each field replicate. Sites are Pier Pilings (PP), Green Sands (GS), and Mitigation Ponds (MP).*

Broad-Band High-Resolution Microcalorimetry for Biological and Materials Science Applications on the Advanced Light Source

Principal Investigators: Stephen P. Cramer, Jeffrey Beeman, Eugene Haller, Norman Madden (Berkeley Laboratory), Mark Le Gros, and Eric Silver (Smithsonian Astrophysical Observatory)

Project No.: 95007

Funding: $102,900 (FY 95)

Project Description

We propose to investigate a new high-resolution x-ray microcalorimeter for use on the ALS. We will attempt to demonstrate the use of the detector on the ALS and we will perform internal source experiments to demonstrate the advantages of using a microcalorimeter for x-ray spectroscopy. This instrument has potential commercial value, and it will significantly improve the efficiency and sensitivity of a wide range of fundamental and applied science measurements. Potential applications for this device include x-ray magnetic circular dichroism; spin polarized x-ray absorption; and, eventually, table-top EXAFS and medical imaging. Our ultimate goal is to improve the sensitivity of these analytical techniques by at least an order of magnitude. The detector also has potential as an analytical instrument for use on electron microscopes. Based on the results of this feasibility study, we will propose that outside funding agencies support the development of a dedicated microcalorimeter spectrometer for the ALS.

Our approach is to replace the solid-state detectors and crystal or grating spectrographs with a spectrometer that incorporates the best features of both of these detectors. A laboratory version of the microcalorimeter has already been developed with an energy resolution of 18 eV. This resolution has been obtained with a 10–50 Hz input count rate. In principle, 1 eV and kilohertz count rates are possible. We will use this system to perform initial experiments and simultaneously develop a detector system tailored to the needs of the ALS user community.

Accomplishments

The x-ray microcalorimeter is a powerful spectroscopic tool that is destined to revolutionize many fields of x-ray science. This device promises energy resolution of order 1 eV, with unity quantum efficiency over a >20 keV energy bandwidth. A microcalorimeter possesses the energy resolution of a crystal with the stopping power and broad-band response of an ionization detector. During the LDRD funding period, significant advances in our detector performance have occurred; currently an energy resolution of 7 eV FWHM at 6 keV has been demonstrated. This resolution is more than an order of magnitude greater than the best ionization detector.

The high efficiency and resolution of the microcalorimeter enable the detailed study of chemical bonding via measurement of x-ray spectra. Crystal spectrometers have been used for this purpose for many years; however, this technique requires strong sources and long measurement times. A microcalorimeter makes the x-ray chemical analysis of trace quantities of radioactively labeled compounds practical. In an effort to develop experimental techniques that use this new analysis tool, a preliminary radioactive source measurement was performed. We studied the oxidation-state-dependent x-ray spectrum of ^{55}Fe labeled inorganic compounds. The structure of the Mn K x-ray spectrum depends upon the electronic spin state of the iron atom. At the time of the experiments, our detectors exhibited a FWHM 18 eV, and we were unable to clearly resolve the subtle spin-state-dependent differences in the Mn K spectrum. Using our best current detector (see Fig. 2), these differences would be easily observed. This detector is a specialized device developed specifically for chemistry and other ALS applications.

We planned to use the spectrometer built by Drs. Le Gros and Silver to perform experiments on the ALS. Due to scheduling difficulties, this goal was not achieved during the funding cycle. Fortunately, construction of the next generation x-ray spectrometer is ahead of schedule, and in 3 to 4 months the new system should be operational, enabling the continuation of experiments on the ALS. The prototype ALS spectrometer resulting in part from the FY 95 LDRD is an engineering development model operated from a liquid helium bath. Dr. Le Gros will remain at Berkeley Lab during FY 96 in order to complete this instrument.

Outside funding was obtained for the construction of a spectrometer suitable for use on a Scanning Electron Microscope. The funding is administered by the Smithsonian Astrophysical Observatory (SAO) and the focus of the research is the creation of a low-vibration, liquid-helium-free, cryogenic engine for the

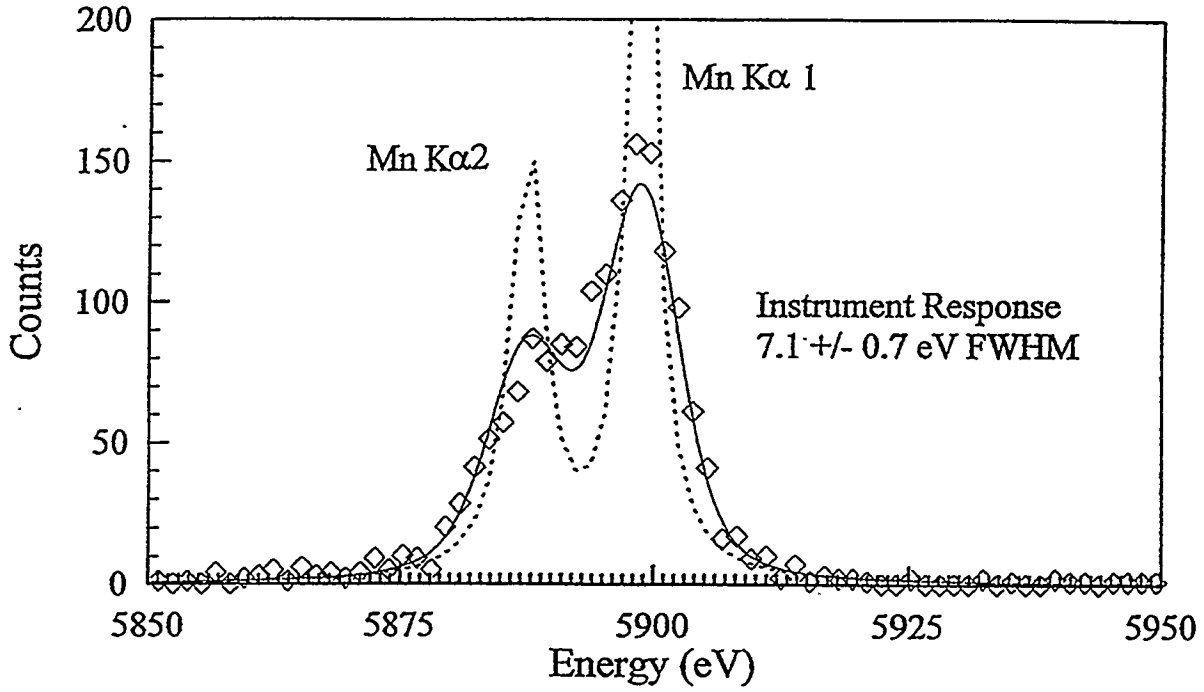

Figure 2. Mn Kα x-ray spectrum showing partial resolution of the Kα 1/Kα 2 doublet.

x-ray microcalorimeter. This development effort will result in a spectrometer that will revolutionize submicron particle analysis, and strongly impact electron microscopy in general. We would have preferred funding for a dedicated ALS spectrometer, but anticipate that continued collaboration with the SAO group will bring about unique experiments on the ALS.

Publication

Le Gros and Silver *et al.* 1995, "Microcalorimeters for Broad-Band X-ray Spectroscopy," submitted to *X-ray Spectrometry* .

Research to Support the Development of Energy-Efficient, Low-Polluting Automobiles

Principal Investigators: M.D. Levine, N. Brown, D. Grether, R. Harley, D. Hopkins, K. Jackson, D. Littlejohn, D. Lucas, M. Madou, F. McLarnon, R. Sawyer, I. Shepherd, H. Stadler, H. Taha, T. Wenzel

Project No.: 95008

Funding: $138,000 (FY 95)

Project Description

The United States has embarked on a major series of efforts to create an automobile with much greater fuel economy and much lower emissions. This project focused on expanding existing laboratory expertise in three critical areas:

- Investigation of new power sources for low-NO_x emitting automobiles
- Creation of microsensors that will be a key component of advanced automobiles
- Analysis of the impact of vehicle technologies on urban air quality

Accomplishments

Low-NO_x Emitting Automobiles

Scientists and regulators are beginning to agree that our worst air quality problems cannot be resolved without achieving significant reductions in NO_x emissions, an ozone precursor. Nationally, on-road vehicles account for over 30% of the total NO_x emissions. We assessed two approaches to advance the development of low-NO_x power sources for electric or hybrid electric vehicles: catalytic combustion turbines and zinc/air batteries. Both approaches have the potential of significant impact in the intermediate term; however, they have had inadequate attention to date.

Our preliminary assessment on the potential for catalytic combustion to serve as a means to reduce NO_x emissions suggests that the technology has the potential to achieve significant success. Additional R&D efforts are needed to establish a convincing proof of concept. We have met with high-level representatives of industry and agencies to promote a national research program on catalytic combustion, and have found considerable interest in the research community and some within the auto industry. We have proposed that a National Academy of Sciences study be initiated to investigate this approach in much greater depth.

Our assessment of zinc/air batteries convinced us of the value of pursuing the concept further. Based on this assessment, we had sufficient information to advance the development of bifunctional air electrodes and to test thin zinc/air battery cells. Additional funding for this work has been approved.

Microsensors for Advanced Automobiles

Sensors are already widely used in today's vehicles. However, we believe that the performance and cost effectiveness of existing sensors could be greatly improved by making them much smaller. This can be done by microfabrication (or micromachining), a process that uses batch-type, thin-film deposition techniques originally developed to manufacture electronic integrated circuits. At present, micromachined sensors are used in automobiles for controlling airbag release and as pressure sensors for various applications. Micromachining these sensors has led to dramatic reductions in production costs. Berkeley Lab's Center for X-ray Optics has developed a processing capability well suited to fabricating such sensors. The basis of the capability is a technology that combines deep x-ray lithography, microelectroplating, and molding processes. Sensors and microstructures fabricated by this process can have lateral dimensions as small as 10 micrometers, vertical dimensions less than one millimeter, and submicron tolerances.

We have performed a detailed assessment of the role that different microsensors can play in automobiles. The project has prepared an extensive report on the topic, which includes an assessment of the opportunities for Berkeley Lab to develop specific microsensors for application in the next generation of automobiles. The assessment (1) identified major opportunities for automotive microsensors and microactuators; (2) ranked their impact on fuel economy or their effectiveness in measuring emissions; and (3) proposed the best micromachining approach for the highest ranking sensors. Two especially promising opportunities for the Laboratory are developing microsensors that measure exhaust gas concentrations and measure mass air flow.

Impact of Vehicle Technologies on Urban Air Quality

In the third area, we focused on improving the scientific understanding of the level and sources of

emissions from current vehicle technologies. Better understanding of the emissions characteristics of current technologies will allow accurate evaluation of the impact of new automotive technologies on air quality.

We have made four major accomplishments in this area over the past year:

- We analyzed data measured by remote sensing devices to better understand the emissions from malfunctioning vehicles as they are driven in actual use. Our analysis indicates that the malfunction probability of emission control systems in relatively new (2- to 5-year-old) vehicles is strongly dependent on vehicle model. This result has very interesting implications for emission control policy.
- We used tunnel and roadside monitors to measure real-world emission levels of nitrous acid (an ozone precursor) and nitrous oxide (a greenhouse gas).
- We reviewed the literature on emissions from small engines likely to be used in hybrid electric vehicles.
- We continued to upgrade our capabilities to perform air quality analyses of the LA Basin, as well as performed simulations of the Basin.

Publications

M. Ross, R. Goodwin, R. Watkins, M. Wang, T. Wenzel, "Real-World Emissions from Model Year 1993, 2000, and 2010 Passenger Cars," to be published as LBL-37977.

M. Ross and T. Wenzel, "Real-World Emissions from Conventional Cars: MY1993 and MY2010," to be published in *Is Technology Enough? Sustainable Transportation-Energy Strategies*, American Council for an Energy-Efficient Economy.

T. Wenzel and M. Ross, "Emissions from Modern Passenger Cars with Malfunctioning Emissions Controls," to be published as SAE 960067, Society of Automotive Engineers.

M. Madou, "Sensor and Micromachining Needs in Transportation—LBL's Role," *Microfabrication Applications*, Palo Alto, California (1995).

Building Performance Assurance

Principal Investigator: Stephen E. Selkowitz

Project No.: 95009

Funding: $369,800 (FY 95)

Project Description

Despite significant advances in building technology and the promulgation of tighter building standards, buildings still consume one third of all U.S. energy, at a cost of $200 billion per year, with $85 billion used in commercial buildings. Half of this is very likely wasted, compared to what could be achieved. The goal of this project is to explore the technical underpinnings of a new approach to intervening in the life cycle of buildings so as to make them more resource efficient. The long-term goal is not only to capture the wasted energy in the commercial building sector, but to provide even greater financial savings for building owners by improving comfort and productivity in conjunction with energy-related workplace improvements.

In any construction or retrofit cycle of a building, there are four major stages: design, build, commission, and operate. The information needs and decision-making process at each stage are different, and there is typically a fundamental disconnect in the flow of information between each of these stages. Information that is generated at one life-cycle stage is either not available in an appropriate form for decision making at the next stage and thus must be recreated at great cost, or is translated imperfectly between decision makers and phases in a way that increases the likelihood of errors. We expect to be able to create new information management systems and tools for assessing and tracking building performance so that these bottlenecks and losses can be avoided and the benefits of an integrated, life-cycle, cradle-to-cradle approach can be captured.

Our activities are proceeding along three parallel tracks. First, we will use our understanding of building physics and decision-making needs and the Berkeley Lab's computer science and information systems expertise to develop the conceptual framework for a life-cycle information system. This information

system, which is a representation of the decision-making process, the physical building elements, and all their performance attributes over time, must accommodate the needs of many different simulation tools and many different users. It must be sufficiently robust to accommodate growth and expansion and the inevitable changes over time in computer hardware and software. Second, we will demonstrate the specific benefits of using such an approach by developing several new tools and building assessment procedures that utilize the new information system, capture new data from the building, and add value for the building owners and occupants (for example, by tuning building performance in the commissioning phase and tracking performance over time). We expect this work to take place in an occupied testbed building and involve investigations of sensor needs and data-acquisition systems. Finally, we will develop partnerships with key building industry actors for continuation of our research and implementation efforts.

Accomplishments

We have completed several important steps in realizing the vision outlined in our original proposal. We have refined our overall vision of building performance assurance over the building life cycle and have generated considerable interest in this approach among several potential sponsors (e.g., DOE, utilities, and manufacturers). As a vehicle for explaining and testing our concepts and approaches, we have developed a computer based mock-up that incorporates working portions of the new tools we have developed and mock-ups of other yet-to-be-developed capabilities. We have had extensive discussions and visits with a number of organizations that have become involved in the project. We have explored the functional requirements and developed some initial specifications for the Building Life-Cycle Information System (BLISS) envisioned as the centerpiece of our effort. In a related effort, we are working with an industry consortium (the Industry Alliance for Interoperability), which we expect will build an object-oriented software framework that we will incorporate into our BLISS model. Moving to the experimental arena, we arranged access to Soda Hall, the new EECS building on the UC campus, and set up an instrumentation and data-collection system that is focused on the performance of the building's chiller system. We have developed a chiller commissioning procedure and supporting software tools that will verify the detailed energy performance of the chiller system and update the BLISS chiller model. As we move from the commissioning phase to ongoing building operations, a new performance tracking tool has been developed. This tool allows a portion of the collected data (1.5 GB per month) to be sorted, analyzed, and visualized so that key performance metrics can be extracted and compared to expected values. A powerful software emulation tool has also been created and calibrated against the measured performance data. (See Fig. 3.) Using data visualization techniques to compare simulation results from the emulation tool to measured chiller performance data, we are able to compare energy performance against expectations. With this emulator, the energy benefits of new control strategies can be investigated and tested before they are implemented in the building. Ultimately, this will provide the capability for model-based diagnostics and control.

Although our focus has been to develop and test these approaches on a single building, the ultimate challenge is to apply these techniques to a large percentage of the nation's buildings. Many of these buildings are too small to justify the cost of individual on-site engineering expertise. We have developed a concept for Remote Building Operations and Management, which involves linking local building energy management systems to a central data archive and analysis center, using the Internet and a distributed computer architecture with wide bandwidth and security features. Development of this concept, which is a direct outgrowth of this project, has been funded for FY 96 by the DOE Office of Scientific Computing. We have also attracted some support from industrial participants, who are now actively exploring how they can expand and later implement elements of this project.

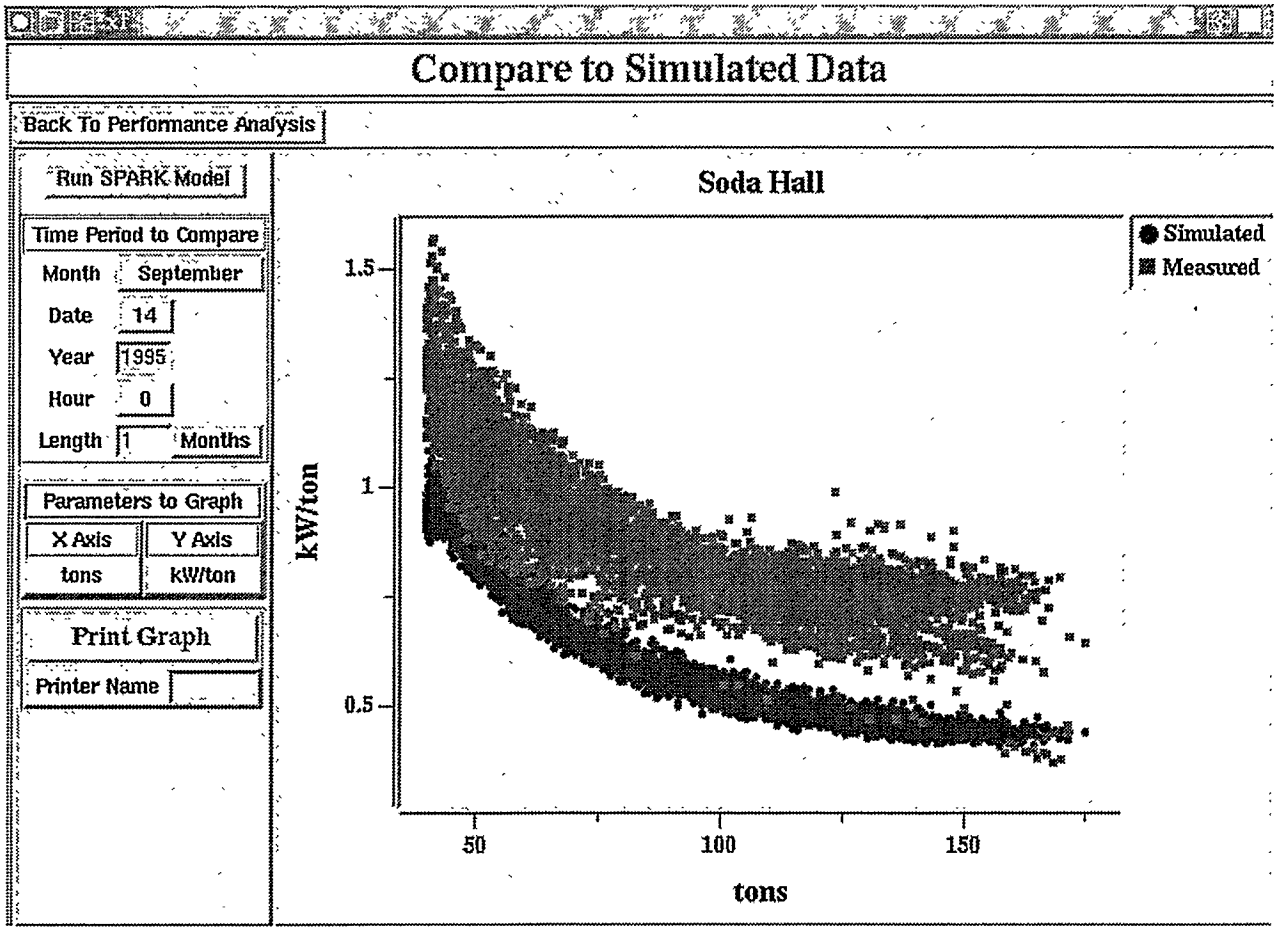

Figure 3. Screen from the new Chiller Performance Tracker. The efficiency of the chiller (in power per ton of delivered cooling, kW/ton) is reported over a range of load conditions (tons of cooling required). Measured data over a one-month period (upper band of light gray points) are compared to a software emulation of the chiller (lower band of darker points) under the same operating conditions. The discrepancy between the curves (less efficient performance than predicted) suggests that the chiller system needs refurbishment. This type of model-based chiller system tracker can also be used for optimization studies in the future.

Engineering Division

Development of Microchemical Methods for Biological Assays

Principal Investigators: Joseph M. Jaklevic and Jocelyn C. Schultz

Project No.: 93008

Funding: $69,400 (FY 95)
$94,700 (FY 94)
$46,900 (FY 93)

Project Description

The aim of this project is to develop methods for performing biochemical procedures in sub-microliter quantities arrayed in multiple reaction cells, and to develop a high-speed DNA sequencer based on the use of ultrathin (50–150 μm) slab gels. The result of such a program will be the ability to perform biochemical assays in large numbers at reduced costs and/or at faster rates. The methods will have applications in emerging biotechnological areas such as genome sequencing and large-scale clinical assays.

To miniaturize biochemical procedures, large arrays of small-area reaction cells can be fabricated using standard photolithographic nanofabrication methods. Successive masking and processing steps can be used to create physical wells in an appropriate substrate or, alternatively, a patterned surface treatment can be used to create hydrophobic barriers around individual reaction cells. Dispensing in nanoliter quantities can be achieved with droplet-on-demand ink-jet dispensers. Our work to date has focused on developing these dispensers for our applications.

Using ultrathin polyacrylamide gels in automated fluorescence sequencers is a means to greatly speed up DNA sequencing through miniaturization. The efficiency of heat transfer in ultrathin gels (50–150 μm) permits the use of electric fields larger than those used in standard thickness (0.35–0.5 mm) electrophoresis gels, and thus DNA separation speeds can be increased ~ 8 times. In our system, a 488 nm laser beam passes transversely through the width of the gel to excite all of the DNA lanes simultaneously. A linear array of lenses and fiber optics collects the fluorescence from the excited chromophore attached to the DNA fragments. A cooled charge-coupled device (CCD) solid-state array detects the light. A similar system is being developed in our group for use with standard-thickness gels. The high-spatial resolution of this fiber optic detector offers the possibility of densely spacing the DNA lanes across the width of the gel, thus maximizing the number of samples that can be run at one time. The eventual coupling of the thin-gel format to microfabricated arrays for preprocessing of the DNA templates could constitute a significant improvement in sequencing technology.

Accomplishments

Sub-Microliter Dispenser

A droplet-on-demand ink-jet dispenser was designed, built, and tested. In order to optimize and quantify the dispenser's performance, an apparatus was assembled that allowed strobed microscopic viewing of the droplet stream (typically at 250 Hz). Droplets of 0.4 nl volume (90 μm diameter) with a velocity of 3 m/s could be dispensed with a 50 V pulse, and the dispenser could operate consistently for more than an hour. The droplets shot out at least 15 mm from the dispenser orifice in a straight path. It was also verified that the dispenser could reliably generate single droplets on demand.

Ultrathin Slab Gels for High-Speed, Automated DNA Sequencing

A complete automated fluorescent sequencer based on an ultrathin gel format was assembled. This apparatus includes optics that direct the laser beam; Berkeley Lab-built water-cooled gel frame and electrophoresis cell; a linear lens array that images the fluorescent light onto a Berkeley Lab-built fiber optic array; the optics necessary to image the other end of the fiber optic array on the cooled charge-coupled device camera; and a computer to collect, store, and process the camera images. A compact arrangement of two prisms and a mirror, placed after the last focusing lens, allows us to precisely adjust the position of the laser beam through a window at the side of the gel plates and into the gap between the plates.

This year a second generation water-cooled gel frame and electrophoresis cell was designed and built. The improvements in design allow us to much more reliably attain both high laser transmission through the window into the gel as well as excellent gel and liquid sealing. The latter are important for the formation and maintenance of good gel quality and the prevention of electrical shorts to ground at the high voltages applied. Also this year, a much improved positioner for the linear array of lenses and fiber optics was designed and built. This allows us to more readily and precisely adjust the position of the array over the fluorescent light.

Experiments to date have been carried out at 100 V/cm on a 100-μm thick gel. This is approximately twice the field under which the standard 0.35-mm-thick gel can be run. The sequencing therefore occurs twice as fast on the ultrathin system under these conditions than with standard thickness gels. Furthermore, the quality of the data is comparable for the two systems under these conditions. However, since the ultrathin gel frame is only half the width, and therefore can accommodate only half the number of samples as the standard thickness gel frame, the throughput of each of the two systems under these two sets of conditions is equal. In the future, higher fields, using either the 100-μm thick or thinner gels and different gel compositions, will be investigated and are expected to increase the throughput of the ultrathin gel system.

The majority of experiments to date have focused on optimizing the sample loading process of the ultrathin gel system. Standard-thickness gel frames are typically held vertically and loaded by inserting a syringe needle into the sample well between the two glass plates comprising the gel frame. The ultrathin gel frame is positioned horizontally, and the DNA sample is injected into a slot perpendicular to the plane of the gel. Originally, the sample wells were formed out of the polyacrylamide gel matrix, as they are in the standard-thickness slab gel. Due to concern that the DNA was adhering to the walls of the sample well and the difficulties in seeing these wells during the loading process, we have tried machined "combs" to form the sample wells. The process of optimizing the material, the shape of the comb teeth, and improving their sealing to provide leak-proof sample wells continues. However, we have already shown that improved DNA band profiles can be obtained with this approach.

In conclusion, we have a working ultrathin slab gel DNA sequencer that with further optimization should provide increased throughput over the standard thickness gel sequencer.

Publications

W.F. Kolbe, J.C. Schultz, and J. Jin, "High-Throughput Fluorescent Sequencer Development," to be presented at the DOE Human Genome Program Contractor-Grantee Workshop V, Santa Fe, New Mexico, Jan. 28–Feb. 1, 1996.

W.F. Kolbe, J.C. Schultz, and J.S. Zelver, "Fluorescent Sequencer Development," presented at the DOE Human Genome Program Contractor-Grantee Workshop IV, Santa Fe, New Mexico, Nov. 13–17, 1994.

Advance Towards the Next Generation of Pixellated Detectors for Protein Crystallography

Principal Investigators: Jacques Millaud, Thomas Earnest, Howard Padmore, and David Nygren

Project No.: 95010

Funding: $293,700 (FY 95)

Project Description

This proposal seeks to develop and build a pixel detector that will be used for the detection of x-rays at the Advanced Light Source (ALS). This detector can be used in a number of applications of synchrotron radiation, including biological x-ray crystallography, medical imaging, and high-energy physics. The initial application will be in the field of x-ray crystallography at the new macromolecular crystallography facility presently being developed at the ALS. The development of this new detector technology will ultimately benefit researchers using x-ray crystallography in the Structural Biology and Life Sciences divisions at Berkeley Lab, as well as researchers in other fields who require fast x-ray detectors to optimally utilize the high flux of x-rays generated by the ALS.

We will integrate the advances in material science, Application-Specific Integrated Circuit (ASIC) architecture and design, and advanced packaging into

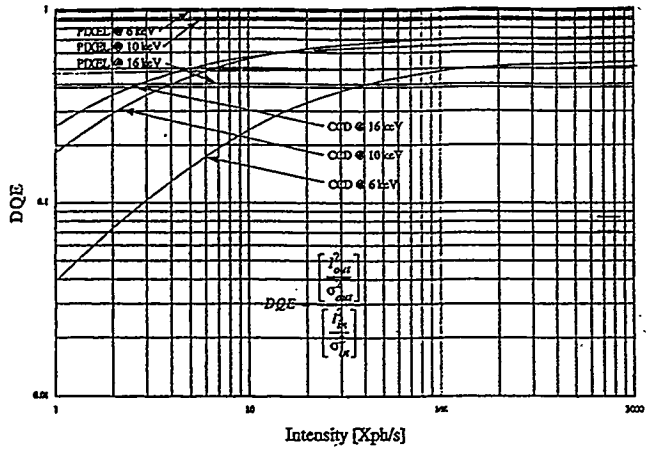

Figure 1. Comparative detector quantum efficiency for pixels and CCD-based detectors.

a small pixel detector system. This detector, with a granularity of 150 μm x 150 μm, will eliminate some of the limitations of CCD-based detector systems currently in the design stage. It will offer true pulse-counting statistics; reduce the point-spread function of the phosphor conversion CCD approach; and provide fast, adjustable electronic shutter and high and variable frame repetition rate while maintaining or improving the signal-to-noise ratio. This detector will open up new opportunities in time-resolved crystallography.

Accomplishments

Substantial progress and achievements have been made, far exceeding the scope of the FY 1995 LDRD:

1. The design of the detector system architecture has been finalized.
2. Functional blocks corresponding to the pixel processor analog front end and the column architecture have been designed, laid out, fabricated, and tested. They fully meet, and in a number of cases exceed, the original specifications.
3. Several configurations of detector arrays have been fabricated. Dark current is very low (~pA/pixel).
4. A characterization system built around an 8 x 8 array is in the completion stage. It will be used to qualify noise, speed, spatial uniformity, and cross talk.

The concept of using event-driven smart pixel detectors for protein crystallography experiments is proving to be of major importance for the whole field of x-ray crystallography. Time-resolved crystallography as well as monochromatic crystallography will benefit from the unlimited dynamic range and frameless operation associated with the column architecture and the high-quantum efficiency of the detector.

Concepts and preliminary results have been presented at several meetings (BSR95, APS users group, IEEE symposium) and through numerous interactions with experts in the field of crystallography and instrumentation. Offers of collaboration from Rutherford Appleton Laboratory and Daresbury in the UK are being discussed. Our collaborators at UC San Diego (Xuong, *et al.*) are designing the data acquisition part of the detector system.

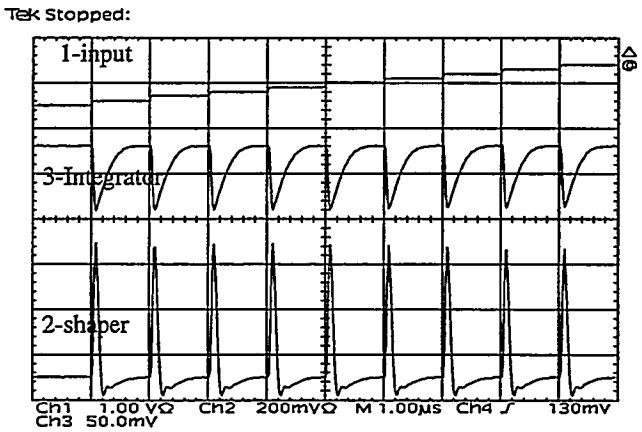

Figure 2. Fast integrator reset at 1 MHz counting rate.

Publications

N.-H. Xuong, P. Datte, E. Beuville, J. Millaud, and D. Nygren, "A Very Advanced Detector for Synchrotron Radiation," *Proceedings of the 16th European Crystallographic Meeting (ECM 16)*, Lundt, Sweden, August 1995.

J. Millaud and D. Nygren, "The Column Architecture—A Novel Architecture for Event Driven 2d Imagers," to be published in *Proceedings of the 1995*

IEEE Nucl. Science Symposium, San Francisco, California.

B. Turko, E. Beuville, J. Millaud, and H. Yaver, "A/D Processing System for a 64 Element Pixel Detector," to be published in *Proceedings of the 1995 IEEE Nucl. Science Symposium*, San Francisco, California.

E. Beuville, C. Cork, T. Earnest, J. Millaud, D. Nygren, H. Padmore, B. Turko, W. Mar, and G. Zizka, "A 2d Smart Pixel Detector for Time Resolved Crystallography," *Proceedings of the APS Conference*, October 16–20, 1995; to be published in *Review of Scientific Instrumentation*.

Integrated Molecular Cytogenetics Workstation

Principal Investigators: Damir Sudar and Joe W. Gray

Project No.: 95022

Funding: $57,200 (FY 95)

Project Description

The goal of this LDRD proposal is the development of a molecular cytogenetics imaging workstation that integrates all facilities of the experimental prototype workstations currently in use at the Resource for Molecular Cytogenetics. The Integrated Molecular Cytogenetics Workstation will be capable of scanning a microscope slide for metaphases and acquiring high-resolution multicolor digital images of fluorescently labeled microscopic specimens. Furthermore, analysis programs for fluorescence intensity measurements, CGH analysis, and fractional length metaphase mapping will be ported to or developed for this workstation.

The hardware and software components of the target platform consisting of a research fluorescence microscope, CCD camera, multi bandpass filterset, microscope automation, and a Macintosh computer must be configured. First, a CGH analysis package has to be built using a karyotyping module and a CGH analysis strategy. Image data will then be collected using the Resource QUIPS systems or the Vysis SmartCapture system. Subsequently, a flexible image acquisition system will be developed based on the Berkeley Lab QUIPS system. This system is then to be augmented with metaphase finding capability, which will be a stepping stone towards automated scanning applications such as rare-event detection, spot counting, etc. Using the CGH analysis framework, the fractional length metaphase mapping capability will be ported to the system. The metaphase finding capability and high-resolution analysis (CGH and mapping) will be integrated.

Accomplishments

In collaboration with Vysis, Inc., we have developed an image-processing library (VyLib) that integrates all the relevant functionality of the low-level commercial image processing library into our prototype molecular cytogenetics workstation. A detailed report is available that describes the library (VyLib) in some detail. VyLib will be the basis for all new developments.

Based on VyLib, we developed a new software package for the accurate mapping of locations along the medial axis of chromosomes in a metaphase spread and implemented and tested a novel approach to measuring ratio intensities of fluorescent labels, which is an integral part of CGH imaging.

Also, we developed a method to quantitatively assess the quality of images for CGH analysis. The software implementation of this method is currently being evaluated and will be integrated in the standard CGH analysis package.

Using the common software framework, we are planning the development of automated microscope scanning and analysis capabilities in order to implement metaphase finding, rare-event detection, and hybridization spot counting.

One result of this work is a CGH analysis package running on the Macintosh computer. An alpha version of this software was shown publicly at the 45th annual meeting of the American Society of Human Genetics in Minneapolis on October 24–28, 1995.

Electron Crystallography of Selected Membrane Proteins

Principal Investigator: Bing Jap

Project No.: 94009

Funding: $147,600 (FY 95)
$80,000 (FY 94)

Project Description

The emphasis of our program has been on developing the means to produce crystals suitable for high-resolution electron crystallography of two proteins—the Cystic Fibrosis Transmembrane Conductance Regulator (CFTR) and the platelet membrane protein receptor, GPIIb-IIIa (integrin $\alpha_{2b}\beta_3$). Each project began at a different stage of structural study.

For GPIIb-IIIa, the program began with the availability of milligram quantities of the purified protein. Therefore, work could begin immediately on developing and evaluating crystallization protocols. To produce two-dimensional crystals of this receptor, we have pursued methods for reconstituting membrane proteins with lipids. In a typical scenario, detergent solubilized protein and lipid are combined and then dialyzed so as to slowly remove the detergent, hopefully allowing the lipid and protein to form a complex in which the protein is organized into periodic arrays within lipid bilayers. Parameters critical to this process include detergent and lipid type, pH, ionic strength, and temperature. This project is part of an ongoing collaboration with Dr. Joel Bennett of the University of Pennsylvania, School of Medicine.

The case for the CFTR has been significantly different. As no source for milligram quantities of pure protein was available at the start of this project, the first order of business was to develop a reliable method for overexpressing the protein prior to purification and crystallization for its subsequent structural determination. In the previous year, we cloned the CFTR gene for overexpression in the vaccinia virus. This year we concentrated our efforts on purifying the virus and on characterizing the transfected CV-1 cells for the overexpression of CFTR.

The long-term goal of the project is to provide the structural basis for understanding the functional mechanisms of these proteins, which in turn could provide a molecular explanation of diseases associated with defects in these proteins. This information will play a key role in the development of therapeutics.

Accomplishments

Since our last report we have succeeded in reconstituting GPIIb-IIIa with lipids to form bilayer patches that contain small crystalline arrays of the receptor. Preliminary electron crystallography studies of these specimens in negative stain demonstrates that some of these patches yield diffraction to about 15 Å resolution. There were, however, indications that the negative staining procedure deteriorates crystal quality. Recently, we have begun to record low-dose/low-temperature electron micrographs of these specimens embedded in sugar. The latest results from these efforts are encouraging. In the computed Fourier transforms of images of these samples, significant reflection amplitudes are present for some reflections at about 5Å resolution. Before proceeding with full data collection, we need to improve the crystals both in terms of crystal size and long-range order. We therefore are focusing on refining the crystallization protocol.

We have been successful in expressing CFTR protein in CV-1 cells using the vaccinia virus expression system. This was accomplished in spite of the antiquated equipment available, which caused several major problems. A preparation of detergent-solubilized transfected CV-1 cells shows the presence of CFTR protein in the form of a positive reaction with antibodies directed against the recombinant protein. We have also proceeded to evaluate the expression level of CFTR in CV-1 cells that have been infected with our recombinant virus. Parameters being optimized for high-level expression of CFTR include the virus-to-cell ratio and the duration of cell incubation after virus infection. Also, we have begun to evaluate the expression of CFTR in several other cell lines in order to determine the best cell line for overexpression.

Propagation of Genetically Damaged Hemopoietic Stem Cell Progeny

Principal Investigators: Maria Pallavicini, Malak Shoukry, and George Brecher

Project No.: 94010

Funding: $49,000 (FY 95)
$44,600 (FY 94)

Project Description

Biological health effect risks from environmental toxicants are often monitored by measuring genetic damage in cell subpopulations in peripheral blood. Peripheral blood cells derive from a rare subpopulation in bone marrow designated as "stem cells" that has the capability to self-renew and produce blood cells (hemopoiesis) for the lifetime of the organism. It is estimated that 1 out of 50,000 bone marrow cells may be a stem cell. Genetic damage incurred by a stem-cell population will be present in its progeny. Thus, measurement of long-term stable genetic damage in peripheral blood reporter subpopulations (e.g., lymphocytes) following environmental exposure to radiation or carcinogens/mutagens is used to estimate absorbed dose (e.g., dose received by stem cells *in vivo*) at extended periods after exposure.

Assays that estimate systemic dose from measurements using reporter cells in peripheral blood assume that the frequency of genetically variant circulating cells is (1) equivalent to the frequency of variant stem cells, and (2) proportional to the extent of systemic genetic damage. However, it is unclear whether these assumptions are entirely valid. For example, genetically aberrant lymphocytes may arise from both damaged hemopoietic stem cells, as well as from immature lymphocyte subpopulations that survived radiation. The frequency of aberrant lymphocytes in peripheral blood may be altered by clonal expansion of lymphocyte subpopulations in response to immunologic stimuli. Dose estimation and risk assessment is dependent upon a clear understanding of the relationship between the frequency of genetically damaged stem cells and genetically aberrant reporter populations. We are pursuing studies to increase understanding of the dynamics of hemopoiesis by determining the relationship between radiation dose, stem-cell genetic damage, and propagation of genetically damaged cells throughout the hemopoietic system.

Assessment of genetic damage in blood cells and stem cells requires assays to detect alterations in the genome of the target subpopulation. Cells with severe chromosome abnormalities are unlikely to survive for extended periods. Stable genetic alterations (i.e., chromosome translocations) are more likely to result in biologic health effects because these abnormalities are compatible with cell survival and, if present in a stem-cell population, should be maintained for the lifetime of the organism. Fluorescent tagging of chromosomes using fluorescence *in situ* hybridization (FISH) with chromosome-specific probes allows visualization of translocations in mitotic cells. Thus, the translocation frequency response (tfr) assay can be used to estimate exposure dose. Measurement of tfr in phenotypic or functionally defined hemopoietic subpopulations allows evaluation of the propagation of progeny from genetically damaged stem cells. We are using combined genotype/phenotype approaches to investigate whether translocation frequency in peripheral blood lymphocytes (1) reflects genetic damage in hemopoietic stem cells, (2) is independent of chromosome type, and (3) reflects a genetic predisposition to radiation damage.

Accomplishments

The radiation translocation frequency response *in vivo* of peripheral blood lymphocytes was measured using FISH with paint probes for chromosomes 1+2 and X+3 (Fig. 1). A semiquadratic linear dose response relationship between radiation dose and translocation frequency was established. The translocation

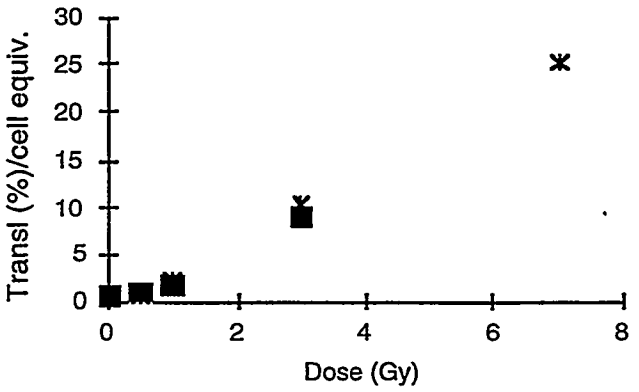

Figure 1. Average PBL translocation frequency response measured at 6 weeks (*) and at 16 weeks (■).

relationship between radiation dose and translocation frequency was established. The translocation frequency was constant at 6 and 16 weeks post exposure at each dose. These data suggest that either (1) genetically damaged lymphocytes represent long-lived lymphocytes, or (2) genetically damaged stem cells are generating the aberrant lymphocytes. If the genetically aberrant lymphocytes arose from damaged stem cells, then these stem cells should continue to produce progeny carrying the same structural aberrations following transplant into another host. These studies are in progress.

Our analyses also indicate that chromosomes 1+2 are involved in 30% more translocations then X+3, suggesting preferential breakage of one or both of these chromosomes at 0.5–3.0 Gy. Further studies confirmed that the increased translocation frequency was attributed to breaks in chromosome 2. The region of chromosome 2 involved in translocations is syntenous to human chromosome 201q13, which shows recurrent deletions in therapy or environmentally induced leukemias. However, C57Bl mice show a low incidence (<0.001%) of radiation-induced leukemia (RIL). On the other hand, SJL mice show a high propensity (25%) to develop radiation-induced leukemia (RIL). In a small group of animals, FISH analyses revealed similar translocation frequencies among C57BL and SJL mice. These data suggest that loss of translocations involving chromosome 2 are necessary, but not sufficient for transformation. Furthermore, these findings, albeit preliminary, suggest that the tfr may not be useful to identify individuals at risk of developing RIL. Analyses of additional animals will be required to confirm these speculations.

In summary, our data demonstrate that the frequency of genetically damaged lymphocytes remains constant within irradiated animals for at least 4 months post exposure. However, preferential radiation induced breaks in chromosome 2 in both radiation-sensitive and resistant strains suggest that not all chromosomes are at equal risk of radiation damage. Studies to identify the genetic basis for preferential breaks on chromosome 2, and radiation-induced stem-cell damage and leukemogenesis are planned.

Creation of Transgenic Mice Containing a Library of P1 Clones Encompassing the Down's Syndrome Region from Chromosome 21

Principal Investigator: Edward M. Rubin

Project No.: 94011

Funding: $265,900 (FY 95)
$189,900 (FY 94)

Project Description

Down's syndrome (DS) pathology is caused by trisomy of chromosome 21. The characteristic DS phenotypes include mental retardation, immune deficiencies, heart and gut abnormalities, and typical facial and body features. Mouse chromosome 16 has been shown to share extensive synteny with human chromosome 21. Mice trisomic for chromosome 16, therefore, has been used as a model for DS phenotype studies in the past. The goal of this project was to create a series of transgenic mice, each containing a defined piece of human DNA from the DS region of the chromosome. The transgenic mice created through microinjection of human DNA in the forms of P1 and YAC clones would be used to assess phenotypic changes in the organism. This would allow localization and study of candidate genes responsible for specific DS phenotypes.

Accomplishments

We have accomplished the following:

1. Creation of multiple lines of transgenic mice to contain human DS DNA. A set of overlapping YACs and P1s containing much of the DS region between markers CBR and PCP-4 was introduced into mice.

2. Expression study of transgenes. We have used RT-PCR to determine the expression patterns of two human genes located on the YACs that were introduced into mice.

3. Preliminary behavioral study of transgenic mice. This study suggested that overexpression of a gene or a group of genes located within a 570 Kb YAC might be the cause of learning deficiency in one of the transgenic mice.

Creation of a Library of YAC/P1 Transpolygenic Mice

The clone map we have developed in the DS region of chromosome 21 consists of a complete YAC contig and a P1 contig that extends over part of the YAC contig. There are 5 YACs (230E8, 745H11, 141G6, 152F7, and 285E6) spanning approximately 2 Mb of DNA. Four of these YACs, except for 285E6, were previously reported to be nonchimeric and nondeleted as, suggested by the long-range restriction map comparison between lymphocyte and YAC clone DNA. The YAC contig completely covers the region between CBR and PCP-4. YAC 745H11 was unstable, and therefore was not used in constructing transgenic mice. The omission of 745H11 produced a gap in the YAC contig. This gap was filled by a set of 4 overlapping P1s.

Pups resulting from zygote microinjection with YAC and P1 DNA were first screened by PCR using primers that detected human and vector sequences. Two other approaches, inter-Alu PCR fingerprinting and transmission analysis of the sequence-tagged sites (STSs) on YACs, were used to assess the integrity of the human clones in transgenic mice. For each YAC, we have generated 2 to 10 independent lines of mice carrying full length insertion. Additional 8 to 13 lines of mice carrying incomplete segments of YACs were also created for each YAC. The 4 P1 clones were injected into mice as pools of two overlapping clones. Three different pools of P1 DNA were thus introduced into mice. At least one line of mice was created for each P1 that bridged the gap in the YAC contig.

Expression Study of Transgenes

To investigate whether the human YAC DNA integrated into the mouse genome displayed expression of the resident genes, one transcription unit was examined for each YAC using reverse transcription PCR (RT-PCR). The STS CBR is contained within the gene for human carbonyl reductase, which is considered to be a housekeeping gene. The STS resides within YAC 230E8, and a line of mice containing this YAC expresses the carbonyl reductase gene fairly uniformly in all tissues examined. The STS D21S267 is contained within a transcription unit that has been shown to be expressed predominantly within the human brain. This STS is found within YACs 141G6 and 152F7, and two lines of mice, each containing one of these YACs, express the gene containing this STS. Moreover, expression of the human gene is particularly strong in the mouse brain. Thus, each YAC transgene was demonstrated to express at the appropriate location.

Spatial Learning Impairment in the Transgenic Mice Carrying 152F7 YAC

We have used the Morris water maze task to examine spatial learning impairment in these transgenic mice. Mice were first given training trials with a submerged platform and a visible flag to indicate the platform location in the maze. Mice were then given training trials with a submerged platform at the same location in the maze. Finally, mice were required to swim in the pool without the platform after the training trials (probe test). In the probe test, mice carrying human YAC 152F7 reduced the duration in the quadrant where the platform had been originally located. This learning deficit does not appear in nontransgenic siblings of YAC 152F7, nor in transgenic mice carrying other human YACs. These results suggest that overexpression of a gene or a group of genes in YAC 152F7 may cause the deficit of spatial learning deficit.

Publication

D.J. Smith, Y. Zhu, J.-L. Zhang, J.-F. Cheng, and E. M. Rubin, " Construction of a Panel of Transgenic Mice Containing a Contiguous 2-Mb Set of YAC/P1 Clones from Human Chromosome 21q22.2," *Genomics* **27**, 425 (1995).

A Transgenic Model for Clinical Testing of Progestins and Analysis of Progesterone Receptor Function

Principal Investigator: G. Shyamala

Project No.: 94012

Funding: $69,500 (FY 95)
$59,800 (FY 94)

Project Description

The female sex steroid hormone progesterone has diverse and tissue-specific physiological effects that are mediated through its cognate receptor, namely, the progesterone receptor. The major use of progestins in humans is in hormonal contraception and, as a result, they are the synthetic steroids used by the largest number of women in the world. In this setting, a particular concern is an increase in the incidence of coronary heart disease and other vascular disorders in women. Progestins are also used in the therapeutics of several gynecological diseases related to estrogen/progesterone imbalance, including benign breast diseases and endometrial hyperplasia. However, there is also a growing concern that the successful use of progestins in the clinical treatment of endometrial diseases may have the adverse effect of increasing the risk with respect to mammary carcinogenesis. Therefore, at present, a prodigious effort is being put into research on the synthesis and pharmacology of progestins with the aim of devising steroids with potent progestational activity and minimal metabolic effect.

The progesterone receptor exists in two molecular forms, commonly designated as the "A" and "B" forms. *In vitro* studies indicate that these "A" and "B" forms can have different biological activities depending on the cell and promoter context, and we believe that this accounts for the diverse effects of progesterone observed *in vivo*. Since *in vivo*, both forms of receptors exist to individually identify the effect of the "A" form versus the "B" form, we have proposed to create transgenic mice expressing either the "A" or "B" form of the receptor so that they may serve as experimental models for precise understanding of the role and relative importance of these forms *in vivo*, and hence, the molecular basis for the diverse effects of progesterone. This, in turn, will provide crucial structural information towards the synthesis of new derivatives suitable for clinical use with minimal overlapping activity and hence adverse effects.

Accomplishments

We accomplished our goals insofar as we were able to create transgenic mice carrying either the "A" or the "B" form of the progesterone receptor gene (hereafter referred to as PR-A and PR-B mice). We obtained eight founder lines for PR-A mice and six founder lines for PR-B mice. All of the eight founders of the "A" mice were fertile and transmitted the transgene with fidelity. In contrast, two founders of the PR-B mice did not transmit the gene—one was sterile, and one died prior to mating.

For a preliminary analysis of the phenotypes represented by the transgenic mice, we examined the uterus and the mammary glands. In the uterus, progesterone inhibits epithelial cell proliferation, while in mammary glands, it promotes the epithelial cell proliferation. That is to say, in these two important target tissues for progesterone action, progesterone has opposing effects that, in turn, are known to have major consequences with respect to the susceptibility of these tissues to carcinogenesis.

We found that, compared to wild type mice, PR-A mice exhibited a decrease in uterine growth, while in mammary glands there was an increase in mammary epithelial cell proliferation. In contrast, there were no significant differences between the wild type and PR-B mice with respect to these parameters.

These data suggest that *in vivo* the tissue-specific effects of progesterone may represent the combined activities of the "A" and "B" forms of the progesterone receptor. In the case of the uterus and the mammary glands, this may be essential for maintaining the cellular replicative homeostasis. Therefore, introduction of either form of the receptor as a transgene can upset this homeostasis *in vivo*, which we believe may be responsible for the phenotypic changes associated with the uterus and with the mammary glands of PR-A mice. As originally proposed, we now intend to use these transgenic mice to resolve the mechanisms responsible for the diverse and tissue-specific effects of progestins and their antagonists.

A followup grant to this research has been awarded in the DOD Breast Cancer Research Program.

Variations in Susceptibility to Environmental Oxidants as Studied Using Transgenic Mice

Principal Investigators: Diane L. Tribble, Elaine L. Gong, Edward M. Rubin, and Mary Helen Barcellos-Hoff

Project No.: 94013

Funding: $110,000 (FY 95)
$125,400 (FY 94)

Project Description

Radical-mediated oxidative processes have been implicated in the development of numerous chronic and degenerative diseases, including atherosclerotic heart disease and cancer. Recognition of the ubiquitous pathophysiological consequences of oxidative processes provides a unifying framework for the study of environmentally induced diseases since a diverse array of disease-promoting environmental agents act as oxidants in biological systems. The primary objectives of this project were to identify environmental oxidant stress conditions capable of promoting atherosclerosis in susceptible mice, and to use these atherosclerosis-promoting exposure conditions to investigate the protective effects of human transgenes coding for proteins with antioxidant activity.

Accomplishments

In the first year of this project, we observed that a single dose (8 Gy) of ionizing radiation, administered in conjunction with a high (1.25%) cholesterol diet, accelerates atherosclerosis in susceptible (C57BL/6) mice, as indicated by a threefold greater mean lesion area in the proximal aorta of irradiated versus sham-irradiated mice. Mechanisms underlying the disease-accelerating effects of radiation are not known, but are suggested to involve oxidative tissue damage. Recently, in collaborative studies with Dr. Jay Heinecke, we observed that levels of tyrosine metabolites indicative of hydroxyl radical-mediated protein modification (*ortho-*, *meta-*, and di-tyrosine) are only modestly elevated (15–30%) in aortic tissue obtained post irradiation. This suggests that aortic cells are able to respond effectively to the oxidant stress imposed by ionizing radiation at the dose used in these studies, and thus, that marked oxidative injury to the vasculature is not essential to the atherosclerosis-accelerating effects of radiation. We are currently investigating whether the acute antioxidant response leads to perturbations in cellular antioxidant capacity and redox state, which in turn may affect the subsequent response to oxidative injury and lead to alterations in the expression of critical regulatory proteins.

Irradiation had no effect on plasma lipid or lipoprotein levels in C57BL/6 mice either on chow or the 1.25% cholesterol diet, providing further evidence that the atherosclerosis-promoting effects are due largely to vascular alterations. Disease acceleration was observed only in animals exposed to high cholesterol diets, however, suggesting that radiation-induced vascular alterations are not sufficient alone, but rather occur in conjunction with a conducive lipoprotein milieu. Previous studies in the laboratory of Dr. Rubin showed that animals transgenic for apo A–I_h, the primary structural protein of high-density lipoproteins (HDL), are particularly resistant to diet-induced atherogenesis. Such effects are attributed to the participation of HDL in reverse cholesterol transport, although recent reports have suggested that HDL also may reduce atherosclerosis by inhibiting atherogenic oxidative processes. To investigate whether HDL offers protection against radiation-induced atherosclerosis, we initiated studies aimed at examining the extent to which this process is inhibited in Apo A–I_h transgenic mice. If radiation-induced atherosclerosis is found to be reduced in Apo A–I_h transgenics relative to littermate controls, future investigations will address the extent to which these effects are due to HDL antioxidant effects.

The antioxidant effects of HDL have been suggested to involve removal and inactivation of biologically active lipid oxidation products from vascular cells and low-density lipoproteins (LDL). In order to study these processes more directly, we developed a method for monitoring HDL- and LDL-specific oxidation in mixed systems (e.g., mixtures of these lipoprotein populations or of lipoproteins and cells). Results obtained using this methodology support a direct antioxidant effect of HDL *in vitro* (e.g., HDL inhibited oxidation within the LDL particle without undergoing simultaneous oxidation). In future studies, we will attempt to adapt this methodology to the study of lipoprotein oxidation *in vivo*, a process that has thus far evaded direct examination. Such measures will then be used to investigate the effects of HDL and other antioxidants on atherogenic oxidative processes in transgenic and irradiated mice.

Among the reactive oxygen species generated *in vivo*, the superoxide anion (O_2–) has been implicated as a primary mediator of atherogenic oxidative modifications. In many cases, the atherogenic potential of O_2– has been inferred from observations of an attenuating effect of superoxide dismutase (SOD). SOD has been shown to inhibit macrophage- and vascular cell-mediated lipoprotein oxidation, and leukocyte adhesion to the vascular endothelium, and to promote endothelium-derived relaxing-factor-induced vasodilation. To evaluate the pathogenic involvement of O_2– and SOD in diet-induced atherogenesis, we examined atherosclerosis susceptibility in fat-fed C57BL/6 mice expressing the intracellular form of human copper–zinc SOD (CuZn–SOD_h) in collaborative studies with Dr. Charles J. Epstein. SOD activity was found to be elevated two to threefold in aortic tissue and peritoneal macrophages from CuZn-SOD_h-transgenics, yet there were no measurable differences in aortic lesion areas relative to littermate controls after 18 weeks on an atherogenic diet.

The lack of an antiatherogenic effect of CuZn–SOD does not rule out the involvement of O_2– in the development of atherosclerosis. Among the various alternative explanations for these results, we are currently evaluating whether protective effects are observed over a different range of SOD activities (e.g., such as may be attained by inhibition rather than amplification of activity) and whether localization of SOD in the extracellular compartment is critical to its protective effects. With regard to the latter, we have observed that, despite the elevation in intracellular SOD activity, phorbol ester-stimulated O_2– release is not decreased in peritoneal macrophages derived from SOD transgenics. Thus, macrophage-mediated LDL oxidation and vascular damage are unlikely to be affected by amplification of intracellular SOD activity. In future studies, we will evaluate atherosclerosis susceptibility in extracellular SOD knockouts and over-expressors.

Observations of a protective effect of CuZn–SOD also may depend on the degree to which oxidative stress is a feature of the atherosclerosis-inducing conditions. Studies are currently underway to examine whether susceptibility to radiation-induced atherosclerosis is altered in CuZn–SOD_h-transgenics.

Publications

E.L. Gong, M.H. Barcellos-Hoff, J. Verstuyft, E.M. Rubin, and D.L. Tribble, "Atherogenic Effects of Radiation Exposure in Fat-Fed C57BL/6 Mice," *Proceedings of the Radiation Research Society*, April 1995.

D.L. Tribble, E.L. Gong, E.L. Carlson, J. Verstuyft, and C.J. Epstein. "Fatty Streak Formation in Fat-Fed Mice Expressing Human Copper-Zinc Superoxide Dismutase," *Circulation* **91**, I-229 (1995).

D.L. Tribble, B.M. Chu, E.L. Gong, F. vanVenrooij, and A.V. Nichols, "HDL Antioxidant Effects as Assessed Using a Nonexchangeable Probe to Monitor Particle-Specific Peroxidative Stress in LDL-HDL Mixtures," *J. Lipid Res.* **36**, 2580 (1995).

Isolation of Genetic Suppressor Elements in Human Mammary Epithelial Cells

Principal Investigator: Paul Yaswen

Project No.: 95011

Funding: $67,000 (FY 95)

Project Description

Development of human breast cancer is thought to involve multiple genetic changes in the genes that regulate growth and differentiation of human mammary epithelial cells (HMECs). Finding the genes and elucidating the pathways involved is a key step in understanding the pathogenesis of this disease. In order to directly isolate and identify genes whose normal functions are suppressed during malignant transformation of HMECs, we will employ a phenotypic selection method that allows fast recovery and identification of *functional* gene fragments. We have created a retroviral library of potential genetic suppressor elements (GSEs) from homogeneous cultures of normal finite lifespan HMECs. This library can be used to infect growing cultures of HMECs.

Our long-term goals are to select infected HMEC cultures for: (1) cellular immortalization, (2) resistance to TGFβ-mediated growth inhibition, and (3) anchorage independent growth. Cells that continue to grow under selective conditions (repeated passaging, TGFβ exposure, suspension in methylcellulose) will be harvested, and inserted retroviral DNA will be rescued by polymerase

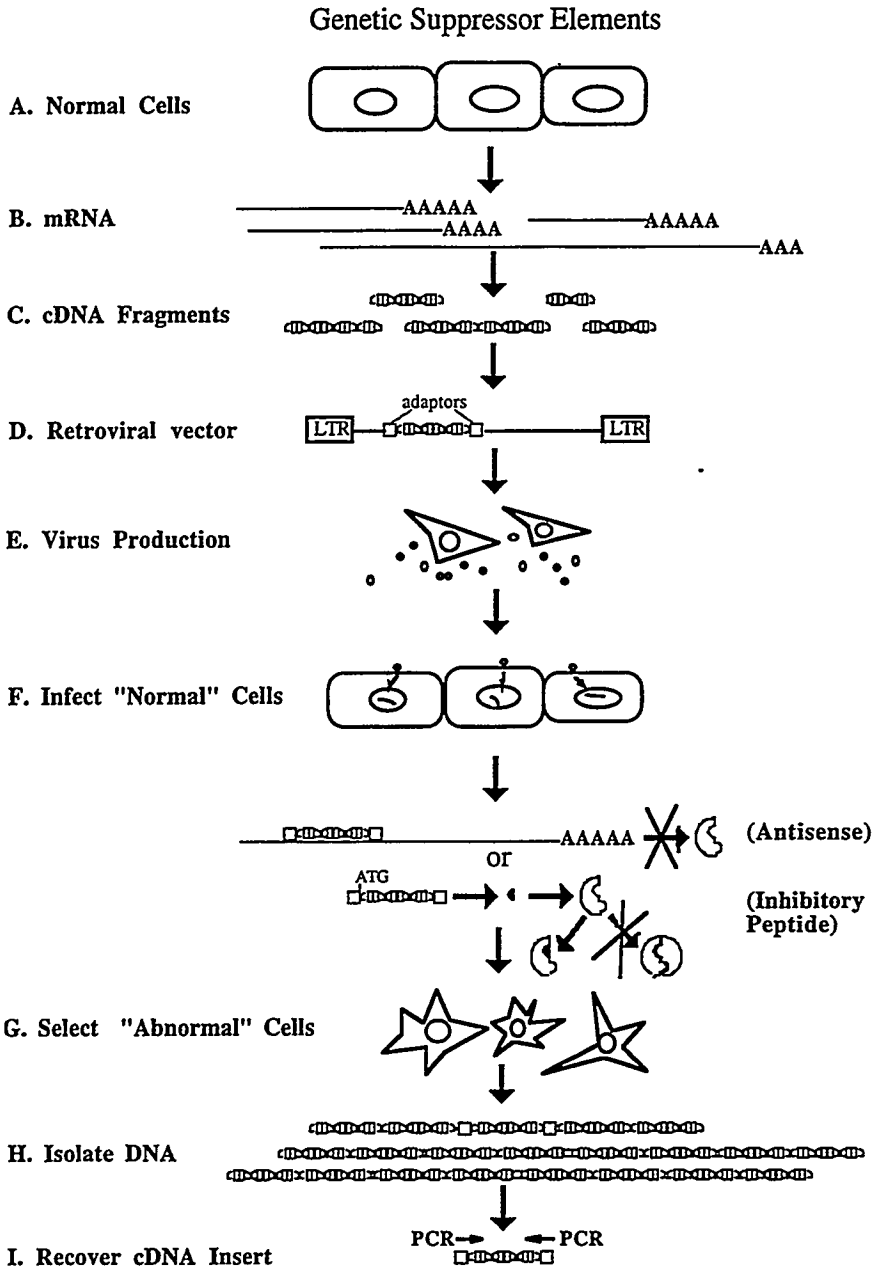

Figure 2. Isolation of Genetic Suppressor Elements (GSEs). Normal human mammary epithelial cells (A) will be harvested, and mRNA prepared. The mRNA (B) will be reversed transcribed using random oligonucleotide primers. the resulting cDNA (C) will be ligated to synthetic adaptors and inserted into a retroviral vector. The retroviral library (D) will be transfected into packaging cells in order to form infectious virus (E). Recipient human mammary epithelial cells (F) will then be infected with the retroviral library. cDNAs that function as GSEs will form antisense RNAs to block mRNA translation, or short peptides to block protein interactions. Partially or fully immortalized human mammary epithelial cells (G) resulting from GSE expression will be obtained after prolonged passage in monolayer cultures. Genomic DNA (H), containing inserted retroviruses, will be purified from selected cell clones and used to recover GSEs (I) by PCR.

chain reaction (PCR). After an additional round of screening, the inserted cDNA fragments will be sequenced and used to characterize biochemical pathways that are disrupted during malignant transformation. The gene fragments identified by this protocol can then be used as potential diagnostic markers, and to develop more detailed models of breast cancer progression. In our present experiments, we are particularly interested in isolating GSEs corresponding to genes that ordinarily suppress immortalization in HMECs. Such genes are likely to include suppressors of telomerase activity. Since telomerase activity is not found in most adult human somatic cells and does not appear to be essential for normal tissue homeostasis, it represents a unique target for new, potentially less toxic, therapeutic strategies.

Accomplishments

We have compared retroviral vectors and packaging systems in order to optimize the infection efficiency and cDNA expression in HMECs. Using the *kat* system of retroviral packaging constructs and retroviral expression vectors, we have consistently obtained infection rates of greater than 60% in target HMECs. Our transfections of packaging cells have also been optimized to 60–80% to ensure that a complex population of retroviral constructs can be packaged. We have synthesized random primed cDNA from poly(A)+ RNA of subconfluent cultures of normal HMEC, and have inserted it into the *kat* system expression vector in order to generate a retroviral library of potential GSEs.

Our retroviral cDNA library has been introduced into two extended life cultures, 184Aa and 184Be. Culture 184Aa is a clonal isolate that is known to contain the same mutations in the p16/CDKN2 locus that are found in its immortalized derivative, 184A1. Mutations at this locus are often found in cell lines derived from many tumor types, including breast carcinomas, but are less abundant in primary tumors. This has led to speculation that p16 mutations may be predisposing to immortalization or adaptation to *in vitro* conditions, although clearly in the case of 184Aa, these mutations are not sufficient by themselves to achieve immortalization. Control 184Aa and 184Be cultures reproducibly cease proliferation by passages 15 and 10, respectively. In each case, approximately 4–6 weeks after infection, there are obvious clonal areas of high mitotic activity in the cultures infected with the cDNA library, but no such areas in cultures infected with the control virus. Whether the highly mitotic cells have been fully immortalized remains to be determined.

Cell colonies displaying prolonged growth in monolayer cultures will be clonally expanded and cellular DNA extracted. cDNA inserts will be amplified from the cellular DNA by PCR using primers corresponding to flanking retroviral vector sequences. After isolating gene fragments that consistently confer selectable phenotypic changes in targeted HMECs, our priorities will be the structural characterization of their cellular targets, and analysis of changes in gene expression/function in breast tumor cell lines, primary tumors and metastases.

Materials Sciences Division

Electronic Thermalization in Metals and Semiconductors

Principal Investigator: Jeffrey Bokor

Project No.: 93014

Funding: $122,400 (FY 95)
$169,500 (FY 94)
$180,900 (FY 93)

Project Description

Our goal is to obtain information on hot-electron relaxation mechanisms and rates in a variety of metals and semiconductors. This information can be used to optimize electronic device performance in the nanoscale regime and to design laser photochemical processes on metal and semiconductor surfaces. We are also exploring the use of laser-stimulated desorption to help solve the important problem of stiction in surface micromachining technology.

Time-resolved photoemission spectroscopy is used for directly measuring laser-excited hot-electron energy distributions, and the time evolution of these distributions as they thermalize and equilibrate by various energy-loss and momentum-exchange processes. A new technique for electron heating is being studied. This technique involves the use of THz-bandwidth electromagnetic pulses radiated from large-area ultrafast photoconducting antennas.

In conjunction with this experimental effort, theoretical models capable of describing the results are being developed, and the relevant scattering parameters are being determined by comparison with experimental results.

Accomplishments

We have demonstrated the first practical application of hot-electron mediated laser stimulated desorption. A reduction of the adhesion between polysilicon surface-micromachined structures and an underlying silicon substrate is achieved using ultra-short-pulse laser irradiation. Polysilicon cantilevers that adhere to the substrate after final rinse and dry (stiction) are freed after irradiation by 800-nm-wavelength laser pulses with a duration of 150 fs and fluence of up to 40 mJ/cm^2. Longer pulse widths of 2.7 ps result in significantly reduced effectiveness, which we interpret as evidence that the process depends heavily on the presence of high electron temperatures in silicon. The process is explained in terms of hot-electron induced desorption of a residual capillary water layer at the interface between the cantilever and substrate. Stiction is a common problem affecting yield in surface micromachined devices such as accelerometers and displays.

The detailed dynamics of hot electrons excited by such short pulses in silicon are being investigated using time-resolved photoemission spectroscopy. Conduction band electrons created by pulsed laser excitation at 800 nm have been clearly detected using our photoemission apparatus. We observe a very rapid (100–200 fs) decay of the total carrier population in the near surface region. This is somewhat puzzling since bulk conduction band electrons should have a lifetime in the range of hundreds of nanoseconds. Two alternative models are under investigation to explain these results. One model involves ultrafast surface dynamics. The second model is related to photoemission selection rules that, for the ultraviolet wavelength we use, strongly emphasize only the hottest carriers in the photoemission signal. Further experiments will clarify the situation.

A high-intensity source of THz electromagnetic pulses at a 1-kHz repetition rate has been completed and characterized. Using larger aperture GaAs photoconducting antennas with 3-cm-gap electrodes, we have generated pulses with 0.4 μJ energy at 1 kHz repetition rate. By focusing this beam with a parabolic mirror, peak electric fields of 150 kV/cm are produced. This high electric field strength is well into the regime that leads to hot-carrier transport effects in semiconductors. Detailed theoretical calculations based on energy balance equations predict carrier heating in silicon up to 0.4 eV of the effective carrier temperature, and strong velocity saturation. Experiments to directly observe these effects are currently in progress.

Publications

N.C. Tien, S. Jeong, L.M. Phinney, K. Fushinobu, and J. Bokor, "Surface Adhesion Reduction in Silicon Microstructures Using Femtosecond Pulses," *Appl. Phys. Lett.* (Jan. 8, 1996).

E. Budiarto, S. Jeong, J. Son, J. Margolies, and J. Bokor, "High Power Terahertz Radiation at 1 Khz Repetition Rate," *IEEE LEOS Conference Proceedings*, San Francisco (Nov. 1995).

E. Budiarto, J. Margolies, S. Jeong, J. Son, and J. Bokor, "High Intensity THz Pulses at 1 kHz Repetition Rate," submitted to *IEEE J. Quantum Electron.*

Near-Field Scanning Optical Microscopy/Spectroscopy of Low-Dimensional Systems at 50-nm Resolution

Principal Investigators: Shimon Weiss, D. Frank Ogletree, and Daniel S. Chemla

Project No.: 94015

Funding: $112,100 (FY 95)
$133,500 (FY 94)

Project Description

The development of the near-field scanning optical microscope (NSOM) enables the combining of super-resolution ($\lambda/40$) with various optical spectroscopies such as fluorescence, excitation, Raman, nonlinear and time-resolved spectroscopies. In addition, the unique properties of the near-field light allow the obtaining of exquisite sensitivity by enhancing the signal/background ratio. They also allow mapping of the dipole moment of a single fluorophore. Imaging, dipole moment determination, and fluorescence spectroscopy of single-dye molecules have recently been demonstrated.

The main objective of this research is to further enhance the NSOM spectroscopic capabilities, and to use it to study the physical and chemical properties of mesoscopic systems. Two main efforts are being pursued. One is the application of single molecule detection (SMD) to biology, and the other is the study of novel mesoscopic materials systems such as semiconductor nanocrystals, self-assembly monolayers, and thin molecular films.

Accomplishments

The NSOM head was incorporated into a conventional upright microscope (Zeiss Axioscope). Various detection schemes with fluorescence imaging, fluorescence time traces, emission spectra, and radiative lifetime by time-correlated photon counting, all with single molecule sensitivity, were incorporated into the setup. Dual-color excitation and/or dual-color detection capabilities were also added.

We have used the NSOM to study energy transfer on molecular level. Fluorescence resonance energy transfer (FRET) (Förster energy transfer) is a standard spectroscopic technique for measuring distances in the 10–75 Å range in relevant biological systems. Energy is transferred from a donor molecule to an acceptor molecule via an induced-dipole, induced-dipole interaction, with the transfer efficiency depending on the inverse-sixth-power of the distance between the donor and acceptor and on their relative orientations. With the aid of the NSOM, we observed FRET between a single donor fluorophore and a single acceptor fluorophore linked by a short dsDNA molecule. Dynamic events such as photobleaching and possibly rotational diffusion, which result in spectral changes in the emission from the FRET pair, were detected. The photodestructions dynamics of donor or acceptor were used to determine the presence and efficiency of the energy transfer. Figure 1 shows such an event, where acceptor photobleached and donor emission increased as a result. To the best of our knowledge, these measurements demonstrate the first single and pair molecule detection that are attached to biological macro-molecules. We believe that the NSOM-FRET technique is a potentially powerful tool for studying dynamic phenomena such as conformational changes in proteins, protein–DNA interactions and molecular motors.

Another current effort is the study of the fluctuations in the room temperature emission rate from single dye molecules that are excited in the near field. Preliminary results indicate transitions to long (~ seconds) and short (~ milliseconds) lived dark states. The nature of these dark states is currently being studied.

A third effort is the imaging and spectroscopy of individual semiconductor CdSe nanocrystals.

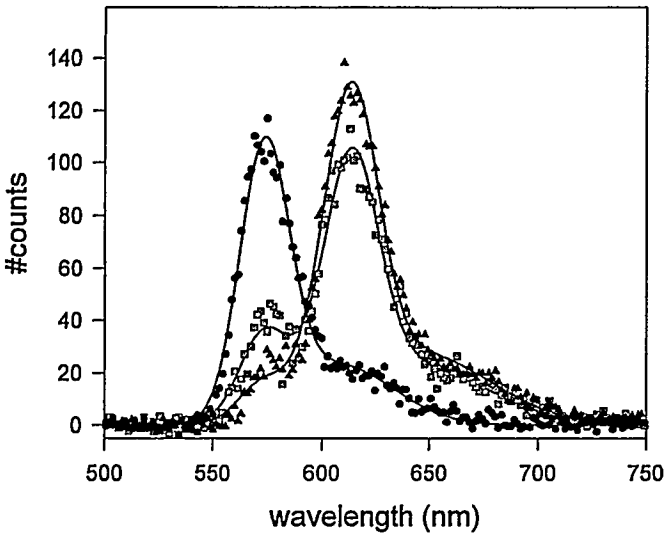

Figure 1. Three successive spectra from a single pair. Shown are the spectra before (triangles), intermediate (squares), and after (circles) the bleaching of the acceptor molecule (peak at 610 nm). The increase of donor emission (peak at 570 nm) after destruction of acceptor is indicative of energy transfer.

Publication

T. Ha, Th. Enderle, D.F. Ogletree, D.S. Chemla, P. Selvin, and S. Weiss, "Fluorescence resonance energy transfer between a single donor and a single acceptor molecule," submitted for publication to *Proceedings of the National Academy of Science.*

Electron-Beam Lithographic Fabrication of Submicron Junctions for Coulomb Blockade Arrays

Principal Investigator: John Clarke

Project No.: 93015

Funding: $89,000 (FY 95)
$59,000 (FY 94)
$119,800 (FY 93)

Project Description

The goal of this project is to study dynamic critical phenomena via electrical measurements of large arrays of small metallic islands linked by submicron tunnel junctions. The arrays are fabricated close to a ground plane, giving each island a well defined capacitance to ground C_g that is large compared to the junction capacitance C. Electrons introduced into such an array by application of a voltage or current bias perceive the array as a randomly rough energy landscape, due to the presence of randomly trapped charges near each island. Because the arrays are produced by electron-beam lithography, many of the parameters of the system are under designer control. For instance, the dimensionality of the array, the range of interactions of the electrons, the system size, and the amount and type of disorder present in the system can all be varied in well-defined ways. As a result, these arrays are expected to provide a good model system for the study of dynamic critical phenomena.

Accomplishments

The ground plane is a degenerately doped Si substrate; electrical isolation from the array is provided by 100 nm of thermal oxide grown on the surface of the substrate. The array pattern is defined using electron-beam lithography with a JEOL 6400 electron microscope. To produce tunnel junctions, we deposit two Al films in successive, angled evaporations with an intervening oxidation step. In the past year we have produced arrays with intentionally introduced disorder by varying the island shape from site to site. A random number generator was used to choose the island shape at a given site from a list of predetermined shapes; a different disorder realization can easily be produced by using a different seed for the random number generator. An electron micrograph of a test sample is shown in Fig. 2; the random distribution of island shapes can be clearly seen.

We have produced a two-dimensional (2D) array of 40 by 40 islands on a side in which the island areas vary from 0.87 μm^2 to 2.10 μm^2, in nine steps, corresponding to an estimated range in capacitance to ground C_g of 0.6 fF to 1.5 fF. We have performed electrical measurement on this sample in a dilution refrigerator in the presence of a magnetic field of 0.5 T, which renders the Al films normal.

In Fig. 3(a) we see a Coulomb blockade region around zero voltage. There is a threshold voltage V_T of approximately 220μV, above which the current rises and eventually enters a linear asymptotic regime, as can be seen in the inset. We verify that the capacitance to ground C_g varies from island to island

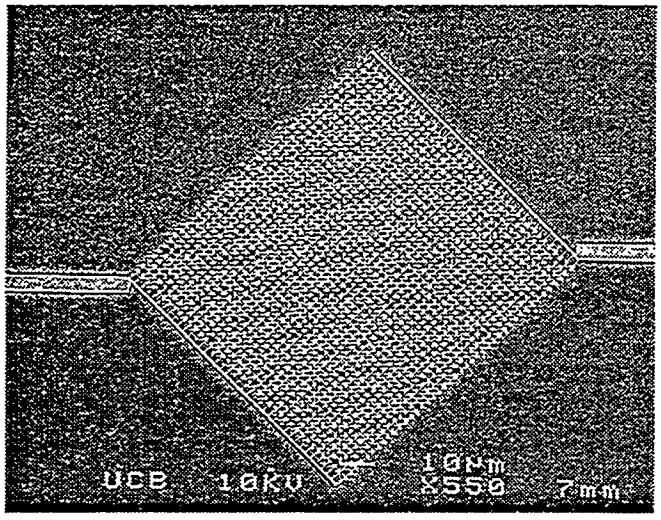

Figure 2. Electron micrograph of a 40 by 40 disordered test array. The random variation in island area across the array is clearly visible.

by current biasing the array just above V_T and measuring changes ΔV in the voltage across the array as a function of the voltage V_g between the array and the ground plane. For an array with a single island shape, we expect ΔV to be periodic in V_g with period e/C_g. As can be seen in Fig. 3(b), ΔV is not simply a periodic function of V_g. We have used a fast Fourier transform to calculate an estimated power spectrum for the data in Fig. 3(b), as shown in the inset; to reduce noise we averaged power spectra of four different sets of data covering the same range in V_g. The resulting spectrum shows several clear peaks, indicating the multiple periodic nature of ΔV vs. V_g, and demonstrating the presence of multiple island shapes.

We have examined the I-V characteristics in Fig. 3(a) for scaling behavior by plotting the current versus a reduced voltage $v = V/V_T - 1$. In arrays with no intentionally introduced disorder in the island shapes, we found earlier that the current and voltage follow a scaling law $I \sim (V/V_T - 1)^{\zeta}$. However, the data in Fig. 3(a) do not follow this scaling law for any reasonable choice of threshold voltage V_T. It appears that the dynamic critical phenomenon in these arrays is affected by the nature of the disorder present in the array; further theoretical investigation of this issue is called for.

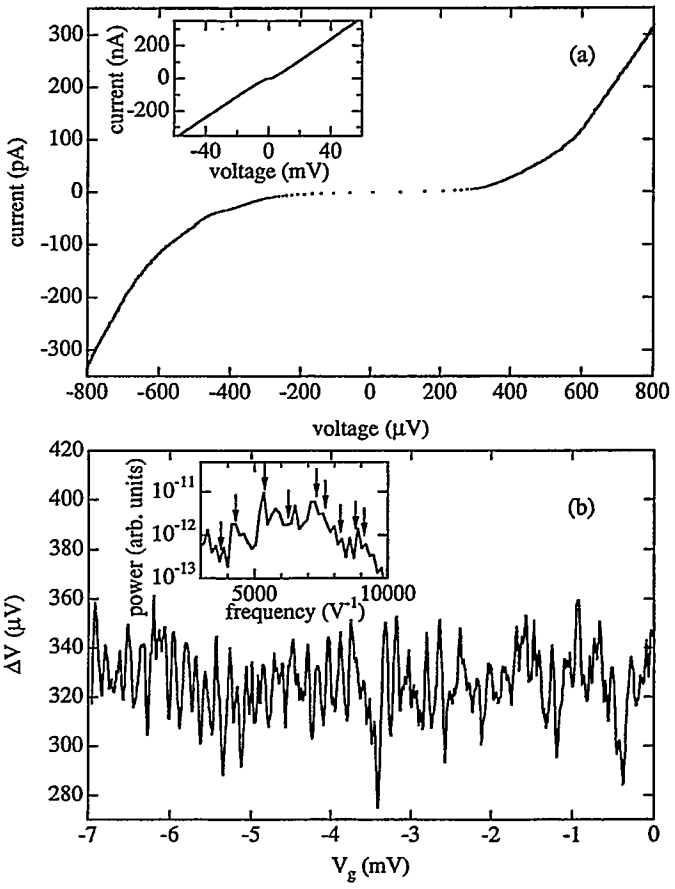

Figure 3. (a) I-V characteristic for the 40 by 40 disordered 2D array showing the presence of a threshold voltage of 220 µV and nonlinear conduction above threshold. The inset shows the asymptotic linear regime at high current. (b) Voltage across the array vs. gate voltage V_g at a bias current of 10 pA. The array voltage is clearly not simply a periodic function of V_g. The inset shows the power spectrum of the data. The arrows mark expected peak positions estimated from the measured island areas.

Publications

T.R. Ho, A.J. Rimberg, and J. Clarke, "Scaling Behavior in the Current-Voltage Characteristic of a One-Dimensional Array of Small Metallic Islands," *Bull. Am. Phys. Soc.* 40, 259 (1995).

A.J. Rimberg, T.R. Ho, and J. Clarke, "Scaling Behavior in the Current-Voltage Characteristic of a Two-Dimensional Array of Small Metallic Islands," *Bull. Am. Phys. Soc.* **40**, 259 (1995).

A.J. Rimberg, T.R. Ho, and J. Clarke, "Scaling Behavior in the Current-Voltage Characteristics of One and Two-Dimensional Arrays of Small Metallic Islands," *Phys. Rev. Lett.* **74**, 4714 (1995).

A.J. Rimberg, T.R. Ho, and J. Clarke, "Current-Voltage Characteristics of a Two-Dimensional Array of Strongly Coupled Small Metallic Islands," abstract submitted for the 1996 March Meeting of the APS.

T.R. Ho, A.J. Rimberg, and J. Clarke, "Intentionally Introduced Disorder in a Two-Dimensional Array of Small Metallic Islands," abstract submitted for the 1996 March Meeting of the APS.

New Directions for In Situ Electron Microscopy at High Spatial Resolution

Principal Investigator: Ulrich Dahmen

Project No.: 94016

Funding: $158,400 (FY 95)
$100,400 (FY 94)

Project Description

The success of electron microscopy as a technique for materials characterization is due to its unparalleled spatial resolution. However, major limitations are posed by the fact that most observations are static, allowing only indirect conclusions about the mechanism of microstructure evolution. *In situ* microscopy overcomes these limitations through direct dynamic high-resolution observation at temperature, in a field, under stress, in ultrahigh vacuum, or in a gas atmosphere. However, *in situ* microscopy to date has been mostly a qualitative technique.

This research will explore the potential of *in situ* electron microscopy, with emphasis on high spatial resolution, controlled sample geometries, and new electron optical techniques. Its goal is to examine the possibility of developing transmission electron microscopy (TEM) as a quantitative technique for the measurement of mechanisms and kinetics critical to the understanding of materials, and thereby build a framework to prepare the NCEM for new instrumentation and a new focus on high-resolution dynamic investigations.

It is in the exploratory nature of this proposal to assess the feasibility of several different approaches to *in situ* electron microscopy, including the use of crystallographic templates to generate model microstructures, microfabrication techniques for preparation of specific sample geometries, low-drift specimen holders capable of high resolution at elevated temperature, and electron holography using field emission sources.

Accomplishments

High Resolution In Situ Observations of Crystal Melting and Solidification

After showing for the first time that high-resolution electron microscopy can provide direct observations of melting and solidification of small inclusions, we continue by investigating the size dependence of melting and solidification. Nanosized Pb particles were formed in an Al bicrystal matrix by ion implantation and annealing. The Al bicrystals were prepared at Berkeley Lab and alloyed with Pb by ion implantation at Risø National Labs in Denmark. The Pb inclusions were octahedral, in shape and the Pb lattice was parallel to the Al matrix. Observations along ⟨110⟩ directions therefore provided optimized conditions for high resolution imaging. High-resolution observations of melting and solidification of Pb particles showed extremely interesting size-dependent superheating and supercooling, thermal migration, and thermal fluctuations. The behavior of Pb inclusions at grain boundaries was distinctly different from that of bulk inclusions and has been documented by high-resolution electron microscopy of equilibrium shapes. It was found that grain boundary inclusions such as those shown in Fig. 4 are faceted toward one grain and rounded toward the other grain. This can be understood by a modified Winterbottom construction in which the distance between the Wulff centers of the two half shapes is a measure of the grain boundary energy. Measurement of twin and grain boundary energies as a function of boundary inclination is currently underway. In addition, there are indications that the interface structure has a strong influence on the melting and solidification behavior of grain boundary inclusions. Image simulations to permit precise measurements of inclusion sizes and shapes have laid the foundation for a quantitative understanding of the fascinating size- and shape-dependent thermal behavior of these inclusions.

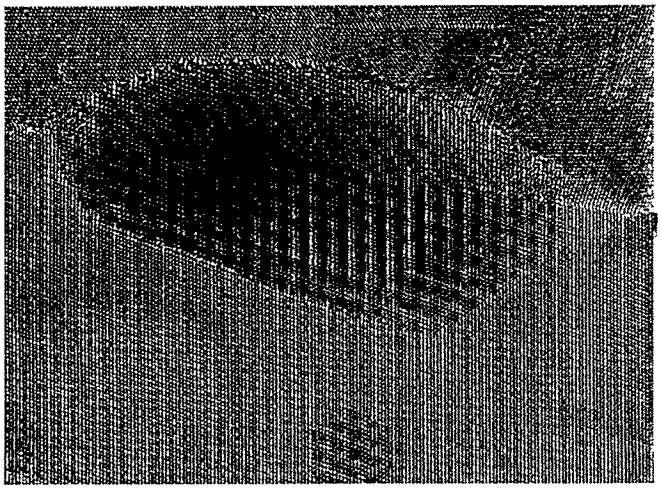

Figure 4. HREM image of grain boundary inclusion produced by ion implantation of Pb into mazed bicrystal films of Al. The inclusion shape is faceted toward one grain and rounded toward the other.

In Situ Deformation Studies

Based on initial tests that demonstrated the feasibility of *in situ* indentation experiments with a modified version of a straining holder for the 1.5 MeV High Voltage Microscope, a new *in situ* nanoindentation stage was designed and built in collaboration with M. Wall from LLNL. The stage uses an exchangeable diamond or sapphire tip that can be positioned accurately with piezoelectric drives to indent an electron transparent thin film and follow the transition from elastic to plastic deformation. The design, shown in Fig. 5, illustrates that sufficient sensitivity for controlled indentation experiments has been achieved. We have demonstrated that the stepper motors provide mechanical control to within ±10 nm over a range of more than 5 mm. In addition, the piezoelectric drives give control to within ±1 nm with a range of several hundred nanometers. Initial tests using a sapphire-tipped indenter with excellent control and reproducibility have been successful.

A remote control interface for *in situ* experiments on the 1.5 MeV HVEM has been developed in collaboration with B. Parvin from ICSD and a group of scientists at NCEM. This interface, first demonstrated publicly at the August meeting of the Microscopy Society of America in Kansas City, allows users to run heating, cooling, tilting, and, eventually, deformation experiments remotely or in a conference mode.

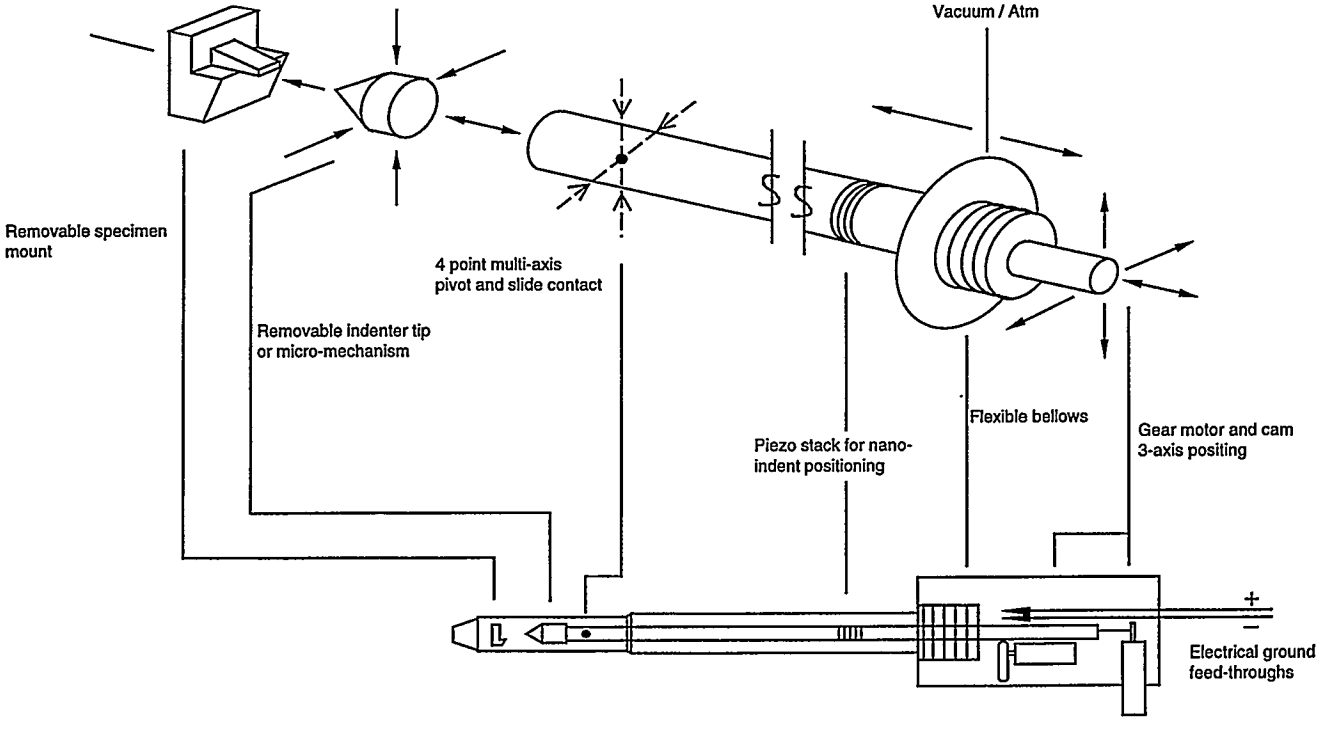

Figure 5. Schematic of in situ *indentation holder for 1.5 MeV High Voltage Electron Microscope.*

Publications

S.Q. Xiao, E. Johnson, S. Hinderberger, A. Johansen, K.K. Bourdelle, and U. Dahmen, "*In Situ* Observations of Nanometer-Size Pb Inclusions in Al Near Their Melting Point," *J. Microscopy* 180, 61 (1995).

E. Johnson, S. Hinderberger, S.Q. Xiao, U. Dahmen, and A. Johansen, "Structure and Morphology of Nanosized Lead Inclusions in Aluminum Grain Boundaries," *Interface Science*, in press.

S. Paciornik, S.Q. Xiao, S. Hinderberger, E. Johnson, and U. Dahmen, "Automated Measurement of Size and Visibility of Small Inclusions in HREM Images," *Proc. MSA* 53, 648 (1995).

S.Q. Xiao, S. Paciornik,, R. Kilaas, E. Johnson and U. Dahmen, "Modeling and Simulation of Octahedral Pb Inclusions in Al," *Proc. MSA* 53 (1995).

B. Parvin, D. Agarwal, D. Owen, M.A. O'Keefe, K.H. Westmacott, U. Dahmen, and R. Gronsky, "A Project for On-Line Remote Control of a High-Voltage TEM," *Proc. MSA* 53, 82 (1995).

M.A. Wall, T.W. Barbee, and U. Dahmen, "Techniques for *In Situ* HVEM Mechanical Deformation of Nanostructured Materials," *Proc. MSA* 53, 240 (1995).

Quantum Hall Plateau Transitions and the Hubbard Model

Principal Investigator: Dung-Hai Lee

Project No.: 94018

Funding: $86,400 (FY 95)
$18,300 (FY 94)

Project Description

The goal of this project is to understand a fundamentally unsolved problem in the Quantum Hall Effect. The hallmark of the Quantum Hall Effect is the pinning of the Hall resistance at multiples of h/e^2. This happens when a two-dimensional electron gas is submitted to strong magnetic fields. Until now it has not been known how the Hall resistance evolves from one quantized value to another. The purpose of this project is to understand such evolution.

Accomplishments

Significant progress was made this year in the understanding of the effects of electron–electron interaction on the critical properties of the plateau transition. A long-standing puzzle in the Quantum Hall Effect has been why the experimentally measured critical static exponent for the plateau transition agrees so well with the theoretical prediction when the electrons are assumed not to interact. This agreement is particularly puzzling in view of the fact that the dynamical exponent does not agree between the two.

In collaboration with Z. Wang at Boston University, it was shown that (1) if the electron–electron Coulomb interaction is screened, then the critical properties will be unaffected by the interaction. In that case, both the static and dynamical exponents should agree with the noninteracting theory. (2) If the Coulomb interaction remains unscreened, then the mean-field effects change the dynamical exponent while preserving the static one. The effects of the interaction beyond mean-field are shown to be unimportant.

These results set a precedent where the critical behavior of metal-insulator transition is unaffected by the electron–electron interaction. In all previous examples, interaction has altered all of the exponents of the transition.

Publications

D-H. Lee and Z. Wang, "Transitions Between Hall Plateaus and the Dimerization Transition of a Hubbard Chain," to be published in *Phil. Mag. Lett.* (1996).

D-H. Lee and Z. Wang, "The Effects of Electron–Electron Interaction on the Transitions Between Hall Plateaus," submitted to *Phys. Rev. Lett.*

Interaction of Hydrogen and Hydrocarbon Molecules with Indium Antimonide Surface: Chemistry of Etching

Principal Investigator: Roya Maboudian

Project No: 94019

Funding : $77,700 (FY 95)
$42,100 (FY 94)

Project Description

This project employs high-resolution electron-energy-loss spectroscopy (HREELS), low-energy electron diffraction (LEED), temperature–programmed desorption (TPD), and Auger electron spectroscopy (AES) to investigate the interaction of atomic hydrogen and saturated (methane and ethane) and unsaturated (ethylene and acetylene) hydrocarbon molecules with the well-characterized surface of indium antimonide, as a first step toward understanding the mechanisms involved in hydrocarbon-based reactive ion etching.

Accomplishments

The assembly of the ultrahigh vacuum chamber has been completed. The key instrument is the HREELS, capable of 2 meV energy resolution. HREELS indicates the presence of surface species (such as C–H in Fig. 6) by probing their vibrational modes. It can also be used to probe plasmon excitations and thus acquire information about free-carrier concentrations in the near surface region. TPD makes use of a quadrupole mass spectrometer (QMS) to identify desorbing species and to determine kinetic parameters such as the activation energy of desorption. An example of a TPD spectrum, for the case of deuterium adsorption on Si(100), is shown in Fig. 7. LEED gives information about the long-range order of clean and adsorbate covered surfaces, while AES provides information about the chemical composition of these surfaces.

These techniques have been used to study the chemistry of atomic hydrogen (and deuterium) with a well-characterized Si(100)-(2 × 1) surface. For low hydrogen coverages, we observe a 2 × 1 pattern with LEED, the Si–H stretch with HREELS, and the monohydride desorption peak with TPD. These

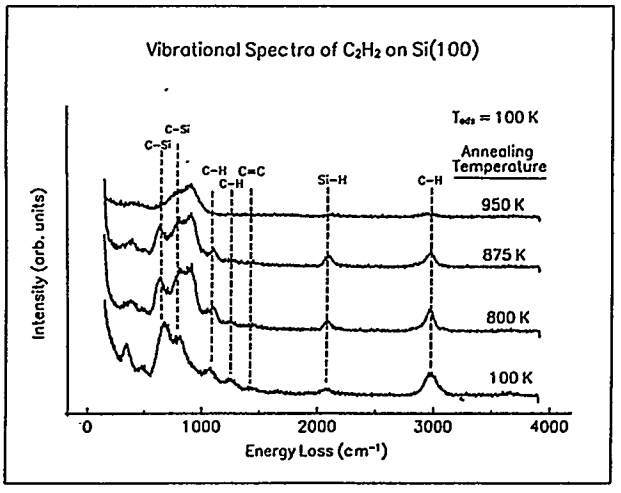

Figure 6. HREEL spectra for acetylene adsorption followed by annealing at various substrate temperatures on a Si(100)-(2 × 1) surface.

observations all indicate the presence of the only monohydride species. As coverage increases the LEED pattern changes to 1 × 1, the Si–H2 scissor mode appears in addition to the Si–H stretch, and the dihydride desorption peak appears in TPD (see Fig. 7). These observations indicate that the dihydride species is now also present. From the TPD peaks, the activation energy for monohydride desorption is calculated to be about 50 kcal/mol. These are all in agreement with the literature.

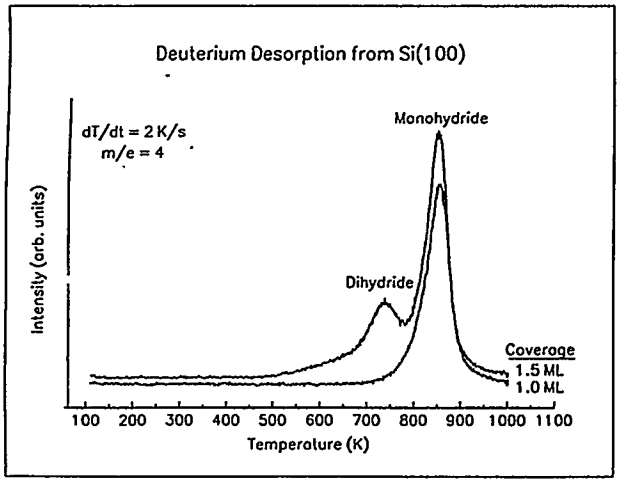

Figure 7. TPD spectra for deuterium desorption from Si(100)-(2 × 1) surface at two different initial coverages.

Experiments have also been carried out for acetylene adsorption on Si. Here the literature reports the nondissociative adsorption of acetylene on Si dimers. Upon heating, the acetylene primarily decomposes, with a small fraction desorbing intact. Hydrogen desorbs while carbon is left on the surface. Our TPD results are consistent with this picture, showing a large hydrogen desorption peak and a very small acetylene peak. HREELS results also agree with the aforementioned picture (see Fig. 6). As acetylene is heated to successively higher temperatures, the intensity of the C–H stretch decreases as the acetylene begins to decompose. The intensity of the Si–H stretch increases as some dissociated H atoms react with Si. Finally, at 950 K, all the acetylene has decomposed and the hydrogen has desorbed. Only Si–C loss peaks are still observed. These experiments have established that all the equipment is working well and will be effective as tools in studying the mechanisms of hydrocarbon-based reactive ion etching of compound semiconductors such as InSb.

A Low Temperature AFM for Imaging Current Flow in Nanostructures

Principal Investigator: Paul L. McEuen

Project No.: 95012

Funding: $54,900 (FY 95)

Project Description

The goals of this LDRD were: (1) to develop an instrument capable of spatially mapping the patterns of current flow in nanostructured materials, and (2) to use this instrument to explore transport in structures fabricated with electron-beam lithography.

An AFM and cryostat capable of operation at low temperatures (T = 1 K) and high magnetic fields (B = 7 T) will be constructed. The AFM will feature a piezoresistive feedback mechanism and a conducting tip to which CD voltages can be applied. It will be used to study lithographically defined nanostructures on which simultaneous electrical measurements are being performed. A voltage applied to the AFM tip will electrostatically influence current flow directly beneath it. The current flow will be measured as a function of the AFM tip position, yielding a nonometer-scale map of the current flow through the structure.

Accomplishments

During the past year, the low temperature AFM was designed and constructed. It is now operational, and the first experiments are being conducted. In particular, we have used the AFM tip to locally perturb the current flow in a GaAs nanostructure, all at a temperature of T = 0.3 K. This required not only the ability to perform low-T AFM, but also to find, at low temperatures, a single submicron device on which electrical measurements are being performed. To our knowledge, this is the first such system operating in the world. A paper describing these results is in preparation.

In addition to the scanned-gate measurements described above, we have begun to explore the use of the system for noncontact force microscopy. The AFM tip is made to oscillate at its resonant frequency, and changes in the resonant frequency with tip position (due to its local interaction with the device) are being investigated. In particular, we have used the electrostatic interaction between the tip and the device to directly image the local potential inside the nanostructure. Work on this continues.

Publication

K.L. McCormick, M. Huang, G. Pilling, P.L. McEuen, G. Duruoz, and J.S. Harris, Jr., "Low Temperature Scanned Gate Microscopy of GaAs/AlGaAs Nanostructures," in preparation.

Biological X-ray Microscopy

Principal Investigators: W. Meyer-Ilse, J.T. Brown, and D. Attwood

Project No.: 95023

Funding: $40,500 (FY 95)

Project Description

X-ray microscopy is an old idea, which, despite great potential and enthusiasm, did not develop into a widely used tool in biology. Early instruments, particularly those using zone plate lenses, have made regular progress, but have not achieved results that are exciting to the biological community. As firsts of

their kind, these instruments are rather difficult to work with, and generally statements on their performance range from "overstated" to "greatly overstated." With these high expectations, rather challenging biological applications were attracted, but most of these failed, and other less challenging applications have not yet been tested. Therefore, the proof of principle for x-ray microscopy has not yet been achieved. Other modern microscopy techniques, such as the scanning probe and confocal microscopes, have proven useful because a large number of researchers had easy access to these instruments, which were available commercially early on. This has not been the case with x-ray microscopes, which presently require a synchrotron radiation light source for best operation, although we think this will change in a few years with the availability of table-top sized x-ray sources. CXRO is interested in developing x-ray microscopes, which would make x-ray microscopy more widely available. Until then, however, to obtain the proof of principle for x-ray microscopy, we are working closely with biologists to demonstrate the utility of the new instrument, and to build an active user community.

Accomplishments

Using the new High-Resolution Zone-Plate Microscope (XM-1) at the ALS, we developed a number of biological applications for x-ray microscopy. The XM-1 has proven to be a reliable precision instrument for our purposes. The award-winning system for mutually indexing sample positions between the conventional (full-field) x-ray microscope and an integrated, state-of-the-art visible light microscope has enabled us to develop several biological applications. Working together with local and international biologists, we established XM-1 as a new tool in parasitology, investigated novel structures in algae, imaged different chromatin distributions in transgenic sperm cells, and developed techniques for human chromosome imaging. With the XM-1, malaria parasites (see Fig. 8) show details never before seen with visible light or with electron microscopes. (It would be of interest to examine these structures in three dimensions, which would require multiple view capabilities combined with a cryo sample holder.) The sperm cells (Fig. 9) also show great detail and structures never observed *in vitro* with such a high resolution. Transgenic sperm cells appear folded, which is not evident from atomic force microscopy.

The stability of sperm cells against radiation allows for multiple images of unfixed material, which could be utilized in a multiple view (tilt) stage. On the other hand, the work with more radiation-sensitive samples would greatly benefit from a cryo sample holder. Although we were able to take images for up to a few

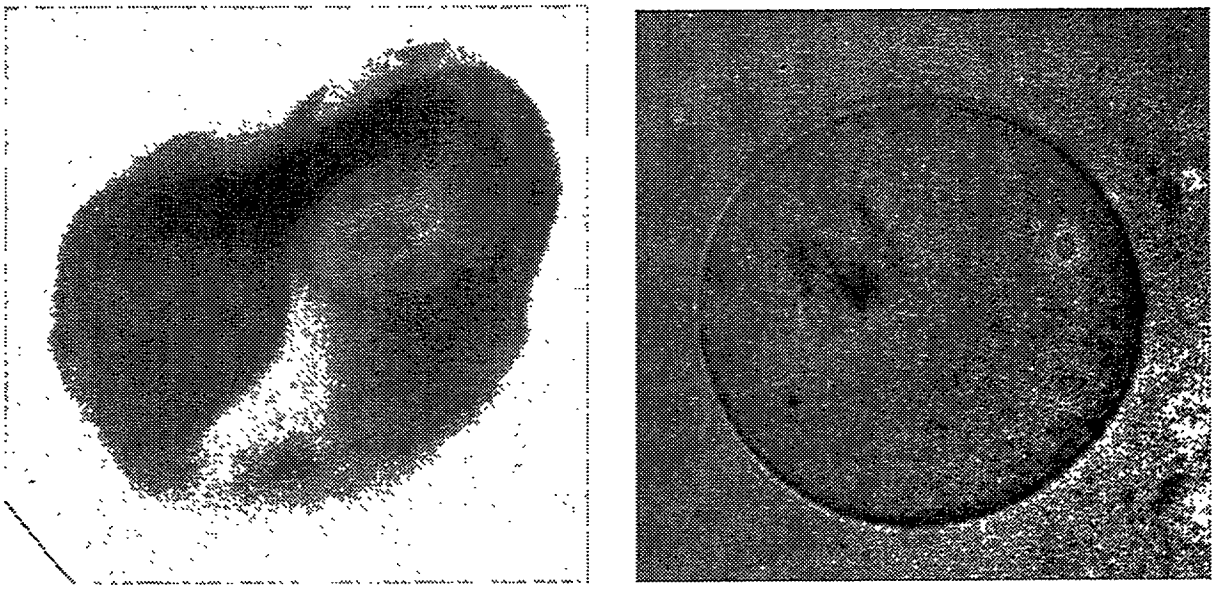

Figure 8. Malaria parasites Plasmodium falciparum *in a human red blood cell (left) and a blood cell ghost (right). Two separate parasites are clearly visible in the left image. (This work was done in collaboration with C. Magowan and M. Moronne, Life Sciences Division, Berkeley Lab.)*

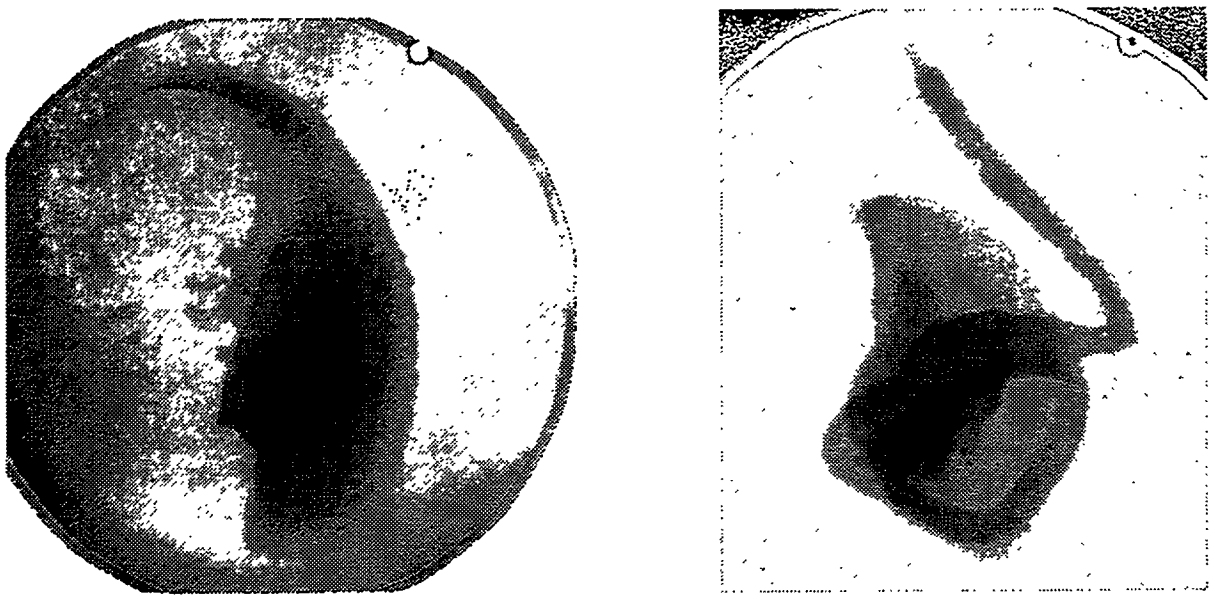

Figure 9. Normal (left) and transgenic (right) sperm cells from mouse in vitro. *These images were taken at 2.4 nm wavelength with a magnification of 2500 and an exposure time of 60 s. (This work was done in collaboration with R. Balhorn, Berkeley Lab.)*

seconds without significant radiation damage, a cryo stage would fix the movement of the sample and permit longer exposure times for better signal-to-noise images. Together with Hector Medecki, we are developing a cryo sample holder and plan, funding permitted, to install multiple view (tilt) capabilities. The results obtained with XM-1 so far show that a modest decrease of dose would notably improve the capabilities of x-ray microscopy. This requires improvements in zone-plate lens efficiencies, which are expected in the near future. For lowest radiation dose, a precision scanning microscope at the ALS would be desirable. Such an instrument would not only minimize the radiation dose to the sample, but also allow us to utilize the advantages of fluorescent labeling techniques.

We used the XM-1 for biological experiments, together with Marie Alberti, Rod Balhorn, Jim Bartholomew, Jacob Bastacky, Tom Ford, Donna Arndt-Jovin, Tom Jovin, Cathie Magowan, Mario Moronne, and Tony Stead. The XM-1's resolution was extensively measured with Yasushi Kagoshima and is occasionally rechecked. With the new zone plates made by Erik Anderson at IBM/Yorktown Heights, we can achieve a resolution better of than 60 nm, measured using a knife-edge test and the 10–90% criterion. This is approximately a factor of only 1.5 away from the theoretical limit. Between May and August of 1995, we recorded about 1350 images, which are still being analyzed by our users. Typical exposure times vary between a fraction of a second to up a few minutes. Although it is relatively uncomplicated to obtain images with this new instrument, the sample preparation is of great importance.

Publications

W. Meyer-Ilse and J.T. Brown, "Biomicroscopy Experiments with XM-1 in Summer 1995," internal report.

W. Meyer-Ilse, C.C. Magowan, and M.M. Moronne, "High Resolution X-ray Microscopy, a New Tool to Investigate Infected Parasites," poster presentation at the Annual Meeting of the American Society of Topical Medicine and Hygiene and the American Society of Parasitologists, San Antonio, Texas, 1995.

Optical Spectroscopy and Microscopy of Magnetic Multilayers

Principal Investigators: Joseph Orenstein and Stuart Parkin (IBM Almaden Research Center)

Project No.: 94020

Funding: $51,400 (FY 95)
$94,400 (FY 94)

Project Description

Synthesis and characterization of artificially structured magnetic materials is a rapidly growing field of research. Recently there has been renewed interest in thin film structures comprised of alternating magnetic and nonmagnetic layers. The interest is fueled by the discovery of huge enhancements in the magnetoresistance (MR) of these structures compared to the MR exhibited by the constituent layers in isolation. This effect, termed giant magnetoresistance (GMR) will be incorporated into the heads used to read data on magnetic disks and tapes. Further advances require the development of new materials and structures that detect magnetic fields with even greater sensitivity.

This program synthesizes novel multilayer structures and develops tools for their characterization. An example of the structures of interest are Co/Cu and Co/Rh multilayers. Although these materials are grown by sputtering, their crystallinity approaches that of MBE-grown materials. The key to achieving excellent crystallinity is the use of a Pt buffer layer between the multilayer and the substrate.

The principal tools for characterization are infrared magneto-optical spectroscopy (IRMOS) and magneto-optical microscopy. In this work, we have used IRMOS as a contactless probe of the in-plane conductivity tensor of GMR films. We have recently constructed a Kerr microscope with submicron resolution for magnetic-domain imaging applications. The microscope images magnetic domains by measuring the spatial variation of Kerr rotation across a sample. This system is designed for studying the role microstructure plays in GMR. Incorporated into the design is the ability to image and measure resistance simultaneously so that correlation of domain structure with transport properties is possible.

Accomplishments

An important problem in magnetic thin films is determining the extent to which the substrate properties influence GMR. We studied Co/Rh multilayers grown on MgO substrates cut so that two different crystalline planes comprise the surface. In one orientation ([100], see Fig. 10[a]), the atoms of the surface are arranged in a square lattice. In the other orientation ([110], see Fig. 10[b]), the atoms form a rectangular lattice and the symmetry of the surface is lowered. The question we sought to answer was whether the anisotropy of the substrate affected the resistivity of the film subsequently grown on top. Our far-infrared optical transmission techniques

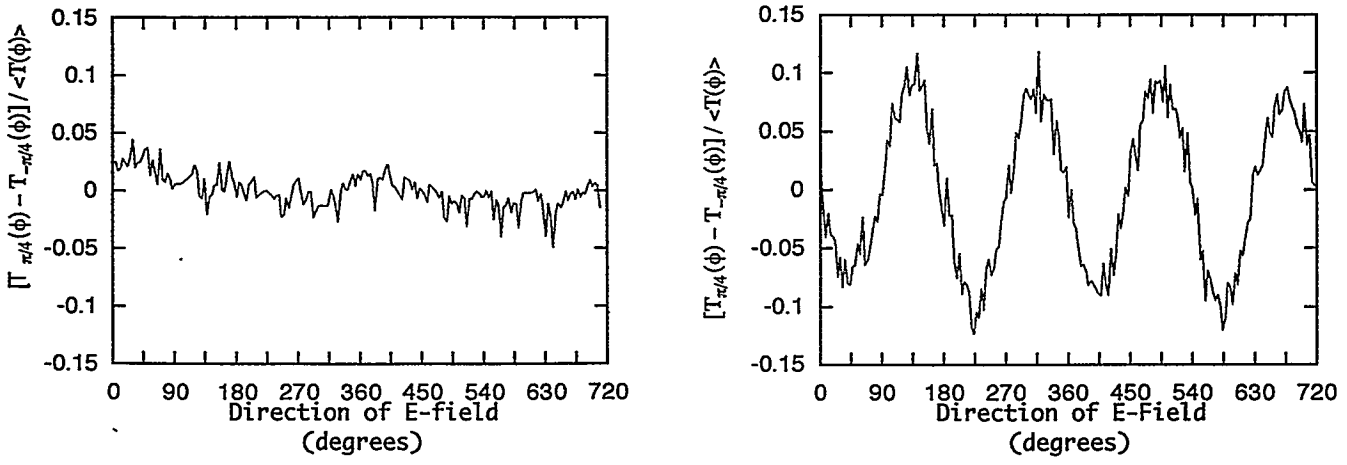

Figure 10. The change in infrared transmission as a function of the direction of electric field vector in the plane of two films: (a) Co/Rh grown on MgO [100]; and (b) Co/Rh grown on MgO [110].

provided an absolute measure of the resistivity anisotropy of the GMR films, and was much more sensitive than conventional transport techniques.

To measure the resistivity anisotropy, we measured the transmission in polarized light as the electric field vector was rotated in the plane of the film. The experimental arrangement is shown in Fig. 11. The infrared source was a Hg-arc lamp, and a ^{4}He-cooled bolometer was used as a detector. The light is polarized by transmission through an array of metallic lines photolithographically patterned on Mylar film.

Figures 10(a) and 10(b) compare the transmission through films grown on MgO [110] and [100] as a function of the electric field orientation. The results beautifully demonstrate the small ($\approx$ 5%) anisotropy in the resistivity of the film in case of the anisotropic substrate. The control (isotropic) substrate results in no conductivity anisotropy.

Our measurements, coupled with x-ray studies and dc magnetotransport measurements, provide a picture of how the substrate affects the GMR. It turns out that the direction with the slightly higher resistivity has a much larger GMR effect. X-ray scattering studies indicate the surface roughness is greater along this axis as well. These observations support the view that spin-dependent interfacial scattering of electrons is the dominant operative mechanism in GMR.

New Directions

Nonlinear optical techniques have recently been employed as probes of interface magnetism. Because symmetry breaking occurs only at the boundaries between distinct centrosymmetric media, second harmonic generation is an excellent probe of interface behavior in our multilayers. We are constructing a microscope to image the second harmonic generation efficiency in magnetic films. Our goal is to couple this system to our Kerr microscope in order to gain a new perspective on microstructure and dynamics affecting GMR.

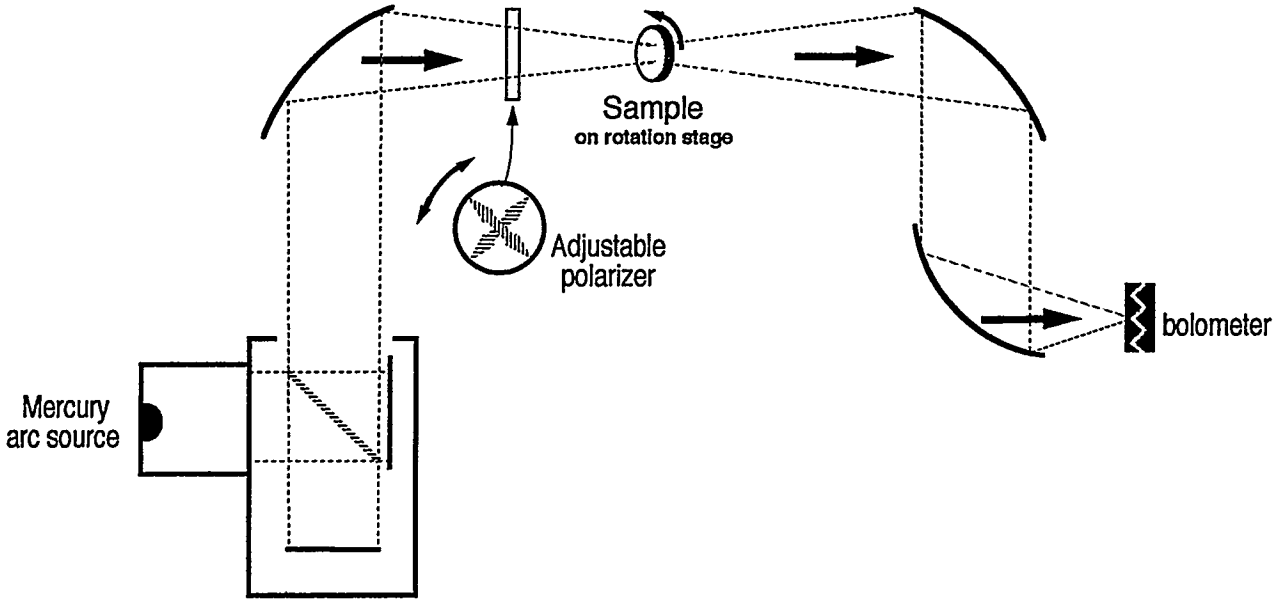

Figure 11. Infrared magneto-optical spectrometer for the measurement of transmission as a function of the angle of the electric field in the plane of a thin film. The polarized transmission is a direct probe of the conductivity of resistivity tensor of the film.

Establishment of the Thermodynamic Temperature Scale in the mK Region

Principal Investigator: Norman Phillips

Project No.: 94021

Funding: $53,100 (FY 95)
$76,700 (FY 94)

Project Description

There are a number of important areas of basic research in condensed-matter physics that have been hampered by the lack of an accurate, well-documented, and easily reproduced temperature scale in the mK region. The most notable examples include ^{3}He, both the normal Fermi-liquid phase and the superfluid phases, and heavy-fermion compounds, particularly heavy-fermion superconductors. Research on these materials could provide definitive tests of Fermi-liquid theory and theories of strongly correlated electron systems, which are of fundamental importance in many branches of condensed-matter physics.

In the 1970s, research at NBS (National Bureau of Standards), now NIST (National Institute of Standards and Technology), with noise and nuclear-orientation (NO) thermometers had already led to the development of a scale down to 16 mK. That scale was promulgated on "fixed-point devices"—devices that contained five superconductors with specified transition temperatures between 16 and 200 mK. These devices are generally recognized as the best available temperature standards in that region, but, because the fixed-point devices do not provide *thermodynamic* standards, the results of this research were not incorporated into the current International Temperature Scale, ITS-90.

ITS-90, the low-temperature end of which is defined in terms of the vapor pressure of ^{3}He, extends only to 0.65 K—and there is reason to suspect small but significant errors even in that scale below 1 K. It is probable that there will be international agreement on a temperature scale to lower temperatures in a few years, but the scale will be based on the melting pressure (or melting curve, MC) of ^{3}He. The MC scale offers a number of attractive features:

- Good sensitivity to below 1 mK.
- The scale is defined continuously.
- Like ITS-90, it is based on a *thermodynamic* property, but in addition there are *thermodynamic* fixed points—three between 1 and 3 mK, and one at 316 mK—that serve as both temperature and pressure standards.
- It is relatively insensitive to magnetic field.
- It is relatively free of the materials problems associated with, for example, superconducting fixed points and resistance thermometers.

The fixed points on the MC scale are an enormous advantage in comparing the realization of the scale between different laboratories and offer a striking improvement relative to the higher temperature vapor-pressure scale for which such comparisons are not reliable. Although there is research in other countries directed to the establishment of the new scale, at this time there is no significant relevant effort in the U.S. The most important element of the project is to extend the MC scale to include the thermodynamic fixed points in the 1–3 mK region.

The instrumentation for the NIST program is largely intact, the cryostat is still usable for that work, and the Director of NIST has made the facility available for our research. Thus, there would be an excellent opportunity to do some preliminary work that would be crucially important to re-establishing the temperature scale project at Berkeley. A timely and significant contribution would also be made to the extension of ITS-90 to lower temperatures.

Accomplishments

Nuclear Cooling Stage

The nuclear cooling stage is essentially complete. A modified technique for soldering Cu wires to the $PrNi_5$ rods has been successfully developed; the power supplies and computer control for the magnetization and demagnetization, including temperature regulation by controlling the field, have been assembled; a modified vacuum can to attach the magnet and cooling stage to the NIST cryostat has been completed.

CMN Thermometry

The cerium magnesium nitrate (CMN) single crystals have been machined and mounted; the mutual inductance bridge has been modified to eliminate a problem that derived from loading of the ratio transformer.

Preparation for Work on the Melting Pressure Scale

A considerable amount of work has been done in intercomparing various Berkeley Lab and NIST thermometers that will be useful in checking the reproducibility of the melting pressure scale. The Berkeley S.R.M. (superconducting fixed point device) has been compared with the NIST "standard" S.R.M.; several additional comparisons of the Berkeley and NIST Rh-Fe thermometers have been made; the piston gauge has been improved by adding a capacitance gauge to measure the pressure in the bell jar (for which a correction must be made); the weights for the gauge have been calibrated. These improvements bring each source of error to ~1 ppm or less.

Although both the preliminary CMN and melting pressure measurements are "ready to go," progress has been impeded by a failure of the $^3He/^4He$ refrigerator, which required some months for repair, and by competition for time with the NIST group that uses the cryostat. We have been promised one run to ourselves in January (the experiments we have done have been done in a dual experiment mode), and we should be able to mount the nuclear cooling stage soon thereafter.

Investigation of Nanometer Magnetism by Using Surface Magneto-Optic Kerr Effect (SMOKE)

Principal Investigator: Zi Q. Qiu

Project No.: 94022

Funding: $59,800 (FY 95)
$25,700 (FY 94)

Project Description

The unique character of the transition metal magnetism is the hybridization of the magnetic electrons with the conduction electrons of the substrate. Thus, it is possible to manipulate the magnetic properties of materials by changing their crystal structure, which has a strong effect on the conducting electrons.

Epitaxial growth of ultrathin films provides a perfect way of stabilizing metastable structural phases because the strain built up in ultrathin film can persist to a certain thickness before relaxing into its bulk form. In addition, the direct hybridization of the electron bands between the substrate and the overlayer provides additional freedom to modify the magnetic properties of a thin film. Thus, it will be very interesting to investigate the metastable phases of the transition metal magnetic thin films.

To explore physical quantities that vary on the atomic scale, we developed the so-called wedged samples. With a wedged sample that has an extremely small slope (10^{-7}), detailed features within one monolayer thickness can be readily explored by measuring the corresponding quantity at different positions on the wedge. In this project, we use SMOKE laser as the probe beam to scan across the wedge to measure the magnetizations at different thicknesses.

Accomplishments

Following the setup of a UHV system, we made significant progress in the past year in the synthesis and characterization of magnetic ultrathin films. We have been able to synthesize new phases of materials that show fascinating properties. In particular, we were able to stabilize the fcc structure of Fe films on Co(100) single crystals. The nature of the structure of Fe is bcc. The fcc phase of Fe exists only at high temperatures (>910°C). Using the MBE technique, we were able to fabricate ~11 atomic layers of the fcc phase of Fe at room temperature. With the aid of the magnetic interaction with the ferromagnetic Co substrate, the magnetic ordering temperature of the fcc Fe was pushed well above room temperature. RHEED and LEED studies indicate that there are two structural phases in the fcc Fe films: fct and fcc. Associated with these two structural phases, the fcc Fe alternates its magnetic nature from a ferromagnetic phase to an antiferromagnetic phase. Using wedged samples, the magnetic properties of the fcc Fe were explored in detail. The following figures summarize our results. Figure 12 is the RHEED intensity during the growth of Fe on fcc Co(100) substrate. Region I has fct structure, Region II has fcc structure, and Region III is the natural bcc phase. Figure 13 is the Kerr intensity as a function of the film thickness. The Kerr intensity is proportional to the film magnetization. In Regions I and III, the Kerr intensity increases linearly as the film thickness increases, indicating a ferromagnetic phase in these two regions. In Region II, the Kerr intensity drops to almost zero and remains as a constant, indicating that the magnetic nature in this region is antiferromagnetic. The fact that the Kerr intensity in Regions I and III follows the same straight line suggests that the magnetic moment of the Fe remains unchanged when the structure changes from bcc to fcc.

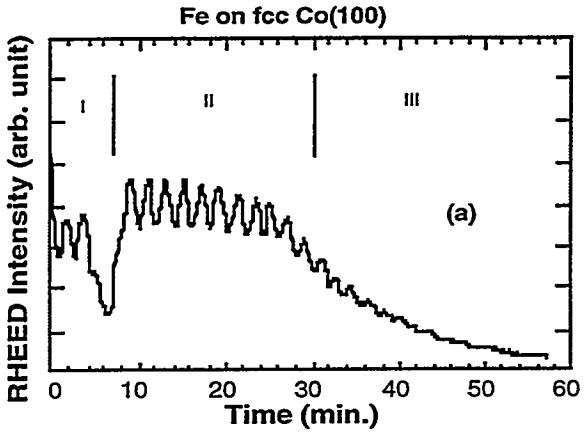

Figure 12. RHEED oscillations during the growth of fcc Fe on fcc Co(100). Three distinct regions can be identified.

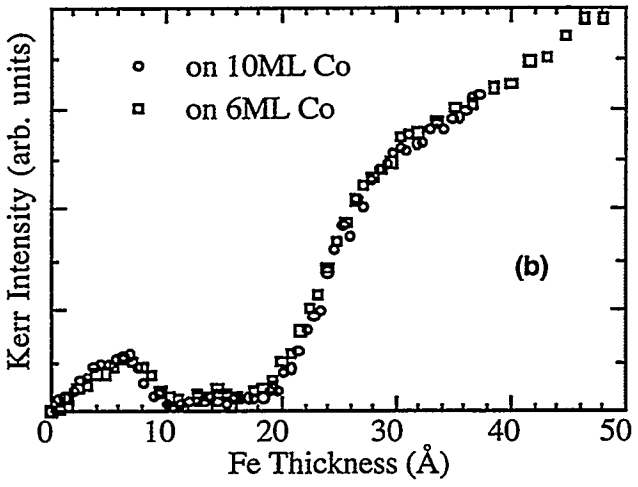

Figure 13. SMOKE measurements on fcc Fe wedges show different magnetic behaviors in the three regions identified by RHEED oscillations.

Publications

Z.Q. Qiu, "Investigation of Magnetic Thin Films Using Wedged Samples," invited talk at the 42nd American Vacuum Society Conference, Oct., 1995.

R.K. Kawakami, E.J. Escorcia-Aparicio, and Z.Q. Qiu, "Antiferromagnetic Coupling in Co/fcc Fe/Co Sandwiches," to be published in *J. Appl. Phys.*

E.J. Escorcia-Aparicio, R.K. Kawakami, and Z.Q. Qiu, "Structural and Magnetic Properties of fcc Fe Films Grown on Co(100)," to be published in *J. Appl. Phys.*

Nanosynthesis

Principal Investigators: Peter G. Schultz and Paul McEuen

Project No.: 94025

Funding: $91,500 (FY 95)
$56,200 (FY 94)

Project Description

The application of the tools of synthetic chemistry to the construction of nanostructures with complex architectures and interconnections requires the development of new techniques. We propose to develop a technique whereby highly localized chemical catalysis on surface atoms or molecules can be carried out using a scanning probe device. By varying the nature of the catalyst and the chemical composition of the surface, it may be possible to construct molecular assemblies not readily accessible by existing microfabrication techniques. This methodology should, for example, make possible the construction of interconnected two-dimensional arrays of nanostructures for sensory or electronic applications.

Modern chemical synthesis has made possible the assembly of such complex molecular structures as the natural product palytoxin and the protein HIV protease. However, in comparison, approaches for the synthesis of nanostructures with comparable control over molecular composition and architecture are still in their infancy. One strategy that offers considerable promise is the adaptation of scanning tunneling or force microscopy to manipulate atoms and molecules on surfaces. These techniques allow imaging of surfaces with atomic resolution and have become important analytical tools in materials science, nanolithography, catalysis science, and, more recently, in the analysis of biomolecules. In addition, both atomic force microscopes (AFMs) and scanning tunneling microscopes are being used to directly modify surfaces, electrochemically as well as mechanically. However, the latter applications are currently limited in resolution and the complexity of structures that can be fabricated. The potential of these approaches for constructing novel nanostructures would be enhanced significantly if the resolution of these microscopes could be combined with the wide array of catalytic transformations available in chemistry.

This project intends to develop an AFM in which the scanning probe has been modified with a metal catalyst that can be used to chemically modify the surface of a self-assembled monolayer (SAM) in a spatially defined fashion. Spatial resolution will be achieved by localization of the catalyst using the scanning probe. The chemically modified surface can be further covalently modified in a second step to generate more complex two-dimensional architectures.

In principle, many different heterogeneous catalysts can be supported on an AFM tip, making possible a variety of chemical transformations, including hydrogenolyses, oxidations, coupling, and polymerization reactions. The system we are initially choosing to investigate uses a platinum catalyst to hydrogenate an azide-derivatized SAM to generate alkyl amino groups with concomitant release of N_2. This catalytic reaction is known to have a very low activation energy and yields no byproducts that could lead to inactivation of the catalytic tip. Because metal-bound hydride is the likely reactive species, the catalytic reaction is also expected to occur only at hose sites in which the tip contacts the surface, resulting in high spatial resolution. In addition, since the reaction occurs only in the presence of a hydrogen donor such as H_2, the reaction can be easily terminated by simple removal of H_2. Finally, free amino or hydroxy groups can be derivatized in high yield in a secondary reaction by a host of molecules, including acids, aldehydes, and metal complexes.

Accomplishments

Highly localized chemical catalysis was carried out on the surface groups of a self-assembled monolayer with a scanning probe device (Fig. 14). With the use of a platinum-coated atomic force microscope tip, the terminal azide groups of the monolayer were catalytically hydrogenated with high spatial resolution. The newly created amino groups were then covalently modified to generate new surface structures. By varying the nature of the catalyst and the chemical composition of the surface, it may be possible to synthesize molecular assemblies not readily produced by existing microfabrication techniques.

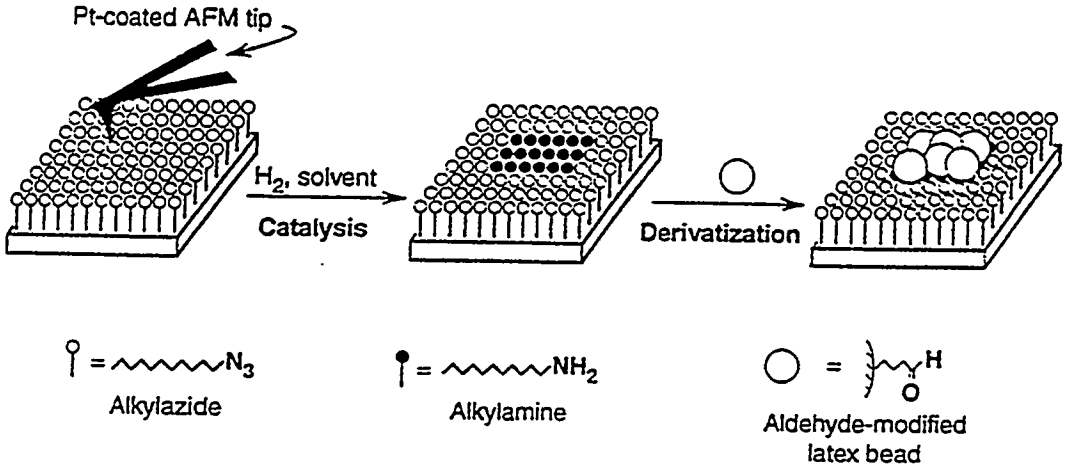

Figure 14. Scanning with a platinum-coated AFM tip over a SAM surface containing terminal azide groups in the presence of H_2 leads to the reduction of azide groups to primary amino groups. Derivatization of the resulting amine surface with aldehyde-modified latex beads or ATTO-TAG results in specific labeling of the reduced areas.

Publication

W.T. Müller, D.L. Klein, T. Lee, J. Clarke, P.L. McEuen, and P.G. Schultz, "A Strategy for the Chemical Synthesis of Nanostructures," *Science* **268**, 272 (1995).

A Combinational Approach to Materials Science

Principal Investigator: Peter G. Schultz

Project No.: 94026

Funding: $83,600 (FY 95)
$184,800 (FY 94)

Project Description

The purpose of this research is to develop a more time-effective, systematic, and economical strategy for the synthesis of new materials. This goal will be accomplished by developing a methodology that allows the parallel synthesis and analysis of new materials with novel electronic, magnetic, optical, and mechanical properties. Such a methodology would allow one to synthesize and characterize materials approximately 10^3 to 10^5 times faster than the current rate. The ability to rapidly synthesize and analyze large libraries of materials should lead to new and exciting solid-state materials composed of previously unexplored combinations of elements. Moreover, the synthesis and analysis of large numbers of diverse chemical structures should add significantly to our understanding of and ability to predict the structural and physical properties of solid-state materials.

The discovery of new materials with novel physical and chemical properties often leads to the development of useful new technologies. Currently, there is tremendous activity in phenomena such as superconductivity, supermagnetic alloys, nonlinear optics, and high-strength materials. However, even though the chemistry of extended solids has been extensively explored, few general principles have emerged that allow one to predict the composition, physical properties, and reaction pathways for the synthesis of such solid-state compounds. Consequently, the discovery of new materials depends largely on the synthesis and analysis of new compounds. Given the approximately 100 elements in the periodic table that can be used to make compositions consisting of three, four, five, or even six elements, the universe of possible new compounds remains largely unexplored. The question then arises whether there is a more efficient, economical, systematic way to discover new materials with novel properties.

One of the processes whereby nature produces molecules with novel functions involves the generation of large collections (libraries) of molecules and systematic screening of these libraries for those molecules with a desired property. One such example is the humoral immune system, which in a matter of weeks sorts through some 10^{12} antibody molecules to find one that specifically binds a foreign pathogen. Recently, this notion of generating and screening large collections of molecules has been applied to the drug discovery process. The discovery of new drugs can be likened to the process of finding a key that fits a lock of unknown structure. One solution to the problem is to simply produce and test a million different keys in the hope that one will fit the lock. Methods have recently been developed for the synthesis of large libraries (up to 10^{12} molecules) of peptides, oligonucleotides, and other small molecules on a time scale of days. This approach promises to have a huge impact on the pharmaceutical industry. Biotechnology companies are being founded to pursue this new opportunity (and currently represent investments of hundreds of millions of dollars and hundreds of new jobs), and most major pharmaceutical companies are building research programs in this area.

This project is to apply this same combinatorial approach to the discovery of new materials. The design of new materials, like drugs, is largely an empirical trial-and-error process. Although theory can provide some guidance, the synthesis and characterization of large numbers of compounds remain the only way to generate materials with new properties. A combinatorial approach toward materials science should be applicable to a large number of targets, such as magnetic materials, efficient heterogeneous catalysts, and doped polymers with novel optical and mechanical properties. We have picked as our first target the combinatorial synthesis of high-temperature superconducting materials. Clearly, high-temperature superconductors represent a target of tremendous practical and theoretical interest. The development of room-temperature superconductors would have an enormous impact on modern technology and industry.

Accomplishments

We reported the first application of the combinatorial approach to the discovery of new solid-state materials with novel physical or chemical properties. Specifically, methodology has been developed that allows the parallel synthesis of spatially addressable arrays containing superconducting copper oxide thin films. Thin film deposition methods are synthetically quite versatile; they offer the ability to construct artificial lattices, epitaxial overlayers, and patterned films of a variety of materials. By sequentially depositing the individual precursors of interest through a series of physical masks, it is possible to generate a spatially defined library of solid-state thin films. Each sample can be varied with respect to elemental composition, the sequence in which the layers are deposited, and the thickness of each layer (including thickness gradients). Subsequent thermal processing provides a library of materials (or devices) whose physical properties can be screened with contact or rapid-scanning probes. The number of compounds that can be simultaneously synthesized by this technique is limited by the spatial resolution of the masks and detectors and by the degree to which synthesis can be carried out on a microscale.

In addition to the above results, the recent development of methods for generating libraries of solid-state compounds has made it possible to apply combinatorial approaches to the discovery of materials. A library of 128 members containing different compositions and stoichiometries of $Ln_xM_yCoO_\delta$ where Ln = Y or La, and M = Pb, Ca, Sr, or Ba, was synthesized by a combination of thin-film deposition and physical masking techniques. Large magnetoresistance has been found in $La_x(Ba, Sr, Ca)_y$-CoO_δ samples, whereas Y-based samples exhibit much smaller magnetoresistive effects. The magnetoresistance of the Co-containing compounds increases as the size of the alkaline earth ion increases, in sharp contrast to Mn-containing compounds, in which the magnetoresistance effect increases as the size of the alkaline earth ion decreases.

Publications

G. Briceño, H. Chang, X. Sun, P.G. Schultz, and X.D. Xiang, "A Class of Cobalt Oxide Magnetoresistance Materials Discovered with Combinatorial Synthesis," *Science* 270, 273 (1995).

X.-D. Xiang, X. Sun, G. Briceño, Y. Lou, K.-A. Wang, H. Chang, W.G. Wallace-Freedman, S.-C. Chen, and P.G. Schultz, "A Combinatorial Approach to Materials Discovery," *Science* 268, 1738 (1995).

Spin-Polarized Photoemission Studies of Magnetic Surfaces, Interfaces, and Films

Principal Investigator: Neville Smith

Project No.: 94027

Funding: $409,900 (FY 95)
$124,300 (FY 94)

Project Description

Photoemission spectroscopy with spin analysis is a valuable method for the study of magnetic systems. The electronic structure of the two spin populations can be determined separately, and one can also infer magnetic alignment in thin films. A call for a stronger research effort in magnetic technology has been emphasized in a number of national reports, and has received reinforcement from the recent discovery of magnetic multilayers with useful transport properties. The ALS is poised to become the world's leading facility for magnetic spectroscopies such as spin-polarized photoemission and x-ray circular dichroism.

The immediate purpose of this proposal is to foster the introduction of spin analysis technology at the ALS. Spin-polarized photoemission will be a major element of the planned undulator beamline. The ultimate goal is to fold the developments of this project into a larger magnetic materials program. Acquisition of the spin-detection technology constitutes a stand-alone, self-contained project.

Accomplishments

Activity during FY 95 was devoted to equipment building and acquisition. In addition, it was decided to expand the scope of the project to include magnetic microscopy, which will perform spin-polarized photoemission and magnetic circular dichroism spectroscopy with fine spatial resolution.

Spin Analysis

Having made the decision to proceed with the "mini-Mott" method of spin analysis, a contract for the construction of such a detector was placed with Florida State University through our collaboration with Professor David Lind of the FSU Physical Department. Delivery is expected in June 1996, at which time the detector will be attached to the back end of the state-of-the-art Scientia photoelectron energy analyzer belonging to Professor Charles Fadley on Beamline 9.3.2 at the ALS. Debugging will commence, and the detector is expected to perform experiments with emphasis on spin-polarized photoelectron diffraction.

Circular Polarization

A quarter-wave phase retarder of the transmission-multilayer type has been designed and constructed at Berkeley Lab under the supervision of Jeff Kortright. The instrument has been installed in an available straight section of the undulator Beamline 7.0, and alignment and characterization studies have already begun. The instrument is shown in Fig. 15. Experiments will start in early 1996, and will focus on magnetic circular dichroism in resonant photoemission from ferromagnetic and rare-earth films (in collaboration with Jim Tobin and Roy Willis), and on microscopy of magnetic thin films using the zone-plate scanning transmission x-ray microscope (in collaboration with Tony Warwick).

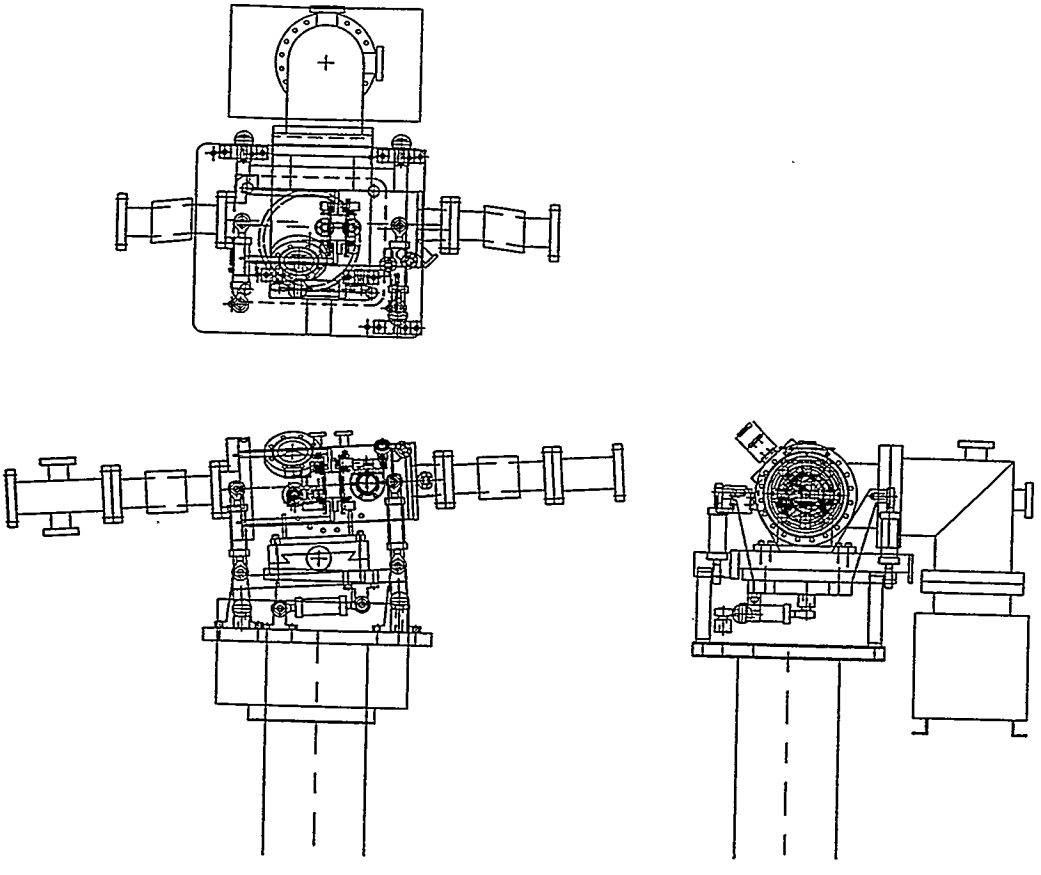

Figure 15. Drawings of the quarter-wave retarder installed on beamline 7.0 at the ALS.

Catalytic Routes to a Cleaner Environment

Principal Investigators: Gabor A. Somorjai, Mark D. Alper, Alexis T. Bell (Program Leaders); with Peter G. Schultz, Jay Keasling, and Fabio H. Ribeiro (Investigators)

Project No.: 95013

Funding: $173,300 (FY 95)

Project Description

As a result of preliminary studies, it was determined that a three-pronged approach to studies of catalytic routes to a cleaner environment was most appropriate to the study and the funding level. In one study, the release of methane, a greenhouse gas, from natural gas-burning automobiles is examined. Heterogeneous catalysts for the removal of that residual gas are pursued. In the second study, the techniques of catalytic antibody generation are used to create an enzyme-like catalyst for the degradation of toxic substances. Availability of this catalyst should greatly increase our understanding of and ability to enhance detoxification of a wide variety of pollutants. The third study, metabolic engineering of catalytically activated pathways in organisms, focuses on the production of biodegradable plastics by bacteria. Use of these plastics would decrease dependence on petroleum, decrease production of harmful byproducts in the production of the plastics, and decrease waste upon disposal.

Accomplishments

Release of Methane

The combustion of exhaust from natural gas-burning vehicles contains small amounts of residual methane (< 1000 ppm), which must be converted to less potent greenhouse species before release into the environment. This conversion requires catalytic methane oxidation in a post-engine convertor (at about 600 K) in the presence of high concentrations of CO_2 and H_2O. While Pd is the most active catalyst for methane oxidation, its activity becomes significant only at temperatures well above 600 K. Our efforts have focused on understanding the factors limiting the activity of Pd. In experiments conducted with Pd/ZrO_2, we have found that the activity of Pd is critically dependent on maintaining the catalyst in an oxidized state as PdO. Excessive heating of the catalyst during the calcination step of catalyst preparation, or inadequate supply of oxygen during reaction, can lead to the conversion of PdO to Pd and a significant loss in catalyst activity. The effects of Pd particle size and support composition, and the presence of water and carbon dioxide in the gas phase are currently being investigated to determine the influence of these factors on the state of Pd oxidation.

Creation of an Enzyme-like Catalyst

A major detoxification pathway used by aerobic organisms involves the conjugation of the tripeptide glutathione (GSH) to the electrophilic center of toxic substances. This reaction is catalyzed by a class of enzymes referred to as the glutathione S-transferases (GST) (EC 2.5.1.18). These enzymes activate the cysteine thiol group of GSH for nucleophilic addition to a variety of substrates, including aryl halides, a,b-unsaturated aldehydes and ketones, and epoxides. Despite the availability of the x-ray crystal structure, the mechanism whereby glutathione transferases catalyze these addition reactions remains unclear. In order to gain a greater understanding of this important biological transformation, as well as to generate new detoxification catalysts, we are investigating whether antibodies can be generated that catalyze similar nucleophilic addition reactions.

Our initial efforts focused on the addition reaction of thiol nucleophiles to the nitro-substituted styrene derivative 1 (Fig. 16). This reaction, which is typical of those catalyzed by GST, involves the formation of a negatively charged transition state. Hapten 4 was designed as an analog of the transition state for adduct formation. The negatively charged carboxylate group of 4 was expected to mimic the negative charge on the aryl nitro group in the transition state. In addition, the polar character of the sulfonamide group

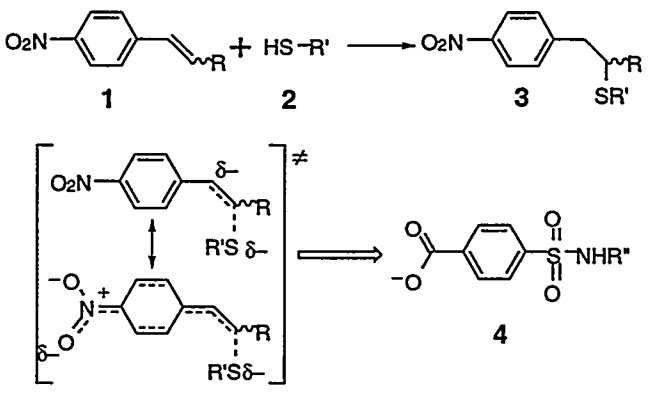

Figure 16. Antibody-catalyzed nucleophilic addition reaction.

might be expected to elicit residues in the antibody combining site capable of electrostatically stabilizing negative charge buildup on the benzylic carbon during the addition reaction.

Two antibodies were identified that catalyze this reaction. Catalysis followed Michaelis–Menten kinetics, and the Lineweaver–Burk plots for both antibody-catalyzed reactions were made. At pH 8.0, the apparent values of kcat and Km for the formation of nucleophilic addition adduct at a fixed concentration of nucleophile 2a (60 mM) were determined: background reaction kuncat = 1.2 4 10-6 s-1; mAb 19F3.1, kcat = 2.2 4 10-3 s-1, Km = 12.6 mM; mAb 19F4.1, kcat = 2.0 4 10-3 s-1, Km = 12.9 mM. The rate accelerations, kcat/kuncat, are 1.8 4 103 (19F3.1) and 1.7 4 103 (19F4.1).

Metabolic Engineering of Catalytically Activated Pathways

A number of years ago it was discovered that a biodegradable, microbial storage polymer, polyhydroxyalkanoate, could replace nonbiodegradable plastics in many applications. By manipulating the culture conditions, one can force a number of microorganisms to accumulate these polymers. Furthermore, it is possible to control the composition of the polymer by addition of supplements to the bacterial growth medium. Known polymers of this type, however, are expensive to produce and purify, and therefore cannot compete well with other plastics. Our methodology is to redirect microbial metabolism and create a new process to produce less expensive, biodegradable polymers that will compete effectively in world plastic markets.

The first step in the proposed work was to develop a model to predict how a redirection of the central metabolic pathways towards the production of the biopolymer polyhydroxybutyrate (PHB) would affect cell growth. At the same time, we began to genetically engineer the host cell, *Escherichia coli*, to divert acetyl-CoA utilization away from acetate secretion towards PHB production.

Development of a Flux-based Model. To predict how the central metabolic pathways should be balanced with the pathways necessary for growth, we developed a steady-state mathematical model to predict fluxes through the various metabolic pathways. This model has been formulated from the known stoichiometry of the metabolic pathways in *Escherichia coli*:

$$\frac{dx}{dt} = \mathbf{S}\cdot\mathbf{v} - \mathbf{b}$$

where **x** is the vector of metabolites, **S** is the stoichiometric matrix, **v** is the vector of reaction rates, and **b** is the demand vector. The demand vector is essentially the requirements to build a cell at a given growth rate (i.e., the necessary amino acids, nucleotides, fatty acids, cell wall components, etc.). As the composition of the cell and the products secreted into the medium vary with growth rate, the demand vector is a function of the growth rate (μ) and the amount and composition of the desired product (p):

$$\mathbf{b} = fn(\mu, p)$$

Since many metabolites participate in multiple metabolic pathways and since there are cyclic pathways in the cell (i.e., TCA cycle), there are more reactions than metabolites (more equations than unknowns). At steady state, one can solve for **v** using the Simplex algorithm by maximizing (or minimizing) a combination of the variables and by placing constraints on the variables. Since the model predicts how the fluxes through the metabolic pathways must be distributed in order to achieve a specific growth rate and product, one can compare the fluxes through the metabolic pathways under various growth conditions and predict which metabolic pathways will be regulated. As an example of the model predictions, we have compared the metabolic fluxes for a cell growing in glucose minimal medium to a cell growing on acetate. The model predicts a significant flux through the glyoxylate bypass in agreement with experimental data. In contrast, the glyoxylate shunt remains closed during growth on glucose or glucose plus acetate. Thus, the model is able to predict which metabolic pathways must be regulated for optimal growth. In the future, we will use the model to predict optimal fluxes of precursors necessary for the production of polyhydroxyalkanoates of a specific composition.

Redirection of Acetate to Polyhydroxyalkanoates. The production of PHB involves the condensation of two acetyl-CoA molecules. In order to divert flux from acetate secretion to production of PHB, we transformed an acetate-secretion mutant (BW16463, *pta ackA*) and its parental strain (BW13711) with a high-copy plasmid (pAET41, compliments of A. Sinskey, MIT) carrying the genes for PHB synthesis. The parental strain carrying the PHB genes secreted less acetate into the medium than the same strain without the plasmid (Fig. 17[a]). The PHB content of the parental strain carrying the *phb* genes was approximately 6% of the dry cell weight (Fig. 17[b]); PHB in the strain with no *phb* genes was undetectable.

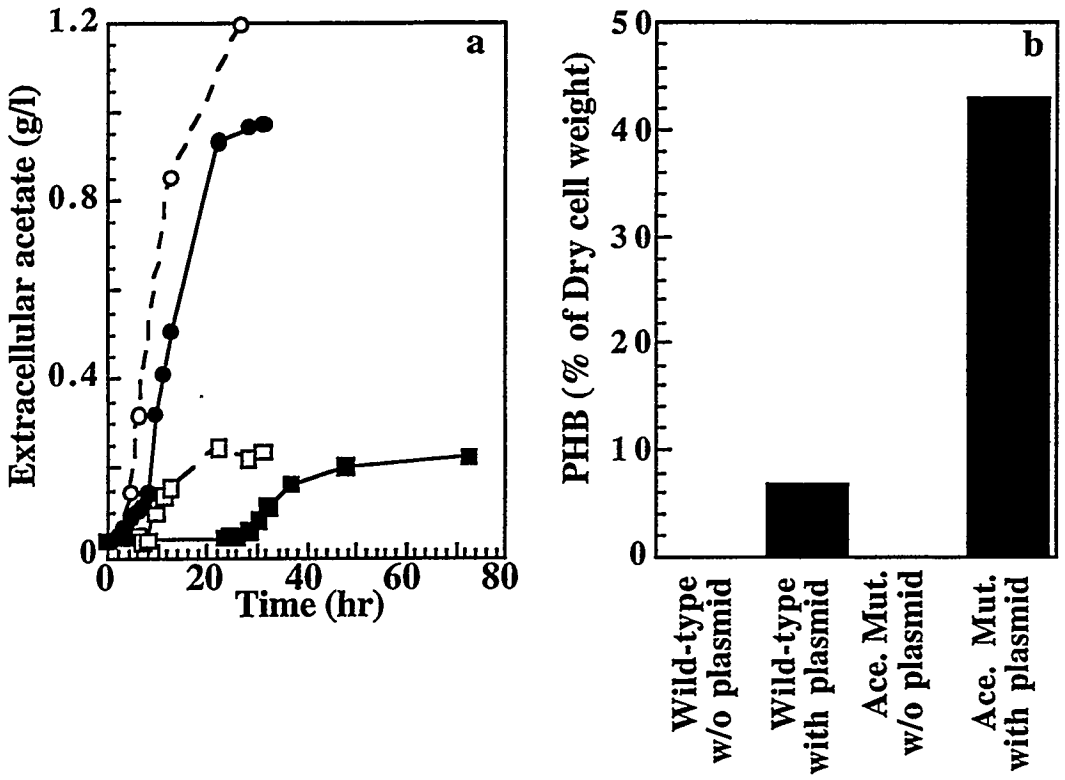

Figure 17. Acetate secretion and PHB production in genetically-engineered acetate mutant and parental strains. (a) Acetate secretion in medium. Open circles: parental strain with no plasmid. Filled circles: parental strain with pAET41 plasmid. Open squares: acetate mutant with no plasmid. Filled squares: acetate mutant with pAET41 plasmid. (b) PHB production.

In contrast, the acetate mutant secreted significantly less acetate into the medium than the parental strain, and the acetate mutant carrying the *phb* genes produced sevenfold more PHB (43% of the dry cell weight) than the parental strain carrying the *phb* genes.

These results are significant for two reasons. First, acetate secretion is an important and unresolved problem in the fermentation industry. Secretion of acetate lowers the pH and reduces productivity. Rerouting excess acetate to formation of PHB reduces acetate secretion and may eventually lead to improved productivity of industrial fermentations. Second, these preliminary results indicate that it should be possible to synthesize copolymers of polyhydroxybutyrate-polyhydroxyvalerate (PHB-co-PHV) in the specified monomer ratios necessary for the production of an economically-viable, biodegradable polymer.

Publications

J. Pramanik and J.D. Keasling, "Flux Distributions Through Metabolic Pathways in *Escherichia coli* Under Various Growth Conditions," to be submitted to *Biotechnology & Bioengineering*.

N. Eliashberg and J.D. Keasling, "Redirection of Acetate to Polyhydroxyalkanoates During Growth of *Escherichia coli* on Glucose," to be submitted to *Biotechnology & Bioengineering*.

E. Fan, Y. Oei, E. Sweet, P.G. Schultz, "Antibodies with Thiol-S-Transferase Activity," submitted to *J. Am. Chem. Soc.*

Time-Resolved Studies of VUV, XUV, and Soft-X-Ray Photo-Induced Chemistry at Surfaces

Principal Investigator: Harry W.K. Tom

Project No.: 93020

Funding: $78,000 (FY 95)
$68,600 (FY 94)
$123,800 (FY 93)

Project Description

The purpose of this research is to study mechanisms by which high-energy photons (VUV, XUV, and soft-x ray) can induce surface chemical reactions. The subtopics of photon-stimulated desorption (PSD) and desorption induced by electronic transitions (DIET) have been a particularly rich and active field of research within surface science and the synchrotron communities. In contrast to previous work that has been limited to the study of ions that have already desorbed from the surface, the intent of our investigations is to probe the atoms or molecules as they react and evolve on the surface, and therefore allow the study of more complex chemical behavior than desorption. The mechanisms of photon-stimulated chemistry are particularly relevant to semiconductor XUV and soft-x-ray photolithography. A better understanding of the reaction mechanisms may open new ways of manipulating surface photochemistry and improving semiconductor processing.

Our experimental approach is to try to time resolve as much of the surface chemical process as possible. This is done by pump-probe spectroscopy using a variety of pump and probe pulses, all with 30–40 fs duration. One measures the change in the probe pulse signal due to the earlier time-arrival of the pump. The probe is either optical second-harmonic generation, photoemission, or total desorption yield. We have approached the topic of x-ray induced surface processes in 3 ways: time-resolved x-ray measurement of core-hole lifetime, studies of surface chemistry enhanced by hot secondary electrons, and studies of hot phonon distributions created by laser excitation of surfaces.

To date there have been no time-resolved measurements of the lifetime of any core-hole excitation. For core holes in atoms, the photoemission spectrum linewidth is probably indicative of the homogenous lifetime. However, in solids, the dominant relaxation processes are complex, involving valence and conduction-band electronic states as well as other higher-lying core states. The x-ray photoemission spectrum is dominated typically by inhomogeneous broadening due to phonons. This broadening is about 20 times as wide as the homogeneous linewidth. In addition to phonon broadening, there are other broadening mechanisms for surface states and adsorbates estimated to be approximately three times the homogeneous lifetime broadening. Time resolving the core-hole lifetime is the only direct measurement of the lifetime. Lifetimes are expected to be <100 fs for most holes. In most cases, hole lifetimes of order 2–10 fs are expected. While we cannot hope to measure such short lifetimes at the present, a direct measurement of some of the longer lived states can help us verify the physics and the relaxation-rate calculations used to predict core lifetimes. By extension, we may then estimate the shorter lived states. Knowing the lifetimes is essential in understanding direct photo-induced chemistry. Long-lived states can efficiently couple electronic energy to atomic kinetic energy and are expected to play a role in ion ejection from surfaces. Short-lived states are expected to be efficient channels of obtaining x-ray absorption and secondary electrons (low-energy electrons) but to be inefficient for direct photo-induced processes.

Our second approach has been to explore the role of hot low-energy electrons in surface chemistry. XUV and x-ray photoexcitation leads to a transient (100–300 fs) and local distribution of hot secondary electrons. The initial core hole is filled by an Auger relaxation process in which one electron fills the hole and another is elected with the excess energy. In this process, however, the ejected electron can inelastically scatter with other electrons, and there are many processes by which the surrounding local valence bands are excited. The emission of secondary low-energy electrons is well known: it is not uncommon for the same order of magnitude of secondary electrons to be emitted as are directly photoemitted by the x-ray photons. However, the importance of these low-energy electrons in the overall picture of x-ray-induced surface chemistry has been ignored. Transient electron temperatures in the vicinity of the original core hole can exceed several 1000 K for 100–300 fs. We have studied the role of hot electrons in the surface system CO adsorbed on Cu(111) by inducing a high electron temperature with a 35 fs, 3 eV laser pulse. On the time-scale of 100 fs, the electron energy bath may be considered decoupled from the lattice

energy bath because the electron-phonon relaxation rate is relatively slow.

The third approach has been to explore the possibility of direct lattice excitation by femtosecond laser excitation. Recently, coherent optical phonons have been observed in bulk materials excited by femtosecond laser pulses. We have observed the first coherent surface optical phonons. These modes are localized on the surface and are thus most likely to play a role in direct surface chemistry.

Accomplishments

Time-resolved X-ray Studies of Core Holes

We have made progress in our original goal of performing the first XUV pump-probe experiments to time resolve XUV-initiated surface processes. We have generated ultrashort pulses of XUV by high harmonic generation of a 800 nm, 35 fs, 70 mJ pulse in an Argon gas jet. The 800 nm laser system works well, delivering pulses with high energy stability and good mode quality to the gas jet. We are currently producing harmonics above ~30 eV in Argon gas, as evidenced by the transmission through appropriate high frequency bandpass filters. The measurement of x-ray pulse durations on the femtosecond time scale is a consistent problem in time-resolved x-ray studies; however, harmonic generation is believed to be completely coherent, so we expect our 73.5 eV pulses to be as short as the 35 fs pulses at 800 nm with which we drive the high harmonics. We await suitable normal incidence x-ray optics to focus 73.5 eV light (49th harmonic of 1.5 eV) onto our sample, solid Magnesium. We will measure the 2p core-hole lifetime of Mg by observing bleaching of the 2p core-hole photoemission line and Auger emission lines by time and energy resolving the electron photoemission induced by two time-delayed 73.5 eV pulses. The binding energy is ~50 eV, so there is adequate excess energy to insure clean photoemission spectroscopy. Although this is an extremely ambitious experimental undertaking, we expect to be able to obtain 2–5% bleaching because normal-incidence x-ray optics should enable us to focus to a spot under 10 microns in diameter and the absorption cross section for absorption is approximately 10 Mbarns. We hope to be able to time resolve the lifetime because our x-ray pulse width should be <35 fs and the lifetime is expected to be greater than 43 fs on the basis of previous x-ray photoemission linewidth measurements, which were corrected for phonon broadening by theoretical analysis.

Role of Hot Substrate Electrons in Surface Chemistry

Using 35 fs, 3 eV pump pulses, we have observed extraordinarily efficient and nonlinear desorption of CO molecules adsorbed on Cu(111) substrates. The experiments measure the yield as a function of pump fluence for 3 CO isotopes. We have found that the heaviest isotope is desorbed with the highest yield and with a higher power law exponent when we fit the yield vs. pump fluence data. These results are consistent with the 35-fs laser pulse inducing a transient electronic excitation that is extremely hot and nonthermal. The optical absorption is sufficient to promote approximately 2% of the electrons per atom. This level of excitation is high but the same order of magnitude as that expected in the immediate vicinity of a core hole when the electronic system must accommodate the ejection of 100 eV of energy in a small region. The enhanced and ultrafast molecular desorption induced by femtosecond laser pulses was reported by us in 1992, and similar studies have been reported for NO and O_2 on metal surfaces. In this study, however, we show that the isotopic mass of the adsorbate is important in this ultrafast process, and, thus, we show that the desorption path must involve strong coupling and high excitation of the CO-metal stretch vibration, as opposed to other lower frequency vibrational modes such as the frustrated rotation or translation.

Role of Direct Phonon Excitation in Surface Chemistry

We have found that optical phonons (periods of order 100 fs) may be excited on surfaces of semiconductors using ultrashort laser pulses. We detect these oscillations on the surface using time-resolved optical second harmonic generation (SHG). SHG is known to be surface sensitive because it is dipole forbidden in the bulk of centrosymmetric media. In this case, even on surfaces of centrosymmetric crystals, the SHG is sufficiently sensitive to detect surface optical phonons. When we irradiate GaAs (100) and (110) crystals with 35 fs pulses, we observe a complex small amplitude oscillation In the time-resolved SHG. The Fourier transform of those oscillations reveals 6 or more oscillation frequencies that we may associate with the GaAs bulk LO phonon, an extended GaAs-vacuum interface LO phonon mode, and 4 local vibrational modes characteristic of the different surface reconstructions. These local vibrational modes vanish after small perturbations of the surface such as oxidation and argon sputtering. These oscillations may be described as coherent phonons in the sense that a relative handful of modes are excited with

definite phase relationships to each other. For a short time, the motion is thus almost classical. Our next step is to consider how these coherent surface phonons couple to adsorbates and whether or not it is possible to drive surface chemistry directly by phonon excitation. We believe the mechanism for exciting these phonons is that excited electronic states screen the internal fields at the surface and release the elastic strain already present at the surface. The same thing should happen locally around a core hole excited by XUV or x-ray light.

Publications

L. Xu, Y.M. Chang and H.W.K. Tom, "Observation of Coherent Surface Optical Phonons by Time-Resolved Second-Harmonic Generation," *Ultrafast Phenomena* IX, Springer-Verlag, Berlin, 1994.

L. Xu, Y.M. Chang and H.W.K. Tom, "First Observation of Coherent Surface Optical Phonons," submitted to *Phys, Rev. Lett.*

Application of Synchrotron Radiation to Processing of Semiconductor Materials

Principal Investigators: Wladyslaw Walukiewicz, Kin Man Yu, Lei Wang, Christian Kisielowski, and Edith Bourret

Project No.: 95014

Funding: $56,400 (FY 95)

Project Description

We have proposed to use high-intensity, tunable synchrotron radiation for selective, atom-specific annealing of semiconductor materials. The possibility of tuning the photon energy to the absorption edge of a specific element allows for a selective deposition of the x-ray energy in artificially structured systems, such as multilayer quantum wells and modulation-doped heterostructures, and to selectively excite specific dopants in the materials. Absorption of a high-energy photon by an atom in the crystal lattice creates an electron in the conduction band and a hole in a core level. The energy absorbed by the atom is either re-emitted or is very rapidly absorbed by the lattice phonons. The whole process occurs on the time scale characteristic for the optical phonon frequencies (of the order of 1 to 10 ps). The large power density absorbed in the lattice can facilitate transformation of crystal lattice defects affecting the materials properties. The initial stage of the project was concerned with solid-phase epitaxial growth and crystallization of amorphous silicon. We have also proposed to use low energy x rays to dissociate carbon clusters in GaAs and InP.

Accomplishments

We have used the ALS to study the effects of x-ray irradiation on the solid-phase regrowth of ion-implanted and as-grown amorphous Si. We have chosen this material because the maximum flux at beamline 10.3 is close to the Si–K absorption edge. The Si samples were irradiated with x rays for the times ranging from 0.3 to 45.0 hr. After the irradiation, the crystallization was induced by thermal annealing. We have conducted extensive structural and electronic characterization of x-ray irradiated and control samples. Rutherford backscattering spectroscopy (RBS) shows an order of magnitude reduction in the concentration of structural defects in the x-ray-treated material. This finding has been confirmed by the transmission electron microscopy (TEM). Figure 18 shows the difference in the quality of the regrown layers in x-ray-treated and untreated Si samples. Both the direct images and the diffraction patterns show a striking improvement in the crystallinity of the x-ray-treated Si. The x-ray-treated layer has regrown completely, whereas a residual amorphous region is found in the untreated sample. We have also found that x-ray irradiation affects the electrical activity of implanted donors and acceptors. An improvement in the donor and a reduction in the acceptor activation efficiency has been observed in the x-ray-treated Si.

Our results have important basic and practical consequences for the solid-phase recrystalization processes that play a crucial role in various aspects of Si device technology. The results indicate that irradiation with x rays "homogenizes" amorphous Si by eliminating microscopic crystalline nucleation centers, forcing a solid-phase epitaxial regrowth from the single crystal substrate. This opens up the possibility for an improvement in the quality of the thin

Figure 18. Transmission electron micrographs (TEM) and electron diffraction patterns of the 525°C 1-hr-annealed Si samples (a) with and (b) without x-ray annealing prior to the thermal treatment. The x-ray annealed sample shows very good crystal quality. A thin ≈30 nm amorphous layer is present in the sample without x-ray annealing. These results are in agreement with the structure of the layers deduced from the Rutherford backscattering spectroscopy data.

crystalline films used in photovoltaic and thin-film transistor technologies. We have also employed a monochromatic x-ray beam to disperse carbon clusters in III-V compounds. The results of Raman measurements show that irradiation with 400 eV x rays results in a decrease in the concentration of graphitic clusters.

Publication

K.-M. Yu, L. Wang, C. Kisielowski, and W. Walukiewicz, "Effect of High Dose X-Ray Irradiation on Solid Phase Epitaxy of Amorphous Silicon," in preparation.

Ultrafast Surface Dynamics with Atomic Resolution

Principal Investigators: Shimon Weiss, D. Frank Ogletree, and Daniel S. Chemla

Project No.: 95015

Funding: $101,400 (FY 95)

Project Description

Many important problems in surface science require high spatial and temporal resolution probes to study phenomena such as vibrational excitations of surfaces

and adsorbed atoms or molecules, electronic excitations on surfaces such as hot electrons in thin metallic films, and optical excitations at semiconductor surfaces and interfaces. Recently, our Berkeley Lab team developed the ultrafast scanning tunneling microscope (USTM), which offers simultaneous imaging of surfaces with few nanometer spatial and subpicosecond temporal resolutions.

The USTM is based on the conventional optical "pump and probe" scheme, which is a stroboscopic measurement of an ultrafast process initiated by a strong pump pulse and probed by a weak probe pulse. In the USTM, a photoconductive switch in series with the STM tip is gated by the probe pulse to sample the tunnel current. The pump laser pulse excites the dynamic phenomena on the surface. Time resolution is obtained by varying the delay between the excitation pulse and the probing pulse.

The original prototype of the USTM was operated under ambient conditions. The purpose of this project is to further improve on the technique and to transfer it to an ultra high vacuum (UHV) chamber where surface processes can be studied on the atomic scale in a controlled environment, and in combination with other surface characterization tools.

Accomplishments

A second prototype of the USTM, still operating at ambient conditions, was designed and built. This prototype enables better sample handling and automated tip-sample approach. More importantly, a wide angle optical access allows us to excite the sample with the pump pulse with three different geometries.

Single point ultrafast tunneling measurements were pursued to obtain a better understanding of the δ-function response of the instrument. The tip fabrication process was improved and shorter tips (30–50 μm long) were fabricated. With these improvements, a record 900 fs resolution time was obtained for resolved tunneling data (see Fig. 19). A theoretical circuit model that describes these measurements was devised and used to describe the lineshape of the measured signals.

An ultrahigh vacuum chamber for use with the USTM was designed and built. A scheme of this design is shown in Fig. 20. Special care was taken to match the different requirements for the ultrafast optics and for the UHV handling of the samples and the STM head.

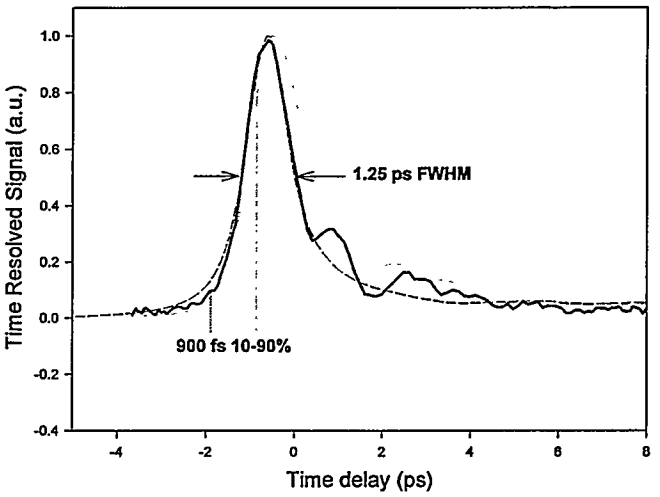

Figure 19. Time-resolved tunneling signals (solid) compared to crashed (dotted) and on-sample measurements (dashed) of picosecond voltage pulses with a 30 μm silver epoxy tip.

To simplify optical alignment, all optical components were placed outside of the chamber. To keep the sample in the chamber within the working distance of the optics, a specially engineered quartz viewport was designed and fabricated. The chamber features a triaxial design, allowing the sample to be rotated away from the optical port to the separate foci of various diagnostic tools, such as a Low Energy Electron Diffraction (LEED) gun, sputtering gun, evaporators, and sample/tip load-and-lock systems. Necessary pumps, valves and vibration isolation system were also purchased. We are currently assembling the UHV USTM and plan to start measurements in the near future.

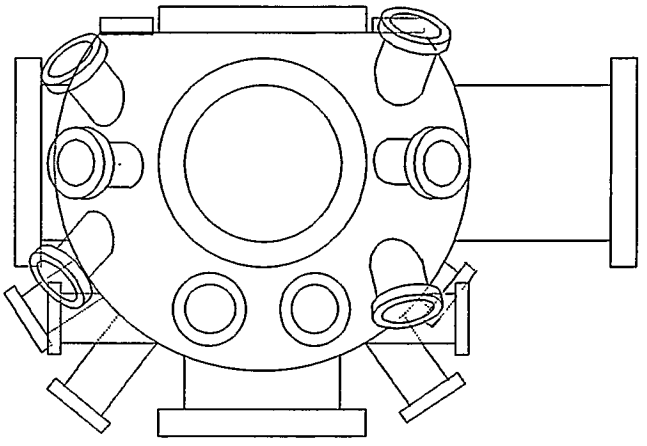

Figure 20. Design of the UHV USTM chamber. Optical port for the ultrafast optics is on the top of the chamber.

Publications

S. Weiss, D. Botkin, D.F. Ogletree, M. Salmeron, and D.S. Chemla, "The Ultrafast Response of a Scanning Tunneling Microscope," *Phys. Stat. Sol. (b)* 188, 343 (1995).

D. Botkin, S. Weiss D.F. Ogletree, M. Salmeron, and D.S. Chemla, "Design Considerations in an Ultrafast Scanning Tunneling Microscope," *Rev. Sci. Instrum.* 66, 4130 (1995).

Conducting and Semiconducting Boron–Nitrogen–Carbon Nanowires

Principal Investigators: Alex K. Zettl, Marvin L. Cohen, and Steven G. Louie

Project No.: 95016

Funding: $43,800 (FY 95)

Project Description

The use of electronic materials on the nanometer length scale is of great importance in new technology. Central to this issue is the development of suitable electronic materials. The "ultimate nanowire" might be one that has high mechanical strength, is chemically inert and easily processed, and has tunable electronic properties (such as thermal and electrical conductivity and energy gap).

The recent discovery in Japan that pure carbon nanotubes can be synthesized rather easily using carbon-arc plasmas has spawned new theoretical and experimental research in this field. Covalently-bonded carbon atoms can form tube-like structures with high mechanical strength and unusual electronic properties. However, from an applications point of view, there are fundamental drawbacks to pure-carbon nanotubes. For example, the conductivity of the tubes depends sensitively on the chirality and diameter of the tubes, parameters that are impossible to control using present synthesis methods.

Preliminary theoretical calculations by M.L. Cohen and S.G. Louie suggest that wire or tube-like structures need not be formed from carbon alone, but may be possible to construct using combinations of boron, nitrogen, and carbon. Boron–nitride, boron–carbide, and boron–carbon–nitride tube-like structures are predicted to be stable and to have unique electronic properties (such as those of a modest-gap semiconductor that could easily be doped by substitutional impurities or impurities inside the tube structure). We believe such structures can be synthesized and that they will have, for many applications, properties vastly superior to any known materials. The synthesis of boron–nitrogen–carbon tubes should have direct impact on future electronic devices fabrication, and possibly other applications as well (e.g., medical). At the same time, such structures would provide unique physical systems for the study of fundamentally new mesoscopic low-dimensional physics.

Accomplishments

This project represents a close-knit collaboration between a theoretical approach (Cohen, Louie) to predict stable materials with desirable properties, and an experimental effort (Zettl) to synthesize and characterize those materials. Tubes containing, for example, just boron and nitrogen, just boron and carbon, and boron, nitrogen, and carbon together are explored.

The major difficulties associated with this project are the successful experimental synthesis and characterization of the materials. As a start, synthesis techniques similar to those used for the manufacture of carbon nanotubes (carbon-arc plasma) are employed. Different amounts of carbon, nitrogen, and boron are introduced into the arc, either by using solid strike-rods of different composition or by injecting different elements in reactive vapor form into the high-temperature growth region. Initial characterization is through TEM imaging, along with TEM analytical characterization.

In this project, new $B_xC_yN_z$ nanotube structures have been successfully synthesized and characterized by TEM. The results are consistent with theoretical predictions. Specifically, nanotubes with stoichiometry BC_3, BC_2N, and BN have been produced. Electron energy loss spectroscopy (EELS) performed at the National Center for Electron Microscopy is used to determine the stoichiometry of individual tubes.

Theoretical studies indicate that $B_xC_yN_z$ tubes may have electronic properties far superior to those of pure carbon nanotubes. The experimental observation made here of concentration gradients in a single tube suggests applications are realizable.

Fully collapsed carbon nanotubes have been discovered experimentally, and are being studied theoretically using elasticity theory.

One patent application has been filed related to this work. Two are in preparation.

Publications

A. Rubio, J.L. Corkill, and M.L. Cohen, "Theory of Graphitic Boron Nitride Nanotubes," *Phys. Rev. B* **49**, 5081 (1994).

Y. Miyamoto, A. Rubio, M.L. Cohen, and S.G. Louie, "Chinal Tubules of Hexagonal BC_2N," *Phys. Rev. B* **50**, 4976 (1994).

X. Blase, A. Rubio, S.G. Louie, and M.L. Cohen, "Stability and Band Gap Constancy of Boron Nitride Nanotubes," *Europhys. Lett.* **28**, 335 (1994).

Y. Miyamoto, A. Rubio, S.G. Louie, and M.L. Cohen, "Electronic Properties of Tubule Forms of BC_3," *Phys. Rev. B* **56**, 18360 (1994).

Z. Weng-Sieh, K. Cherrey, N.G. Chopra, X. Blase, Y. Miyamoto, A. Rubio, M.L. Cohen, S.G. Louie, A. Zettl, and R. Gronsky, "Synthesis of $B_xC_yN_z$ Nanotubes," *Phys. Rev. B* **51**, 11229 (1995).

Y. Miyamoto, A. Rubio, X. Blase, M.L. Cohen, and S.G. Louie, "Ionic Cohesion and Electron Doping of Thin Carbon Tubules with Alkali Atoms," *Phys. Rev. Lett.* **74**, 2993 (1995).

N.G. Chopra, R.J. Luyken, D. Cherrey, V.H. Crespi, M.L. Cohen, S.G. Louie, and A. Zettl, "Boron Nitride Nanotubes," *Science* **269**, 966 (1995).

L.X. Benedict, S.G. Louie, and M.L. Cohen, "Static Polarizabilities of Single-Wall Carbon Nanotubes," *Phys. Rev. B* **52**, 8541 (1995).

N.G. Chopra, L.X. Benedict, V.H. Crespi, M.L. Cohen, S.G. Louie, and A. Zettl, "Fully Collapsed Carbon Nanotubes," *Nature* **377**, 135 (1995).

N.G. Chopra, F. Ross, and A. Zettl, "Electron-Beam Induced Collapse of Carbon Nanotubes," unpublished.

A. Rubio, Y. Miyamoto, X. Blase, M.L. Cohen, and S.G. Louie, "Chiral Conductivities of Nanotubes," unpublished.

Y. Miyamoto, M.L. Cohen, and S.G. Louie, "Theoretical Investigation of Graphitic Carbon Nitride and Possible Tubule Forms," unpublished.

L.X. Benedict, V.H. Crespi, S.G. Louie, and M.L. Cohen, "Relations Between Sheets and Tubes: Static Conductivity and Superconductivity of Carbon Nanotubes," unpublished.

L. Chico, V.H. Crespi, L.X. Benedict, S.G. Louie, and M.L. Cohen, "Pure Carbon Nanoscale Devices: Nanotube Heterojunctions," unpublished.

V.H. Crespi, L.X. Benedict, M.L. Cohen, and S.G. Louie, "Pentaheptium: A Pure-Carbon Planar Metal," unpublished.

Nuclear Science Division

New Techniques for Low-Energy Nuclear Beams

Principal Investigator: Claude Lyneis

Project No.: 95017

Funding: $182,500 (FY 95)

Project Description

The purpose of this proposal was to explore several promising new technical approaches to low-energy research: the production and ionization of radioactive atoms for trapping and ion-implantation experiments; the efficient capture and separation of short-lived heavy elements synthesized in heavy-ion fusion reactions; and the production of high-intensity heavy-ion beams.

Three technical approaches were explored:

- A specialized ion source that can efficiently ionize short-lived radioactive atoms was developed.
- A study to develop a design for a high-efficiency gas-filled separator for compound-nucleus products was performed. The goal was to develop a device that would surpass the capabilities of existing recoil separators and evaluate the efficiency, sensitivity, and analyzing power of the apparatus. Concurrent with this goal was the development of a broad scientific program to enhance efforts in many research areas at the 88-Inch Cyclotron.
- A conceptual design was developed for a new high-performance Electron Cyclotron Resonance (ECR) ion source incorporating new features so as to make a significant advance in ECR technology and boost the heavy-ion performance of the 88-Inch Cyclotron.

Accomplishments

First, a specialized CUSP ion source was designed and constructed to efficiently ionize short-lived radioactive atoms. Preliminary tests using stable CO_2 gas as feed were successfully completed. These tests indicated that the source could produce about 15% of the extracted current from CO_2 as O^{1+}. This is a preliminary step to producing a radioactive beam of $^{14}O^{1+}$ from radioactive carbon monoxide produced by the Cyclotron.

Second, the gas-filled separator study resulted in the design for a gas-filled separator utilizing superconducting magnets. A novel magnet design was developed using a large-angle (165°) superconducting dipole magnet with strong vertically focusing dipole field gradients at the entrance and exit of the magnet. Third-order magnetic optics calculations showed that this design has angular acceptance, separation ability, and resolving power superior to those of existing recoil separators. A preliminary engineering study on the magnet design was also carried out, which showed that the device could be constructed with existing superconducting magnet technology. The separator design and experimental program were validated at the LASSY Gas-Filled Separator Working Group meeting held at Berkeley Lab on September 16–17, 1995. This meeting was attended by Berkeley Lab scientists and engineers as well as separator experts from Jyväskylä, Finland, and GSI.

Finally, the concept for a Third Generation ECR ion source was developed that would incorporate multiple frequency heating, high-mirror-ratio magnetic field confinement, and enhanced supplies of cold electrons. Key issues identified concern the design and construction of a set of superconducting magnet coils to produce the desired magnetic fields. A preliminary coil design was developed and evaluated with respect to critical current densities, magnetic forces on the superconducting coils, and the possibility of using surplus SSC superconducting wire to construct the magnet. This work was carried out in collaboration with the AFRD Supercon Group and utilized three-dimensional magnet codes such as TOSCA to evaluate design options.

Publication

C.M. Lyneis and Z.Q. Xie, "Concept for a Third Generation ECR Source at LBL," *Proceedings of the 12th International Workshop on ECR Ion Sources, Apr. 1995, RIKEN, Japan;* INS-J-182; and LBL-37311.

New Research Directions in Nuclear and Particle Astrophysics (INPA)

Principal Investigators: Robert G. Stokstad, Henry J. Crawford, Douglas M. Lowder, Martin E. Moorhead, David R. Nygren, and Austin Richards

Project No.: 95018

Funding: $57,700 (FY 95)

Project Description

The main purpose of this project is to perform technical and scientific research to define the parameters of a large (1-km-scale) high-energy neutrino astronomical observatory. This builds on the expertise of researchers in the AMANDA (NSF-supported) and DUMAND (DOE-supported) projects, which are forerunners of the km^3 detector.

Development of a proposal for the large neutrino detector requires calculations simulating the response of different detector configurations to (models for) the sources and properties of the incoming neutrinos. Technical advances in the area of smart, low-power electronics for signal processing and in photo-tube design are needed and will be pursued. The building of a community of researchers in support of the large detector will also be promoted.

Accomplishments

The Optical Module (OM) is the basic element of the km^3 detector. A "smart" digital-electronics-based OM has been developed and will be deployed and tested in Antarctic ice by the AMANDA collaboration during this austral summer. The smart OM is based on an integrated microcircuit developed at Berkeley Lab, initially for another purpose, the Analog Transient Waveform Recorder (ATWR IC). This circuit was redesigned and produced for use in the OM environment; it makes possible the recording of the full waveform of a light pulse and accurate nanosecond timing, all with very low power consumption.

Optical beacons based on a new, commercially available blue LED have been developed. These will also be deployed with the test OM described above. These beacons require only a simple two-wire link, rather than a fiber optic link, between OM and surface and are expected to offer much lower cost, shorter pulse width, much higher pulse rates, and greater simplicity and flexibility than the laser system currently in use.

The problem of finding an efficient way to generate and store the Cerenkov light generated by very high energy muons has been addressed, and we are now beginning the construction of a complete simulation shell and definition of the data file formats for different stages of the simulation. Simulation issues have been reviewed, and the outlines of a shell structure for simulation codes were drawn up.

Global Gravitational Anomalies in Three Dimensions

Principal Investigator: Randy Baadhio

Project No.: 95019

Funding: $30,100 (FY 95)

Project Description

The discovery in 1988 by Edward Witten that Quantum Gravity and Quantum Field Theories are exactly soluble in 2+1-dimension has renewed our interest in better understanding three-dimensional physics. Among the most fundamental challenges we are faced with is the occurrence of physical pathologies known as anomalies. Anomalies often ruin the consistency of gauge theories.

The objective of this proposed work is to investigate the occurrence and cancellation of global gravitational anomalies in three-dimensional Quantum Gravity and Quantum Field Theories. These anomalies reflect the theories' lack of invariance under some diffeomorphism groups, particularly those that cannot be smoothly deformed to the identity.

This program represents a new area of research, in part because our knowledge of diffeomorphism groups in three dimensions is meager; furthermore, finding anomaly-free Gauge Theories in three dimensions will greatly improve our understanding of Einstein's Theory of Quantum Gravity in four dimensions. Funding from the LDRD would greatly contribute to better understanding four-dimensional physics through the use of our newly gained knowledge of three-dimensional physics.

Accomplishments

Global anomalies occur when large gauge transformations of a classical field theory fail to be symmetries of the corresponding Quantum Theory. Global gravitational anomalies in particular reflect the lack of invariance of a theory under diffeomorphism groups. As diffeomorphism invariance puts severe constraints on the consistency of gauge theories, the occurrence of global gravitational anomalies is consequently taken as a symptom of a deeply troubled theory, and it thus becomes necessary to cancel the anomalies.

While a fair amount is known about the nature of these anomalies, a good deal is yet to be understood. Quantum Gauge and Quantum Gravity Theories in three dimensions uphold a central importance in physics (for String Theory, Conformal Field Theory, and Condensed Matter Theory) and in mathematics (for the construction of knot and 3-manifold invariants). Because of this importance, the symptoms, manifestations, and cancellation of the pathologies known as global gravitational anomalies were investigated.

There were several obstacles to doing so. One has to do with class of diffeomorphism groups in three dimensions known as equivalence classes of diffeomorphisms, which cannot be smoothly deformed to the identity; these are commonly referred to as mapping class groups. Any concrete study of these pathologies has necessarily relied on our specific knowledge of three-dimensional mapping class groups. I investigated the number of generators and relations that various 3-manifolds have (in which the theories are defined). This approach shed some light on the torsion classes of mapping class groups.

This project research has revealed a wealth of information on a subgroup of the three diffeomorphism group of 3-manifold, the mapping class group. These groups are essential tools in the detection and cancellation of global gravitational anomalies in dimension three.

Having determined the nature of three-dimensional mapping class groups and their torsion classes, the next order of priority was to generalize the Wess–Zumino consistency condition. In some celebrated cases, local anomalies were detected because they were nontrivial solutions of this consistency condition. The Wess–Zumino consistency condition represents a powerful yet simple enough test of anomaly detection. The problem is to generalize this consistency condition, for it is usually expressed in terms of local functional (instead of topological ones). I looked at one-form connections and characteristic forms in three-dimensions, and did succeed in developing a generalized version of the Wess–Zumino consistency condition.

Publications

R.A. Baadhio, "Mapping Class Groups for $D = 2 + 1$ Quantum Gravity and Topological Quantum Field Theories," *Nucl. Phys.* **B441,** 383 (1995).

R.A. Baadhio, *Quantum Topology and Global Anomalies,* Advanced Series in Mathematical Physics, World Scientific (1996), in press.

Integrated Instrumentation System for Drift Chambers, TOF, Cerenkov, and Silicon Vertex Detectors

Principal Investigators: Michael E. Levi and Frederic Kral

Project No.: 95020

Funding: $195,900 (FY 95)

Project Description

The purpose of this program of activities was to effect advances in the area of electronic instrumentation for trigger and data acquisition systems. Using Berkeley Lab's unique strengths in integrated circuit technology and advanced electronics design, coupled with recent advances in microprocessor technology, we have developed a very high speed readout system for certain classes of high energy physics detectors. We developed a timing and amplitude multichannel instrumentation system for use in drift chamber, time-of-flight, or Cerenkov detectors based on a specialized integrated circuit. These detectors require the transfer of data at large volumes and high rates of speed. This project capitalized on the recent invention of a high-speed CMOS monolithic integrated timing circuit at Berkeley Lab. In addition, we devised a method and covered a specialized microprocessor based circuit to enhance the capabilities of silicon vertex detectors and drift chambers for future experiments and provide fast particle tracking information in the formation of a detector trigger. To increase the throughput of high-bandwidth particle tracking data, we relied upon closely coupling the information generated by particle tracking devices with commercially available high-speed embedded processors (500 MIPS).

Accomplishments

Integrated Timing and Amplitude Instrumentation System for Drift Chambers, Time-of-Flight (TOF), and Cerenkov Detectors

Many high energy physics and nuclear science applications require subnanosecond time resolution measurements over many thousands of detector channels. A complete, multichannel timing and amplitude measurement IC for use in drift chamber, time-of-flight, and Cerenkov detector applications was designed and fabricated to address this need. The circuit is capable of measuring both time and amplitude simultaneously. Time is digitized using one eight-channel time-to-digital converter (TDC) comprised of a delay locked loop and eight sets of latches and encoders. Amplitude (for dE/dx) is digitized using a dual-range FADC for each channel. Eight bits of dynamic range with six bits of accuracy are achieved with the dual range. The timing and amplitude information is multiplexed into one DRAM (Dynamic Random Access Memory) trigger latency buffer. Interesting events are then transferred into an SRAM (Static Random Access Memory) readout buffer before the latency time has expired. The design has been optimized to achieve the requisite resolution using the smallest area and lowest power. The single integrated circuit with all these components has been implemented in a 0.8μ triple metal CMOS process.

The TDC used in this application is based on a novel design. Phase-locked loops have been employed in the past to obtain accurate time references for these measurements. An alternative solution, based on a delay-locked loop (DLL) is described. This solution allows for a very high level of integration yet still offers resolution in the subnanosecond regime. A novel phase detector, based on the Muller C element, is used to implement a charge pump where the injected charge approaches zero as the loop approaches lock on the leading edge of an input clock reference. This greatly reduces timing jitter. Software-coded layout generators are used to automatically lay out a highly integrated, multi-channel TDC. This circuit was separately implemented, and test results show a timing jitter of less than 35 ps and better than 135 ps resolution for the TDC circuit. The TDC circuit lends itself to being used as a kernel in a number of other applications, such as clock–pulse alignment and

deskewing, time interval generation for serialization and deserialization schemes in telecommunications, and time-to-digital conversion.

A demonstration chip of the TDC circuit was built using standard 0.8 μm digital technology, with a single poly-silicon layer and three metal layers. The chip was then tested using a fast-pulse generator, a high-resolution (<37 ps) time interval counter, and a logic analyzer, along with some standard test equipment. Under the stated conditions, the loop was stable for clock periods between 16.89 ns (59.2 Mhz) and 25.15 ns (39.8 Mhz), corresponding to a time resolution of 0.53 ns and 0.79 ns, respectively. Time jitter, defined as the rms delay deviation from the expected value, was below 80 ps throughout the measured range of operation, even when no allowance was made for the time jitter of the experimental setup itself. Differential and integral nonlinearity showed values of the same order of magnitude, both staying below one third of a least significant bit throughout the range. Plots of the worst case integral nonlinearity (INL) and differential nonlinearity (DNL) are shown in Fig. 1.

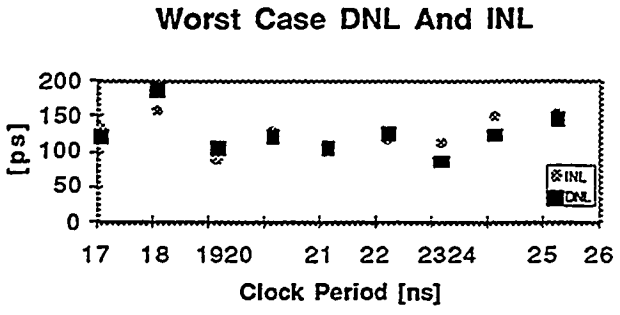

Figure 1. Plot of TDC Integral and Differential Nonlinearity.

Silicon Vertex Detector Back-end Electronics Readout and Trigger

The existence of inexpensive high-speed processors makes it possible to use powerful CPUs at an early point in the DAQ stream. The detector hits, accepted by the lowest-level trigger, arriving at rates of up to 10 kHz, can be analyzed with sophisticated algorithms by such processors. Finally, the increased speed of embedded processors makes software-based algorithms attractive for use in a silicon-based trigger system. The trigger system not only affects the quality of the physics that is done but, in fact, determines the range of physics that can be studied.

Triggering future high-energy-physics detectors will be much more difficult than the triggering of any existing detector. A combination of factors (beam crossing rate, cross-section, etc.) forces the complexity and amount of triggering electronics to be many orders of magnitude more complicated than what has been presently accomplished.

One of the key features of future detectors will be that the particle tracking detectors, especially silicon vertex detectors, will participate in the lowest levels of the trigger. With many interesting types of events containing vertex information, the silicon vertex detector can greatly aid in reducing the amount of data that need to be analyzed in higher levels of the trigger. Thus, trigger primitives have to be provided to the trigger logic at high rate and short latency.

By adding powerful high-speed processors to the low-level readout system, the processor can compute track segments for use by subsequent trigger levels. We have designed a readout system using a commercially available high-end processor, and then benchmarked the performance for the trigger primitive formation. A VME-based silicon vertex detector readout board containing a PowerPC processor board was fabricated and is shown in Fig. 2. The algorithms for constructing tracking segments used by the global tracking trigger need to operate at high speed while handling pattern recognition problems stemming from expected backgrounds. Several fast algorithms for silicon track finding have been simulated and were benchmarked on the PowerPC processor. These benchmarks indicated that a trigger could be formed in software at a rate of 10 KHz using the information from a silicon vertex detector.

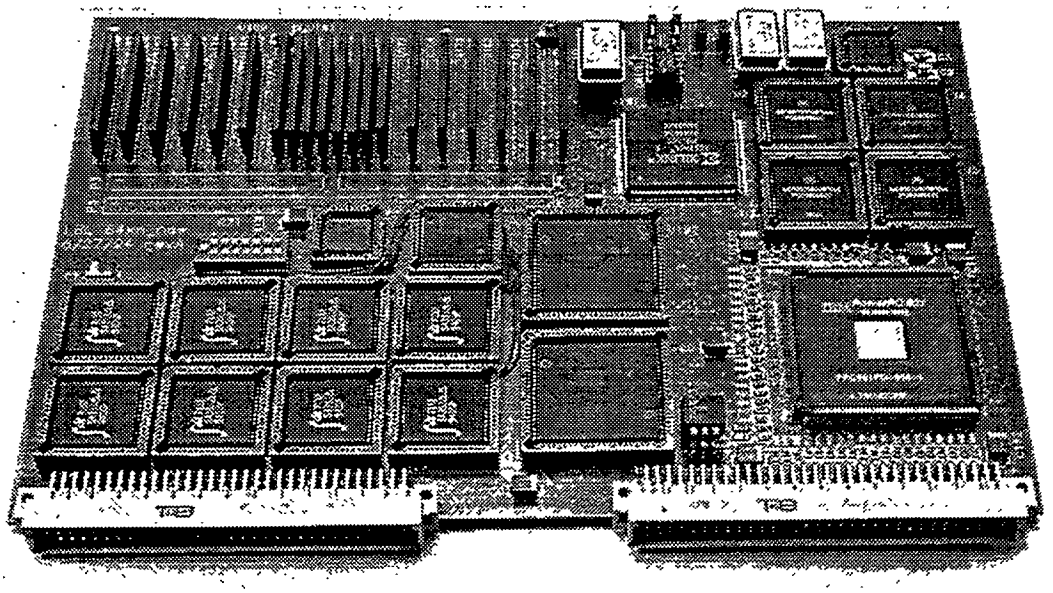

Figure 2. Photograph of an early prototype of a readout board for a silicon vertex detector containing a 250 MIPS processor capable of performing high-speed trigger decisions.

Publications

D.M. Santos, A. Chan, D. DeBusshere, S. Dow, and J. Flask, "A Multi-Channel Time-to-Digital Converter Chip for Drift Chamber Readout," presented at the IEEE 1995 Nuclear Science Symposium and Medical Imaging Conference, Oct. 21–28; LBL-38029.

D.M. Santos, S.F. Dow, and M.E. Levi, "A CMOS Delay Looped Loop and Sub-Nanosecond Time-to-Digital Converter Chip," presented at the IEEE 1995 Nuclear Science Symposium and Medical Imaging Conference, Oct. 21–28; LBL-38040.

Development of High-Resistivity Charge-Coupled Devices for Imaging

Principal Investigators: S. Perlmutter, G. Goldhaber, C. Pennypacker, H. Spieler, S. Holland, R. Stover (UC Santa Cruz), and P. Suni (Orbit Semiconductors)

Project No.: 95021

Funding: $87,800 (FY 95)

Project Description

There is a critical shortage of high-quantum-efficiency, blue, or x-ray-sensitive Charge-Coupled

Devices (CCDs). The only viable method at present to obtain the quantum efficiency and spectral sensitivity needed is to "thin" them. Photons can then reach the potential wells created by epitaxial layers from the "backside," i.e., the side without epitaxial layers. We propose to pursue the development of CCDs with fully depleted substrates to reduce or eliminate the need for thinning. The critical key to this development is a fabrication process developed at Berkeley Lab that yields high-quality detector diodes together with high-density, low-noise electronic circuitry on fully depleted substrates. A key aspect of this process is that it is fully compatible with conventional IC fabrication. The original goal was to apply the Berkeley Lab technique to an existing CCD foundry process so as to exploit the extensive R&D that has gone into the development of CCDs with the extremely high charge transfer efficiency crucial to astronomical imaging. The possibility of fabricating CCDs of this type would greatly improve the yield of astronomical devices and find many other applications. However, our industrial partner (Orbit Semiconductor) withdrew from all R&D during the project, which caused us to rethink the role that Berkeley Lab could play in this development. The conclusion was that the Laboratory will develop internally a CCD process on high-resistivity silicon with the ultimate goal being high-quantum-efficiency, low-noise devices suitable for use in astronomical imaging.

In the course of detector R&D for the SSC, a group in the Berkeley Lab Physics Division has developed a silicon-device fabrication process that allows the first demonstration of the monolithic integration of high-quality detector diodes with high-density, low-noise electronic circuitry. The process consistently achieves a high yield of very low dark current detectors. It is also fully compatible with conventional IC processes. It has been demonstrated with both PMOS and full CMOS circuitry. The key to this process is the utilization of a highly efficient gettering technique that actively removes detrimental impurities from the active volume. However, in the original detector process the gettering structure resulted in an unacceptably thick dead layer, with resultant poor quantum efficiency for visible-light photons. As a result, a significant amount of development work at the Laboratory was required in order to realize a thin backside dead layer that still maintains the low dark current needed for scientific CCDs. After Orbit Semiconductor dropped out of the project, it was decided that Berkeley Lab would proceed with the design and fabrication work necessary to realize proof-of-principle devices, with the eventual goal being the development of a large pixel count device suitable for astronomical imaging.

Accomplishments

As mentioned previously, the original detector fabrication process did not allow for high-quantum-efficiency, visible-light photon detection because of the need for a fairly thick (approximately 1 μm) layer of doped polysilicon on the wafer backside. The process was modified in such a way that the thickness of the backside layer was significantly reduced while still maintaining low dark currents and process compatibility with standard IC processing techniques.

Figure 3 shows the quantum efficiency of a backside-illuminated, Berkeley-Lab-fabricated photodiode (the curve labeled "QE for BSI, AR (Moses)"). With a simple silicon dioxide antireflection coating, a quantum efficiency of 85% at 650 nm was achieved. This result implies that all "red" photons that are not reflected from the surface are detected as collected charge. The quantum efficiency in the 800–1000 nm range (important for many astronomical studies) is already significantly higher than in the current "thinned" CCDs being used at telescopes. These results were realized by processing the device with the usual thick gettering layer intact throughout all high-temperature processes, which are the most

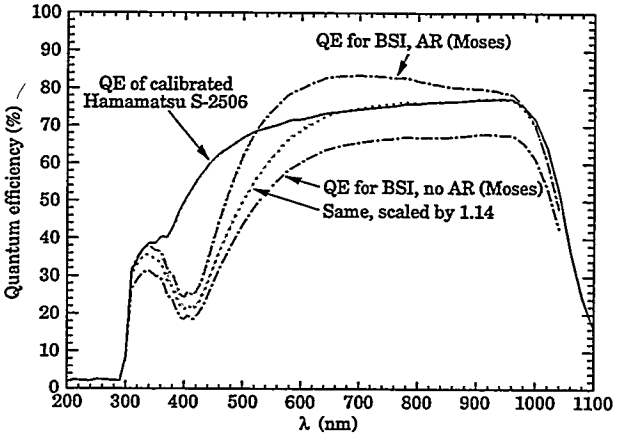

Figure 3. Measured quantum efficiencies of back side illuminated photodiodes, with and without antireflection coatings ($\lambda_0/4$ at $\lambda_0 = 480$ nm). For comparison purposes, the "no AR" case is also shown scaled by 1.14. the "blue problem" is indicated by the shaded region, where the blue response is suppressed. As discussed, performance in this region has since been improved by using thinner polysilicon rear windows.

critical in terms of contamination, that could lead to high dark currents. After the final high-temperature process, the thick backside layer was chemically etched away, and a thin layer of *in situ* doped polysilicon was then deposited at the fairly low process temperature of 650°C. The data in Fig. 3 are for a 0.1 μm thick backside polysilicon layer. During the course of the LDRD, we also fabricated devices with a thinner layer (350 Å) in order to improve the response at shorter wavelengths. We achieved a quantum efficiency of 70% at 480 nm with the 350-Å-thick polysilicon layer and indium tin oxide antireflection coating. We have recently fabricated devices with backside polysilicon layers as thin as 100 Å, with quantum efficiency measurements pending. We are also in the process of developing a backside coating process using indium tin oxide, which is a transparent conducting oxide. This layer is needed to reduce the high resistance of the thin backside polysilicon contact, and simultaneously will act as the antireflection coating.

In addition to the work on the wafer backside layer, we have also designed a mask set that will allow for the fabrication of proof-of-principle devices. As part of this design process two-dimensional process and device simulation has been employed in order to explore the pertinent process and layout parameters that determine the actual behavior of the device. The simulations show that an output transistor with a buried channel implant will function properly in high-resistivity silicon, therefore allowing for the critical integration of the first amplifier directly on chip. This is necessary in order to have a high charge-to-voltage conversion and, hence, large signal-to-noise ratio. Included on the mask set are individual output transistors of varying geometry, capacitor test structures, process monitors, and three individual 200 × 200 pixel CCDs. Also, long (approximately 1.4 cm) one-dimensional CCD structures are included in order to measure charge transfer efficiency. Fabrication of the devices at the Berkeley Lab Microsystems Laboratory is presently underway, utilizing a triple-level polysilicon process developed at Berkeley Laboratory.

Publications

D. Groom, "Effect of Antireflective Quartz Coating on a Silicon Photodiode," INPA internal memo.

Two invention disclosures and additional publications regarding the backside illuminated photodiode and CCD test structure are anticipated.

Structural Biology Division

Hyperthermophilic Microorganisms

Principal Investigator: Rosalind Kim

Project No.: 94029

Funding: $99,900 (FY 95)
$108,000 (FY 94)

Project Description

The purpose of this project is to exploit the biological information resident in the genomes of microorganisms living at extreme environments and understand the ecological niches that these organisms inhabit and their adaptations to these niches. Project goals include:

- Isolation of thermostable enzymes capable of catalysis at extremely high temperatures.
- Development of a fermentation technology designed to exploit the properties of these organisms.
- Understanding the enzymatic catalysis of unusual chemical transformations.
- Isolation of an enormous collection of patentable sequences of direct industrial utility.
- Providing insight into the means by which enzymes can be rendered thermostable.
- Generating a source of protein crystals better matched to higher resolution structural studies than those of existing protein crystals.

The information needed to encode thermoresistant forms of approximately 3000 different enzymes would be provided by the sequence of the genome of a single microorganism. Based upon experience with other microorganisms, this task will require sequencing between 3 and 5 million base pairs of DNA.

Accomplishments

The following systems are being worked on presently:

First, *Pyrococcus furiosus* genomic DNA was obtained from Dr. Robert Kelly of North Carolina State University. We prepared a lambda genomic DNA library, and the DNA polymerase gene was cloned using primers synthesized against the gene based on the sequence published by the Yoshizumi Inhino Biotechnology Research Laboratory in Japan. The gene has been cloned into pET16B vector, and the background strain is BL21(DE3)pACYC. In this construction, the protein carries a His-Tag at the amino terminus and the molecular weight is 92 kilodaltons. The three steps in purification of the crude extract are: 1) metal chelator column; 2) chromatofocusing column; and 3) gel filtration column. The protein yield is 3–10 mg/l of culture. About 50% of the DNA polymerase expressed is soluble. This protein has been crystallized.

The EfTu gene has also been cloned, and presently tests are being done to determine levels of expression.

Next, cells of *Methanococcus jannaschii* were obtained from Dr. Douglas Clark of the University of California, Berkeley. A lambda gem 11 library was prepared, and we are in the process of cloning the EfTu gene as well as other potentially industrially important genes.

In addition, using a Model 491 Prep cell from BioRad, we have been able to isolate seven proteins from a heat-treated (110°C, 15 minutes) crude extract from *Pyrococcus furiosus*. We are in the process of determining the N-terminus amino acid sequence of these proteins. When the genomic sequence of this organism becomes available in the next few months, we will be able to then identify where the gene codings for these seven proteins are located.

Figure 1. Crystallization of DNA polymerase from Pyrococcus furiosus *was performed in a solution of 0.08 M ammonium sulfate, 0.05 M Na-cacodylate at pH 6.5, 0.15% NP40, 0.05% Tween 20 and 4.5% polyethylene glycol 6000. The final protein concentration was 12.5 mg/ml. This was equilibrated with 0.16 M ammonium sulfate, 0.1M Na-cacodylate at pH 6.5, 0.3% NP40, 0.1% Tween 20 and 9% PEG 6000 by the vapor-diffusion method. The crystals grew in 14 days at room temperature to a size of 200 ×50 ×50 μm.*

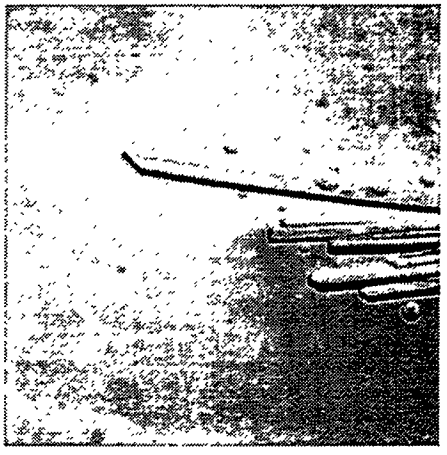

Figure 2. Data were collected on a Rigaku R-AXIS-IIC imaging plate detector with CuKα x-ray from a Rigaku roating anode generator.

SELECT: An Integrated, Science-based Environmental Software Framework

Principal Investigators: Thomas McKone, Sally Benson, Nancy Brown, Joan Daisey, Lois Gold, and Jane Macfarlane

Project No.: 94031

Funding: $434,400 (FY 95)
$375,300 (FY 94)

Project Description

The goal of the SELECT project is to design and develop a flexible, PC-based, object-oriented software system that will integrate, analyze, and present environmental information to managers, engineers, scientists, regulators, and the public. The software will assist the user in selecting cost-effective environmental remediation strategies.

SELECT links together critical components of the remediation process—site characterization, transport calculations, remediation design and performance assessment, multipathway exposure and dose assessment, characterization of upper-bound human cancer risks and risks that incorporate pharmacokinetic and mechanistic considerations, characterization of background hazards and secondary risks that may result from remediation strategies, and economic analysis.

The first step in the methodology is to assess the current and future state of the contaminant plume and the effects over time of each remediation alternative being considered. This is followed by estimating the exposures to a given contaminant for a specified population. Using rodent carcinogenic potency values and human exposure estimates, including (often profound) estimates of uncertainty, cancer risks are estimated. Where possible, pharmacokinetic analyses and mechanisms of carcinogenesis are incorporated in cancer risk assessments. Possible cancer hazard is compared to similarly estimated hazards from typical exposure to rodent carcinogens, e.g., to natural chemicals in the diet, background exposures to airborne chemicals. Costs associated with a specific remediation action are integrated with risk estimates to identify cost-effective strategies. Secondary risks that are produced by remediation are also evaluated. Information visualization tools are used to present information in an understandable form that site managers can use to formulate remediation strategies.

When fully developed, SELECT will accelerate the transfer to industry and regulators of state-of-the-art models and up-to-date information from the national laboratories and will provide the concerned public with a tool that makes the decision process easier to understand. The project currently involves a partnership with McClellan Air Force Base; other partners and users are being sought.

Accomplishments

We have developed a SELECT prototype that runs on a PC and is intended to illustrate a simplified version of the site characterization; a graphic visualization of the development of the concentration field over time; and displays of exposure, risk, and cost effectiveness. The prototype demonstrates the vision of the SELECT software and implements portions of the SELECT methodology. It features:

- Contaminant transport simulations using T2VOC;
- Integration of transport results into exposure spreadsheets of the CALTOX software used by the State of California;
- An easy-to-use interface;
- Real-time estimation of exposure and risk, including risk comparisons; and
- Integrated cost spreadsheets.

Subsurface Transport

The computational program for determining contaminant movement in the soil is T2VOC, a modification of TOUGH2, that calculates the multiphase transport of volatile organic compounds. This model has been used to calculate the fate of trichloroethylene (TCE) for a site at McClellan Air Force Base under the conditions of natural evolution, of connecting nearby residents to the municipal water supply, and of remediation by soil-vapor extraction. An interface to the T2VOC software is currently being integrated into

the SELECT software to facilitate input data specification. In view of the practical limitations of the PC hardware on transport simulation, an effort is underway to compare error analyses due to uncertainty in parameters and choice of conceptual model, by linear and Monte Carlo methods. Simple models for biodegradation are also being considered. See Oldenburg, *et al.*

Exposure

The exposure computation plots dose versus time for each route of human exposure (inhalation, oral, dermal) at the user-specified location. Exposure pathway factors from CALTOX are used for this computation. These data provide an opportunity to compare the route-specific characteristics of a remediation strategy (e.g., for volatile organic chemicals in drinking water as well as from inhalation of shower air). The relationship between pollutant concentration in soil–gas and air exposure to humans in buildings is provided through an additional numerical model. The model is based on the results of study of radon entry by advective transport of soil gases into buildings. A new code (ADEPT) leverages this previous work to provide an ability to determine entry rates of volatile organic compounds (VOCs) into buildings.

We are developing a site-specific atmospheric dispersion model to predict contaminant concentrations in the air at receptor locations near the contaminant source or treatment site. We are using the EPA model ISCLT2. This model requires long-term site-specific meteorological data, which we have located for a five-year period for the McClellan/ Sacramento area. The McClellan-specific model will be interfaced to the SELECT program this summer. We have also obtained ambient air TCE concentration data for a five-year period, measured very close to the McClellan boundary by Cal EPA. We have determined median values for the various years, and these have been included in the comparative risk tables. Ambient air concentrations of TCE pose negligible carcinogenic risk.

Risk: Ranking Possible Carcinogenic Hazards

The Carcinogenic Potency Database (CPDB) is an integral part of the SELECT system. Based on rodent carcinogens in the CPDB, a comparison is presented in SELECT of possible carcinogenic hazards from exposures to site contaminants and a variety of exposures to natural chemicals. Results indicate that, when viewed against the large background of naturally occurring carcinogens in typical portions of common foods, the residues of synthetic pesticides or environmental pollutants rank low. This casts doubt on the relative importance for human cancer risk of low-dose exposures to synthetic chemicals. A database of information that is relevant to developing cancer risk assessments has been developed and will be made easily accessible within SELECT. Included are:

- Carcinogenic potency estimates for approximately 600 rodent carcinogens: (a) TD50 from CPDB, (b) q1* from the US EPA, and (c) q1* from California EPA.
- Mutagenicity evaluations for about 400 rodent carcinogens.
- US OSHA permitted exposures (PEL) and California OSHA PEL.
- Ranking of possible carcinogenic hazards: (a) HERP on 80 rodent carcinogens, and (b) PERP on 75 rodent carcinogens.
- Maximum Contaminant Limits (MCL) in drinking water set by the US EPA and the California EPA
- Ranking of possible TCE hazards for actual exposures in workplace, indoor air, ambient air, and drinking water.

Risk: Assessments Based on Pharmacokinetic-Based and Mechanistic Information

Pharmacokinetic considerations play an important role in cancer risk assessment for chlorinated compounds such as TCE, and thus play an important role in SELECT development. Current estimates of potential human cancer risk for TCE that incorporate such considerations have relied on time-weighted average or integral measures of effective dose applied to the linearized multistage model. Such measures are appropriate only if damage is integrated over time proportional to the instantaneous concentration of the proximate toxic agent.

However, epidemiological, physiologically based pharmacokinetic (PBPK) modeling; and pharmacodynamic and cancer-bioassay studies of TCE and its metabolites are consistent with the hypothesis that TCE-induced rodent liver cancer arises from liver cytotoxicity having a classic threshold-like dose-response, which is likely to correlate better with peak metabolite concentrations in blood perfusing the liver. We therefore obtained PBPK-based risk estimates for TCE based on animal no-observed-adverse-effect levels (NOAELs) and a peak-blood-concentration dose metric, and illustrate estimation of NOAEL-

based Maximum Concentration Limits (MCLs) for human exposures to TCE using novel methods in an analysis being prepared for submission for publication (see Bogen and Gold).

Our results indicate that the current US MCL for TCE in drinking water may be about 40 times lower than the no-effect level. The new methods support quantitation of cancer potencies required in SELECT for volatile organic water contaminants such as TCE.

Risk: Analysis of Comparative Risk-Remediation Strategies

SELECT allows convenient characterization of risks associated with decision-relevant comparisons. This important capability has been demonstrated with regard to upper-bound risks associated with exposures to TCE vs. exposures to water-chlorination byproducts, which may arise from implementation of relevant alternative remediation strategies (e.g., substitution to a surface-water source). A preliminary analysis based on this feature of SELECT is being prepared.

Further information about SELECT can be found on the World Wide Web SELECT Home Page at http://omega.lbl.gov/select/.

Publications

C. Oldenburg, S. Benson, K. Pruess, J. Daisey, N. Brown, L. Gold, and J. Macfarlane, "The SELECT Environmental Remedy Selection Tool: A Platform for T2VOC Multiphase Transport Modeling," *AIChE Symposium Series*, 91(306), 38 (1995); Berkeley Lab Report No. LBL-36634.

K.T. Bogen and L.S. Gold, "Simplified Calculation of PBPK-Based MCLs for Cytotoxic Endpoints: Application to Trichloroethylene Cancer Risk," to be submitted to *Regulatory Toxicology and Pharmacology*.

Acronyms and Abbreviations

ALS	Advanced Light Source
ANAS	Alameda Naval Air Station
ASIC	Application-Specific Integrated Circuit
ATWR	Analog Transient Waveform Recorder Integrated Circuit
BLISS	Building Life-Cycle Information System
BNCT	Boron Neutron Capture Therapy
CCD	charge-coupled device
CD	circular dichroism
CDF	Collider Detector at Fermilab
CERN	European Organization for Nuclear Research
CFTR	Cystic Fibrosis Transmembrane Conductance Regulator
CMN	cerium magnesium nitrate
CMOS	complementary metal–oxide semiconductor
CMT	(High-Resolution Synchrotron Radiation) Computed Microtomography
CPDB	Carcinogenic Potency Database
DDL	delay-locked loop
DIC	dissolved inorganic carbon compounds
DIET	desorption induced by electronic transitions
DNL	differential nonlinearity
DOC	Department of Commerce
DOE	U.S. Department of Energy
DRAM	dynamic random access memory
DS	Down's syndrome
ECR	Electron Cyclotron Resonance
EELS	electron energy loss spectroscopy
EM	electromagnetic
EPA	Environmental Protection Agency
EXAFS	Extended X-ray Absorption Fine Structure
FISH	Fluorescence *in situ* hybridization
FRET	fluorescence resonance energy transfer
GMR	giant magnetoresistance
GSEs	genetic suppressor elements
GSH	tripeptide glutathione
GST	glutathione S-transferases
HDL	high-density lipoproteins
HMECs	human mammary epithelial cells
HREEL	high-resolution electron energy loss
HREM	high-resolution electron microscopy
HVEM	high voltage electron microscope
IC	integrated circuit

ICSD	Information and Computing Sciences Division
INL	integral nonlinearity
IRMOS	infrared magneto-optical spectroscopy
ISL	IsoSpin Laboratory
LANL	Los Alamos National Laboratory
LDL	low-density lipoproteins
LDRD	Laboratory Directed Research and Development
LEED	low-energy electron diffraction
LHC	Large Hardron Collider
LLNL	Lawrence Livermore National Laboratory
MC	melting curve
MCD	magnetic circular dichroism
MCLs	maximum concentration limits
MR	magnetoresistance
NASA	National Aeronautics and Space Administration
NBS	National Bureau of Standards
NCEM	National Center for Electron Microscopy
NEXAFS	Near Edge X-ray Absorption Fine Structure
NIST	National Institute of Standards and Technology
NMR	nuclear magnetic resonance
NO	nuclear orientation
NOAELs	no-observed-adverse-effect levels
NSLS	National Synchrotron Light Source
NSOM	near-field scanning optical microscope
OM	optical mode
PBPK	physiologically based pharmacokinetic
PCR	polymerase chain reaction
PEL	permitted exposures
PEP	Positron–Electron Project
PHB	polyhydroxybutyrate
PSD	photon-stimulated desorption
QMS	quadrupole mass spectrometer
R&D	research and development
RCP	right circular polarized
RCRA	Resource Conservation and Recovery Act
rf	radio standard
RHIC	Relativistic Heavy-Ion Collider
RIL	radiation-induced leukemia
SAM	self-assembled monolayer
SHG	second harmonic generation
SLAC	Stanford Linear Accelerator Center
SMD	single molecule detection
SMOKE	Surface Magneto-Optic Kerr Effect
SNR	signal-to-noise ratio
SOD	superoxide dismutase
SR	synchrotron radiation

SRAM	static random access memory
SSC	Superconducting Super Collider
SSRL	Stanford Synchrotron Radiation Laboratory
STAR	solenoidal tracker at RHIC
STM	scanning tunneling microscope
SXPS	x-ray photoelectron spectroscopy
SXRFM	synchrotron x-ray fluorescence
TCE	trichloroethylene
TDC	time-to-digital converter
TEM	transmission electron microscopy
tfr	translocation frequency response
TOP	time-of-flight
TPD	temperature-programmed desorption
TPPE	two-photon photoemission
UHV	ultra-high vacuum
UHV-STM	ultra-high vacuum scanning tunneling microscope
USTM	ultrafast scanning tunneling microscope
UV	ultraviolet
VOCs	volatile organic compounds
VTX	vertex tracking
VUV	vacuum ultraviolet
XANES	x-ray absorption near-edge spectroscopy microprobe
XSW	x-ray standing wave
XUV	soft-x-ray and extreme ultraviolet (collectively)